Imperial College London

Department of Bioengineering

Evolutionary Biomechanics Laboratory

The Biomechanics and Energetics of Foraging in Leaf-cutter Ants

---

Olivia Kate Walthaus, MSci

Submitted for the degree of Doctor of Philosophy

October 2024

Main supervisor:
Dr. David Labonte

Examiners:
Dr. Angela Kedgley
Prof. Jan-Henning Dirks

Statement of Originality

I, Olivia Kate Walthaus, declare that this thesis is an original report of my research conducted over the past 4 years whilst at Imperial College London. The thesis has been written by me in its entirety and has not been submitted for any previous degree. All experimental assays I either conducted fully or lead and in these instances the collaborative contributions have been indicated clearly, acknowledged and appreciated. All references for supporting literature has been provided along with credit for pictures and figures that are not my own.

Copyright Declaration

The copyright of this thesis rests with the author. Unless otherwise indicated, its contents are licensed under a Creative Commons Attribution-Non Commercial 4.0 International Licence (CC BY-NC). Under this licence, you may copy and redistribute the material in any medium or format. You may also create and distribute modified versions of the work. This is on the condition that: you credit the author and do not use it, or any derivative works, for a commercial purpose. When reusing or sharing this work, ensure you make the licence terms clear to others by naming the licence and linking to the licence text. Where a work has been adapted, you should indicate that the work has been changed and describe those changes. Please seek permission from the copyright holder for uses of this work that are not included in this licence or permitted under UK Copyright Law.

Publications

Some ideas have appeared previously in the following publications:

F. Püffel, O.K. Walthaus, V. Kang, D. Labonte (2023) "Biomechanics of cutting: sharpness, wear sensitivity and the scaling of cutting forces in leaf-cutter ant mandibles" In: *Philosophical Transactions of the Royal Society B*

Acknowledgements

My deepest gratitude goes to Dr David Labonte who is *indeed*, both an incredible supervisor and supportive mentor. Through his unwavering guidance, commitment to scientific rigor, and high standards, I have achieved a lifelong dream of becoming a scientist—something for which words cannot fully express my gratitude. I am especially grateful for his detailed draft iterations, endless patience for last minute conference deadlines and unique motivation in many forms - though my favourite being bets without winners.

All my love and appreciation go to the Evolutionary Biomechanics laboratory and friends at Imperial, each person both past and present has shaped my PhD journey and I am truly grateful to have made friends for life:

I thank Haaris and Henny, for all the breakfasts at Rafaello, trips to the Royal Green William and post conference adventures; Melissa, for being the best badminton partner; Dilanka, for being the badminton player we all aspire to be; Fabi, for never missing a rogue pop culture reference; Freddie, for four years of competitiveness and terrible bets; Oscar, Myriam and Charlie, for making the downstairs office a home away from home; Alex (and Kitri), for being my safe space in London; Sam, for your endless enthusiasm for all things bug; and Maria, Nat, Andrea and Victor for providing an instantly welcoming and supportive environment.

I am grateful to have had the opportunity to supervise and work with passionate and inspiring undergraduate and master's students who have contributed to my thesis; Lina, Finn and Raph, thank you for your hard work.

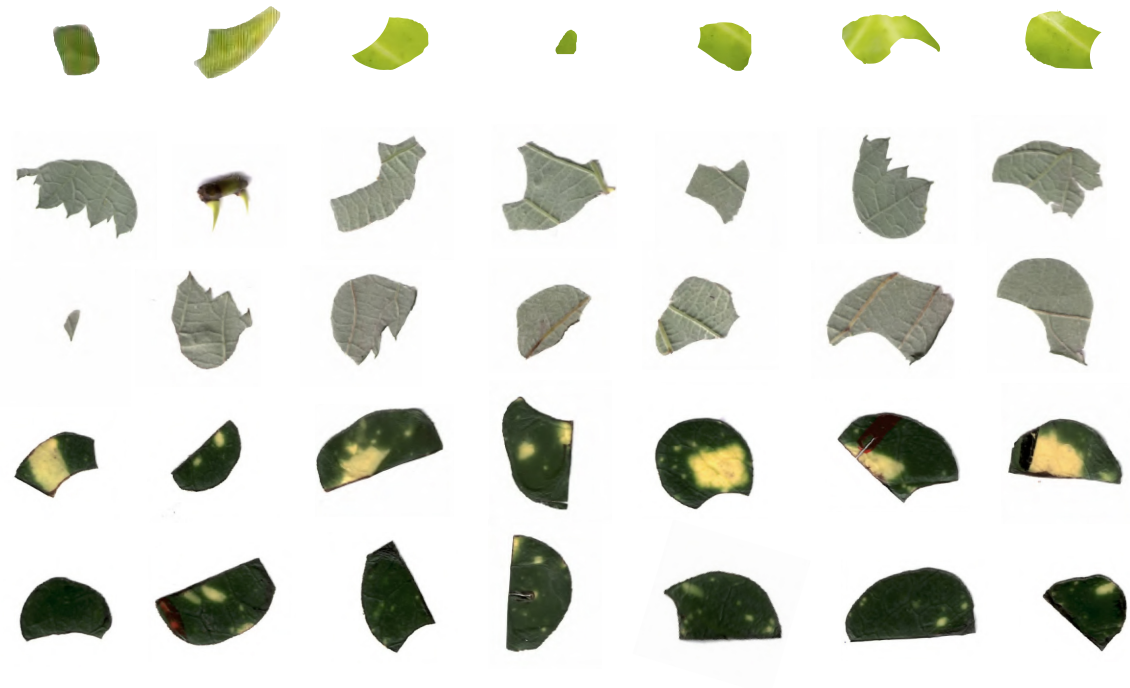
My sincere appreciation to the Department of Bioengineering technical staff, a particular thanks to Ji, Hamid, John, Nana, Paschal and Joel - the department would not run without you.

I finally want to thank my family, this thesis reflects the unwavering love and support I have received all my life. I acknowledge the generations of overlooked talent, missed opportunities and personal sacrifice that have allowed me to reach this immensely privileged position. I am forever grateful for my brother Matt, my best friend, who always keeps me anchored and humble and who is the kindest person I know. I dedicate this thesis to my beloved grandparents, Olive and Ron. Since I was 6 years old, our lively nightly debates on topics in the news shaped my perspective and sparked my curiosity. I have a lifetime of love I can never repay.



"Leaf-cutter ants slice the flesh of hard leaves to create their famous semicircular fragments."

J.R.B. Lighton.



Abstract

Olivia Kate Walthaus

The Biomechanics and Energetics of Foraging in Leaf-cutter Ants

In this thesis, I investigate the mechanical and energetic constraints of leaf cutting—a key aspect of insect herbivore foraging behaviour—using highly polymorphic leaf-cutter ants (*Atta cephalotes*) as a model system. I begin by exploring the factors that influence insect herbivory through the lens of fracture mechanics. I examine how the force required to cut substrates, which vary widely in mechanical properties, changes with both substrate type and worker size. Using a mechanical model, I test predictions on how substrate thickness, toughness, and cutting-edge radius affect cutting force. Cutting forces are found to be size-invariant across worker sizes, as focused ion beam milling (FIB) and scanning electron microscopy (SEM) scans reveal no difference in cutting edge radius. Hence, my results indicate that for pristine tools, cutting force scales directly with leaf toughness and thickness. Next, I assess the variation in metabolic cost of cutting across worker size and substrate. Utilising flow through respirometry, I find that the metabolic power output during cutting remains constant at 30 times the resting rate, regardless of mechanical demand, suggesting that metabolic power output is invariant of substrate properties. Finally, having established the scaling of metabolic power and its independence from substrate mechanical properties, I turn to the scaling of mechanical power. I develop a predictive mechanical model to describe the non-linear variation in cutting speed, which I validate through experimental data. To conclude, I integrate findings from all three experimental chapters of my thesis, deriving a model to estimate changes in cutting efficiency. The result of this work adds a novel perspective to the age-old question - do leaf-cutter ants assign workers to cutting according to ergonomic criteria?

Contents

Acknowledgements **ix**

Abstract **xiii**

1 Introduction **1**
1.1 The evolutionary arms race between insects and plants . . . 1
1.1.1 Plant defences strategies . . . 2
1.1.2 Insect attack adaptations . . . 5
1.2 Energetic costs of insect herbivory . . . 9
1.2.1 Foraging in social insects . . . 9
1.2.2 The insect tracheal system . . . 11
1.2.3 Metabolic rates and how to measure them . . . 11
1.3 Leaf-cutter ants — model insect herbivores . . . 13
1.4 Thesis outline . . . 14

2 The Biomechanics of Cutting **17**
2.1 Introduction . . . 17
2.1.1 A biomechanical perspective on the cutting of thin leaves . . . 18
2.2 Materials & methods . . . 19
2.2.1 Study animals . . . 19
2.2.2 Mandible preparation . . . 22
2.2.3 Model substrates . . . 22
2.2.4 Cutting force set-up . . . 25
2.2.5 Cutting force measurements . . . 26
2.2.6 Mandible “sharpness” measurements . . . 27
2.2.7 Data curation and analysis . . . 28
2.3 Results . . . 29
2.3.1 PDMS pseudoleaves . . . 29
2.3.2 Biological substrates . . . 32
2.3.3 Mandible cutting edge radii are size invariant . . . 34
2.4 Discussion . . . 35
2.4.1 The biomechanics of leaf cutting . . . 36
2.4.2 From pseudoleaves to leaves . . . 37

2.4.3 Mechanical strategies of an evolutionary arms race . . . 38
2.5 Conclusions and outlook . . . 40

3 The Metabolic Cost of Cutting 41
3.1 Introduction . . . 41
3.2 Materials & methods . . . 42
3.2.1 Study animals . . . 42
3.2.2 PDMS pseudoleaves . . . 43
3.2.3 Flow-through respirometry . . . 44
3.2.4 Cutting speed measurements . . . 47
3.2.5 Data curation and statistical analysis . . . 47
3.3 Results . . . 48
3.3.1 Standard metabolic rate . . . 48
3.3.2 Cutting metabolic rate . . . 50
3.3.3 Cutting force and cutting speed . . . 50
3.4 Discussion and conclusions . . . 51
3.4.1 Discontinuous gas exchange; burst frequency, burst volume and their modulation of SMR . . . 53
3.4.2 The diverging scaling of metabolic and mechanical power during cutting . . . 54

4 The Non-linear Variation of Cutting Speed 57
4.1 Introduction . . . 57
4.2 Materials & methods . . . 59
4.2.1 Study organisms . . . 59
4.2.2 Cutting substrates . . . 60
4.2.3 Cutting speed measurements . . . 60
4.2.4 Data curation and statistical analysis . . . 63
4.3 Results . . . 63
4.3.1 Cutting time, fragment size, and cutting speed vary with worker body mass and substrate . . . 63
4.3.2 Energy gained vs energy invested scale with the same mass scaling exponent but differ by a factor of over 2000 . . . 65
4.3.3 Worker size-frequency distribution . . . 66
4.4 Discussion . . . 66
4.4.1 A biomechanical model to rationalise the variation in cutting speed . . . 66
4.4.2 Mechanical power and efficiency . . . 70
4.5 Conclusions and outlook . . . 71

5 Concluding remarks 73

A The Biomechanics of Cutting 79

A.1 Beam calibration co-efficient calculation . . . 79
A.2 The mass insignificant variation of cutting and spacing forces in pseudoleaves. . . . 80
A.3 RM ANCOVA examining the effects of various modulating factors on cutting forces in pseudoleaves . . . 82
A.4 RM ANCOVA examining the effects of various modulating factors on thickness corrected cutting forces in pseudoleaves . . . 84
A.5 The mass insignificant variation of spacing forces in natural leaves. . . . 85
A.6 Nested RM ANCOVA examining the effects of various modulating factors on cutting forces in natural leaves . . . 85
A.7 RM ANCOVA examining the effects of modulating factors on mandible cutting edge radii and wedge angle . . . 87

B The Metabolic Cost of Cutting **89**
B.1 Time constant calculations . . . 89
B.2 Automated peak detection and burst frequency and volume validation . . . 89
B.3 Activity affects discontinuous gas exchange cycles . . . 90
B.4 Preliminary study on 150, 300 and 500 μm PDMS . . . 90
B.5 Mass scaling exponents across *Atta* species . . . 91
B.6 ANCOVA to discern the effects of repeats and mass on burst volume and frequency . 92

C The non-linear variation of cutting speed **93**
C.1 Cutting speed model substrates . . . 93
C.2 Analysis of Covariance (ANCOVA) full statistical analysis . . . 95
C.3 Statistically testing the "goodness-of-fit" of three models for cutting speed . . . 96
C.4 "Null hypothesis" models examples in Laurel . . . 97
C.5 Comparison of linear (K=0) and non-linear hill model (K=4) biomechanical models for cutting speed. . . . 97

Bibliography **99**

List of Figures

1.1 Generalist herbivores, leaf-cutter ants forage on a wide variety of substrates 3
1.2 Plant defences against insect herbivores 5
1.3 Insect adaptations for herbivory 7
1.4 *Atta cephalotes* leaf-cutter ant castes 15

2.1 Sample preparation, cutting force measurements and mandibular wear quantification 21
2.2 The variation of mandibular cutting forces on pseudoleaves 31
2.3 The variation of mandibular cutting forces on leaves 33
2.4 Cutting edge radius and wedge angle variation with mandible wear state and tool geometry 35

3.1 Block diagram for flow through respirometry system 45
3.2 Discontinuous gas exchange — traces, burst frequency and burst volume 49
3.3 The allometry of SMR and CMR and respective CO_2 emission traces 51
3.4 The scaling of cutting speed and its variation with cutting force 52

4.1 Experimental setup to measure cutting speed 61
4.2 Cutting time, fragment mass, and the energetic ratio of leaf-cutting 65
4.3 Cutting speed and worker size distribution across substrates 67
4.4 A biomechanical model to predict the non-linear variation of cutting speed 69

A.1 Cutting force measurement calibration 79
A.2 The mass independence of spacing forces in synthetic substrates 80
A.3 The mass independence of cutting forces in synthetic substrates 81
A.4 The mass independence of spacing forces in synthetic substrates 85

B.1 The effect of movement on discontinuous gas exchange cycles 90

C.1 Linear regressions of cutting speed on linear and log-log space 97
C.2 Visual representation of the Hill relation 97
C.3 Comparison of fit of the biomechanical model for cutting speed using the linear (K=0) and non-linear (K=4, value for vertebrate muscle) hill model. 98

List of Tables

2.1 Mechanical characterisation of model substrates 25

3.1 Respirometry model substrates characterisation 43

4.1 OLS regression describing the relationship of cutting time, fragment mass, and cutting speed for each cutting substrate. 64
4.2 OLS regression describing the relationship of energy invested, and energy gained for each cutting substrate. 66

A.1 A repeated-measures ANCOVA assessing the effects of mass, group, mixing ratio, and thickness on cutting force. 82
A.2 A repeated-measures ANCOVA assessing the effects of mass, group, mixing ratio, and thickness on fracture force. 83
A.3 A repeated-measures ANCOVA assessing the effects of mass, group, mixing ratio, and thickness on spacing force. 83
A.4 A repeated-measures ANCOVA assessing the effects of mass, group, mixing ratio, and *corrected* thickness on cutting force. 84
A.5 A repeated-measures ANCOVA assessing the effects of mass, group, mixing ratio, and *corrected* thickness on fracture force. 85
A.6 A nested repeated-measures ANCOVA to assess the effects of mass, group, and plant type on cutting force in natural substrates. 86
A.7 A nested repeated-measures ANCOVA to assess the effects of mass, group, and plant type on fracture force in natural substrates. 86
A.8 A nested repeated-measures ANCOVA to assess the effects of mass, group, and plant type on spacing force in natural substrates. 86
A.9 A repeated-measures ANCOVA to assess the effects of mass, mandible group, and location on cutting edge radius. 87
A.10 A repeated-measures ANCOVA to assess the effects of mass, mandible group, and location on cutting edge wedge angle. 87

B.1 Mechanical characterisation of preliminary trails pseudoleaves 90
B.2 SMR and CMR for preliminary metabolic cost of cutting trails 91
B.3 Scaling of standard metabolic rate in *Atta* ant species. 91
B.4 ANCOVA to discern the effects of repeats and mass on burst volume. 92

B.5 ANCOVA to discern the effects of repeats and mass on burst frequency. 92

C.1 Cutting speed model substrate material properties 93
C.2 ANCOVA analysis on the effect of body mass and substrate type on cutting time, fragment mass, and cutting speed. 94
C.3 ANCOVA analysis on the effect of body mass and substrate type on energy invested, and energy gained. 95
C.4 ANCOVA analysis on the effect of body mass and substrate type on cut distance, fragment area, and fragment volume. 95
C.5 Statistically testing "goodness-of-fit" for three models to predict the scaling of cutting speed 96

List of Symbols

C	Dimensionless constant
CMR	Cutting metabolic rate
DGC	Discontinuous gas exchange cycles
E	Young's modulus
F_b	Bite force
F_c	Cutting force
$F_{c,c}$	Corrected cutting force
F_f	Fracture force
F_{max}	Maximum bite force
F_s	Spacing force
f_b	Burst frequency
G	Muscle gear ratio
G_c	Tearing energy
h	Substrate thickness
l_f	Muscle fibre length
m	Body mass
m_l	Leaf mass
P	Opposing force
P_{met}	Metabolic power
P_{mech}	Mechanical power
R	Mandible characteristic length
R_c	Callow mandible cutting edge radius
R_f	Forager mandible cutting edge radius
R_s	Scalpel blade cutting edge radius
SMR	Standard metabolic rate
σ_c	Ultimate tensile strength
t_1	Measured laminar thickness
$\bar{t}_1$	Corrected laminar thickness
η	Cutting efficiency
V_b	Burst volume
V_m	Volume of muscle
$V_{tracheal}$	Volume of the insect tracheal system
v_c	Cutting speed

v_{man}	Maximum mandible closing speed
$v_{man,\kappa}$	Maximum mandible closing speed against an external force
v_{max}	Theoretical maximum shortening speed of muscle
v_{rel}	Relative shortening speed of muscle
x_{η}	Calculated most efficient mass
$\bar{x}$	Average mass
$\tilde{x}$	Median mass
x_{mode}	Modal mass
$\dot{\varepsilon}_{\text{max}}$	Maximum muscle strain rate

1 Introduction

Insects account for more than half of all living things on the planet and 90% of all known animal species [1–3]. They can be found across almost all habitats, from the blistering heat of the deserts [4], to the frozen planes of Antarctica [5]. As such, they are unmatched in their breadth physiological adaptations [6]. In the Sahara, the silver ant (*Cataglyphis bombycina*) forages in 60 °C heat whilst moving 108 body lengths per second, making the most of the midday heat to avoid predators [4, 7]. Amongst the beautiful colours of the rainforest the glass-wing butterfly (*Greta oto*) can make regions of its wings almost fully transparent, providing perfect camouflage against any background [8]. In the bustling city of London, hawker dragonflies (*Aeshna*) dance and soar above Hyde Park's ponds catching prey with ease whilst airborne, performing a diverse repertoire of challenging flight manoeuvres using adaptive flight control [9]. To say only that there is remarkable diversity in the specialisations and adaptability of insects would not be doing them sufficient justice, as not only do insects adapt to environments, but they also engineer them.

Ecosystem engineering by insects is a widespread phenomenon and refers to the modification or maintenance of the environment by one species which then impacts others [10, 11].[1] A mutually beneficial example is pollinator-mediated ecosystem engineering [10]. Insect pollinators modulate the reproduction of flowing plants, whilst also depending on them for either a safe space to lay eggs or as a food source [10]. Another example is burying insects: when termites dig underground nests to keep themselves safe from predators, they also improve the structure and drainage of the soil, expanding the range of plants that can grow within that region [13]. However, not all examples of insect ecosystem engineers lead to beneficial outcomes for other species, in fact the most well known example of ecosystem engineering is through insect herbivory [14–17]. Insect herbivores act as ecosystem engineers through the physical and structural modifications of plants [11]. To facilitate successful herbivory insects have evolved highly specialised mouth parts and morphological features to be able to harvest plant matter. In return plants have evolved chemical and mechanical defences to resist such attacks. As such, a 350-million-year long arms race began [18].

1.1 The evolutionary arms race between insects and plants

The co-evolution of plants and insect herbivores predates the dinosaurs [1, 18], and has given rise to increasing species diversity in both herbivores and hosts [19]. So common is this interaction that

[1] The first mention of ecosystem engineering dates back as early as 1881 when Charles Darwin observed that soil structures were altered by earthworms [12].

almost every plant species has been consumed by at least one insect species, [20] in a battle that transcends both ecosystems and scales.[2] Insect herbivores are generally split into generalists or specialists. Generalist herbivores such as leaf-cutter ants (*Atta*) [23], most stick insect species (*Phasmatodea* [24] and leaf-footed bugs (*Coreidae*) [25] feed on multiple host plants from different families (Figure 1.1). Whereas specialists such as the brown planthopper (*Nilaparvata lugens*); (or *rice* brown planthopper as it's more commonly referred to) feed on one or a few plant types from the same family [19, 26]. Whilst the adaptations of specialised herbivores and respective host plant species are countless and each uniquely fascinating, they are beyond the scope of this thesis and as such I will limit myself to a personal favourite example — the monarch butterfly. The monarch butterfly (*Danaus plexippus*) has co-evolved with the milkweed plant (*Asclepias*). A family which produces a secondary compound - cardiac glycosides, which are toxic to the vast majority of insect herbivores [27]. Not only can the monarch butterfly tolerate cardiac glycosides but it has developed a mechanism to sequester them, as a result becoming toxic themselves to potential predators [28].[3]

Across all insect herbivores it is estimated that 10% feed on plants from more than three families [29, 30] and as such occupy a specific ecological niche and are deemed generalists (Figure 1.1) [31]. Whilst the term generalists might evoke the phrase "Jack of all trades, master of none" in truth there are several benefits. Having an abundance of potential food sources means generalist herbivores are less likely to face starvation if one food source gets depleted [32]. Additionally, studies in grasshopper's show that having a more varied diet is conducive to growth [33]. More recently there has been a line of work that shows that utilising a greater range of food sources exposes insects to a wider range of pathogens and thus can lead to a more robust immune response [34]. The ability to feed on a variety of plant families is in itself a remarkable evolutionary adaptation. Leaf material properties, such as toughness, vary by over a factor of 1000 between species [35], additionally different plant species have a range of morphological defensive structures and chemical defences for generalist herbivores to overcome. What features have plants evolved to defend themselves from generalists and in turn what morphological features have generalists evolved to be able to have such a varied diet?

1.1.1 Plant defences strategies

Plants respond to attacks from insect herbivores through an elaborate multi-level defence system. Some mechanisms are indirect such as attraction of the pests natural predators [18, 37]. Others effect herbivores directly, such as the secretions of sticky substances like resin and latex directly stopping an insect in its tracks [19]. Some defences act as immediate barriers to herbivory, such as spines and thorns [38], whilst others are induced to stop herbivory later down the line, like increased toxin production [39]. Within the vast repertoire of plant defences, there are two distinct groups: chemical and mechanical defences to herbivory.

[2] Plants range in shapes and size from mm long duckweed to 100 meter tall Californian red woods [19] insect tools range from puncturing and siphoning needles to large mandibles [21, 22].

[3] This also happens to be an example of one-sided co-evolution, where the milkweed plant gains no benefit from being herbivorised by the monarch butterfly.



FIGURE 1.1: Leaf-cutter ants of the tribe *Attini* are generalist herbivores and have been found to forage on over 20 plant species [23, 36]. Their chosen foraging substrates range from soft petals, to harder leaves and even mushrooms. Within laboratory colonies they have even been found to successfully incorporate oats and corn as a fungus growth substrate. Photo credit: Dr. Sam Fabian.

Chemical defences

I will first, and only briefly, touch on chemical defences as they are beyond the scope of this (mechanically driven) thesis. Chemical defences to herbivory have been studied extensively, filling multiple review papers and books (see [18, 19, 39–41]. The majority of plant chemical defences fall under the category of secondary metabolites — components that are not essential for fundamental life processes but serve a vital ecological role such as herbivory defence [18]. Here I will describe a few relevant subcategories of secondary metabolites. First toxins: toxins are compounds that are deadly to some herbivores or retardant to others. The most notable toxins are alkaloids, with most well-known examples being caffeine and nicotine. These are neurotoxins which directly affect an insect's nervous system [18, 39]. Another subcategory is digestibility reducers such as tannins and lignin. These reduce the nutritional content and palatability of the plant material making the plant less attractive as a food source [42, 43]. Other secondary metabolites include terpenoids, such as menthol which can repel certain insects, and cyanogenic glycosides, which are also toxic. The list is seemingly ever expanding, as even this year (2024) new chemical defences have been identified [44]. However, despite the magnitude and complexity of chemical defences there are two factors that support the prioritisation of the study of mechanical defences. Firstly, no matter how robust the chemical defence,

there will always been at least one insect herbivore than can tolerate them [45, 46]. Secondly, secondary metabolites can only effect insect herbivores when fracture of the plant tissue has occurred, meaning the plant has already suffered damage.

Mechanical defences

Mechanical defences are the first barrier to herbivory. There are several mechanical features that make the initiation of herbivory difficult. The presence of spines and thorns act has both physical and visual deterrents [38, 47]. Waxy cuticle layers not only act as a necessary water barrier for plants but also render leaf surfaces slippery, meaning only insects with specialised adhesive structures can feed on them [48–51]. Finally, trichomes, fine hair-like structures, can cause irritation and mobility difficulties in attacking insect herbivores [52] (Figure 1.2). Additionally, some trichomes are glandular and excrete toxins to deter herbivores [53, 54]. By far the most relevant mechanical defences, are those that would stop herbivory entirely. From a simple mechanical perspective if an insect cannot meet the necessary force requirements to fracture plant tissue, then herbivory does not occur [55] (and the face of this planet would be very different indeed). If for a moment, I take a purely fracture mechanics approach to herbivory, from a plants perspective I can consider a simple equation relating two key material properties to the force required to cut a given leaf (independent of the insect tool used and in absense of additional energetic costs arising from sheet plasticity, bending and buckling) [56]:

$$F = Gh \tag{1.1}$$

Where F is the minimum force required by an insect to cut a leaf, G is leaf toughness and h is leaf thickness.

Thus, from a plant's perspective, to increase the initial barrier to herbivory a plant can either increase its leaves thickness or toughness or a combination of both.[4] Indeed, plant toughness and herbivory patterns do correlate [57, 58]. Several studies on leaf-cutter ants show a preference for less tough substrates and, during cutting, they often avoid tougher areas of plants such as leaf veins and plant stems [59, 60] (See also [61] for similar studies in caterpillars).

The toughness of plant leaves is thought to be proportional to the volume fraction of tissue of the cell wall in the leaf [62] (Figure 1.2). The cell wall is a composite structure comprised of cellulose, hemicellulose, and lignin. Each component combined in a matrix structure that has a toughness of approximately 3.45kJ m^{-2} [62]. It is the matrix structure that gives the cell wall its additional toughness, alone each compound would have an individual toughness 10 times lower. By imbedding cellulose microfibrils in a hemicellulose, and lignin matrix it increases the energy dissipation of the cell

[4] Here I use a fracture mechanics approach to highlight the key relevant mechanical properties within the context of herbivory. I am not implying nor have found any studies whilst writing this review that plants modify these traits instantaneously. Across species there is a natural variation in toughness and thickness of plant leaves.

wall meaning a crack is less likely to propagate completely which would lead to material failure (and successful herbivory). Additionally lignin is largely indigestible to most insect herbivores making it high demand and low reward and as such an inefficient food source [63]. So why should a plant not continuously evolve a larger percentage of leaf to be cell wall, thus increasing toughness and protection against herbivores? While mechanical defences are important, they aren't the plant's primary concern. Increased cell wall thickness can have adverse effects on photosynthesis efficiency. Lignin increases the opacity of the leaf surface, making it more difficult for light to penetrate photosynthetic cells, and makes the leaf surface less porous making essential gas exchange more difficult [64, 65].

The final factor I will consider in increasing the barrier to herbivory mechanically, is increasing leaf thickness. Leaf thickness generally depends on a number of factors, namely the number of layers and length of palisade cells, the placements of veins, and the width of the mesophyll, epidermis, hypodermis and indumentum [66] (Figure 1.2). The role of leaf thickness in preventing herbivory is often overlooked because other mechanical properties, like toughness, are typically standardised for thickness, leading to thickness itself being neglected as an independent factor. However, in the case where thickness was independently considered, leaf thickness and herbivore damage negatively correlated [67]. As with toughness, it would be undesirable to arbitrarily keep increasing thickness as a deterrent to herbivores as there would reach a point where the increase in respiration due to being thicker outweighs the photosynthetic gain.

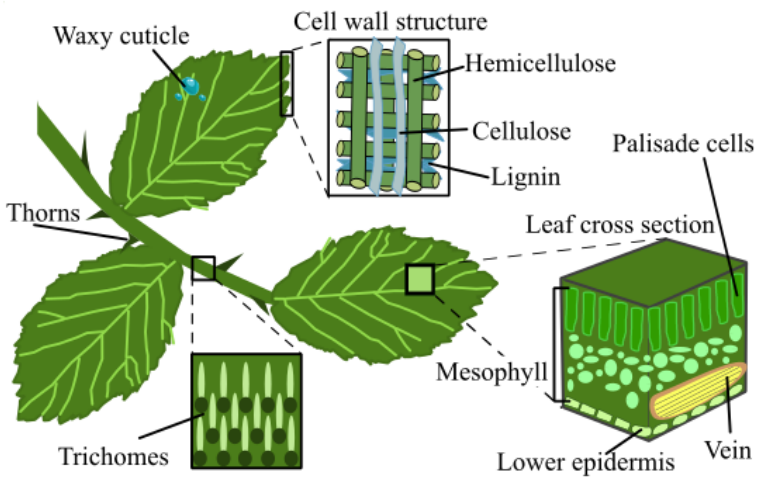


FIGURE 1.2: Plants have evolved various defenses to deter herbivory and increase the barriers against it. Thorns and trichomes, hair-like structures, are examples of mechanical features that act as both visual and physical deterrents. In terms of increasing the initial barrier to herbivory—specifically, the force required to cut plant tissue—two key factors play a role: toughness and thickness. Toughness is associated with cell wall structure, while thickness corresponds to the number of layers within the leaf.

1.1.2 Insect attack adaptations

Given the vast arsenal of defensive strategies plants have evolved, one may consider it a miracle that herbivorous insects have been able to survive to this day. However, co-evolution is no miracle and

insect herbivores are not only able to survive but thrive. Leaf-cutter ants conduct herbivory on such a scale they account for over 15% of the total defoliation in the Neotropics [68–70]. A single swarm of Migratory locust (*Locusta migratoria*) can cover over 100,000 kilometres a day and in that same time eat the same amount as a small town ($\approx$ 10,000 people) [71–73]. The Brown Marmorated Stink Bug (*Halyomorpha halys*) causes millions of pounds worth of crop losses in North America and Europe annually [74, 75]. What enables such prolific herbivory? In short, the insect bite apparatus.

Clissold *et al* stated that in order to fully understand the feeding behaviour of herbivorous insects the biomechanics of the insect bite apparatus must be considered fully [76]. The bite apparatus of insects can be generalised and summarised [5] as two key parts: (i) a pair of mandibles and (ii) the antagonistic muscles that open and close them [78].[6] To maintain strict relevance to the thesis topic, I will assess both components from a mechanical standpoint, focusing on their contributions to herbivore efficacy.

Mandibles

Mandibles are the tools used by insects to cut, slice, pierce or crush plant matter and using a specialised tool for the job significantly improves the outcome — you wouldn't use a spoon to cut a loaf of bread. Across insects the size, shape, and associated musculature of the mandible reflect feeding preferences [77]. Within insects whose diets consist largely of eating seeds, short thick triangular mandibles have evolved, equipped with blunt teeth to enable crushing and grinding [76, 80]. Pollen feeding insects are characterised by lamella shaped mandibles with reduced incisor parts — favouring the scraping of pollen off the plant over the need to slice through tough plant tissue [77]. In order to slice, carry and manipulate the flesh of leaves, sickle shaped mandibles have evolved with razor sharp cutting edges (Figure 1.3).[7] From a mechanical standpoint having a sharp blade reduces energetic penalties arising from tool geometry [81], in the first experimental chapter (Chapter 2) of this thesis I rationalise the effects of tool geometry on cutting force for different substrates and as such will not elaborate further here. The evolution of an ideally shaped tool is just one factor, as in most herbivorous insects, this tool must last a lifetime. Over the course of a lifetime it is estimated that insect herbivores cut many meters of plant tissue [55], during which time, like any tool the mandibles will experience wear. The structure and material properties of mandibles are likely developed to prevent this. Insect mandibles are primarily composed of chitin, a biopolymer which forms in a helicoidal arrangements and is crosslinked with proteins [82, 83]. The chitin-protein complex creates a structure that can absorb impacts without cracking easily, making it well-suited for continuous, repetitive cutting tasks [84]. An additional, yet uncommon adaptation to increase wear resistance is heavy metal deposition within the mandibular teeth [85–87]. Leaf-cutter ants have small amounts of zinc and manganese in their mandible cutting edges increasing hardness and durability of their

[5] This is of course a crude summary of the beautifully complex reality see [77–79].

[6] This is the case for biting insects which are the focus of this thesis; the morphology of the mouthparts of insects that utilise piercing and sucking to feed are distinctively different see [79]

[7] Literally… the cutting edge radii of leaf-cutter ant mandibles were found in this thesis to be as sharp as a pristine razorblade.

mandibles [88] (Figure 1.3). Within this thesis I will examine the effects of arbitrary amounts of wear i.e., by using tools that have developed naturally over the course of an individual's lifetime, on cutting performance (Cutting force – Chapter 2, Cutting speed and mechanical power – Chapter 4). Whilst systematic studies gradually varying wear and quantifying the effect of cutting performance are fascinating, they are beyond the scope of this thesis.[8]

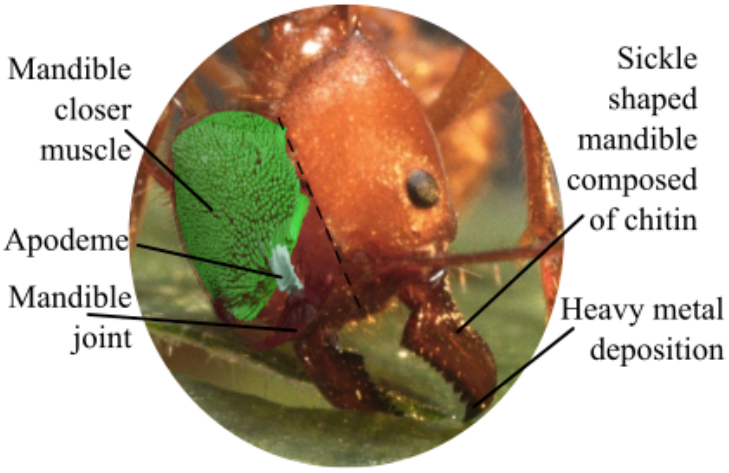


FIGURE 1.3: To slice through the tough tissue of leaves, insects have evolved specialised mouthparts and associated musculature. Their head capsules are filled with enlarged mandible closer muscles, which, when connected via an apodeme to the mandible joint, enable the generation of exceedingly large bite forces. The mandibles themselves are highly specialised tools, sickle-shaped with razor-sharp cutting edges, and are composed of chitin, a durable biopolymer. Heavy metal deposition in the mandibular teeth increases hardness and prevents wear. Photo credit: Dr. Victor Kang. Figure adapted from Dr. Freddie Püffel [89]

Musculature

Whilst mandibles are highly specialised tools that reduce the force required to cut, there still needs to be a system to apply force to do work and fracture the plant tissue. Insect mandibles are actuated by a pair of large muscles which operate antagonistically to open and close them [77, 78]. These muscles generate the large forces required to fracture plant tissue — which I hence refer to as the bite force (also used commonly across other works, see [76, 78, 89–91]). The muscles are connected to the mandible via an apodeme and mandibular joint, which then allows transmission of the bite force on the mandible edge [78, 89] (Figure 1.3). The bite forces are of significant importance for herbivorous insects as they directly determine the range of plant tissues they can harvest [76, 91]. No matter the biological complexity, from a simple mechanical argument cutting cannot occur if the bite force generated by the insect is not greater than the cutting force, the minimum force required to fracture a given plant. Previous work rationalised how the morphological parameters associated with the bite apparatus contributed to the generation of bite forces, finding that the volume of muscle is likely the main factor disproportionally "boosting" the force available [89, 91].[9] Indeed, across insect

[8] But will be evaluated in depth by subsequent PhD students!

[9] This is of course a gross over simplification, but this subject has been already brilliantly described in a previous PhD thesis [92]

herbivores the head capsule is dominated in volume by the mandible closer muscles, in leaf-cutter ants large muscles occupy of 90% of the head capsule [89]. Allowing them to generate forces far in excess of the force required to cut most tropical leaves [91]. Having bite forces far in excess of the required forces gives individuals great behavioural flexibility [55]. Firstly, it means the insect isn't confined to limited food sources [91] (see also [93] for an example vertebrate study). Secondly, from a mechanical standpoint, excess force during cutting provides the potential to increase cutting speed by doing additional work.

Linking cutting force and cutting speed

During cutting, insects activate their large mandible closer muscles, which generate force (bite force, F_b) and do mechanical work. This work is partially expended to meet the minimum fracture requirements of the chosen substrate (cutting force, F_c, Equation 1.1) and propagate a cut; any excess can contribute to the kinetic energy of the mandible, and thus increase cutting speed. How large can this speed get? To answer this question, I introduce the force-velocity properties of muscle: muscle generates its maximum force only during an isometric contraction, when it does not change length. As the muscle strain rate increases, the force it can generate steadily drops, reaching zero at a maximum intrinsic shortening speed. This relation is typically described with an empirical model—the Hill relation [94].

$$F = F_{\text{max}} \cdot \frac{1 - v_{\text{rel}}}{1 + K v_{\text{rel}}} \tag{1.2}$$

Where F is the generated force, F_{max} is the maximal isometric force. v_{rel} is the relative shortening speed of muscle — the ratio of the instantaneous shortening speed v and the theoretically maximum shortening speed v_{max} and K is a dimensionless constant of order unity [95].

In muscle studies, a commonly used value is K=4, typical for invertebrate muscle, though in the simplest linear case (K=0) force declines linearly with speed (see C.2 for a visual representation) [95]. To date, there are no universally accepted values of K for invertebrate muscle. Regardless of the exact value of K, this force velocity trade-off implies that even if sufficient force is available to overcome fracture resistance, the actual cutting speed is constrained by the muscle's force–velocity curve. As contraction speed increases, the available force declines, reducing the ability to accelerate the mandible further. This relationship, captured by the Hill equation, imposes an upper bound on performance. Contextualising cutting force, cutting speed, and bite force within the framework of muscle force–velocity properties is essential for linking cutting mechanics to size-dependent foraging strategies.

In Chapter 4 of this thesis I rationalise how the ratio of the bite and cutting force lead to variations in cutting speed across size and substrate. In conjuction with the variation in cutting forces measured in Chapter 2 I derive a predictive model for mechanical power across size and substrates, based on the Hill relation.

If a greater muscle volume leads to larger bite forces and increased flexibility in cutting speeds, it might seem advantageous to simply maximise investment in muscle mass. However, there are important constraints to consider. Firstly, space within the insect's head capsule is highly limited—muscle must fit within the exoskeletal boundary, which is estimated to be nearly at capacity (approximately 90%). Secondly, and of central importance to this thesis, muscle tissue is extremely costly to build and maintain energetically [96, 97].

This section has outlined the remarkable adaptations that plants and insects have co-evolved. Amidst this biological complexity, mechanical principles impose physical constraints that must be adhered to. Plant tissues have a minimum force threshold required for cutting, and insects must exceed this force to successfully feed. However, herbivory is not driven solely by mechanics— energetic considerations also play a crucial role.

1.2 Energetic costs of insect herbivory

All insect orders from Anisoptera to Zoraptera must obtain, store, and expend energy to grow, reproduce and interact with their environment [98]. Energy is defined as a conserved quantity meaning it can neither be created nor destroyed: it is purely transformational and provides the potential capacity to perform work [99]. When energy is supplied to insects in chemical form through the food they eat, it is either converted via respiration to thermal energy to support basic life processes such as metabolism, stored as chemical energy in growth or as fat reserves, or transferred to their surroundings as work [100]. The minimal energy required to maintain these essential physiological functions is known as standard metabolic rate (SMR) [97]. Any activity beyond this baseline raises an individual's metabolism and as such incurs additional energetic costs. Foraging in herbivorous insects has been studied widely and incurs many energetic costs [101–106]. In the above section I looked at the mechanical constraints of herbivory, as this is a key barrier which limits access to given food sources.[10] In truth, herbivory is just one aspect of insect foraging behaviour — a collective term referring to all steps required to locate acquire and store/consume food sources [112]. Within this section I will assess the energetic costs associated with foraging using social insects — perhaps the most significant foragers in the *Insecta* class [68].

1.2.1 Foraging in social insects

Social insects are able to conduct herbivory on a large scale due to their sophisticated colony structures. An insect is considered eusocial if and only if the following criteria are met: the coexistence of reproductive and non-reproductive castes; at least a two-generation overlap within the colony; and co-operative care for immature individuals [68, 113, 114]. At the evolutionarily advanced grade of eusociality, there is also the presence of distinct castes [68, 113, 114]. Castes are divided by physiological differences, such as reproductive and sterile individuals [68, 113, 114], but also by morphological

[10] Indeed I should note that all foraging aspects also have mechanical constraints; however, it is beyond the scope of this thesis to discuss such here but see [107–111]

differences, where distinct subcastes arise, such as minim, minor, media, and major workers (Figure 1.4). In the most advanced species of social insects, the worker castes exhibit a sophisticated division of labour, which is thought to improve colony efficiency [68, 113, 114]. Foraging is largely conducted by the minor and media castes, while brood care and colony protection are carried out by minims and majors, respectively [68, 113].

Foraging can be divided into three distinct tasks, all of which carry an associated energetic cost: first, locating and traveling to a food source (locomotion); second, harvesting the food (cutting leaves, collecting pollen, etc.); and finally, returning the resource to the nest or colony (laden locomotion) [115, 116]. The costs of locomotion, both terrestrial and aerial, have been widely studied in ants and bees. In grass-cutting ants (*Atta vollenweideri*), the cost of unladen locomotion was found to increase metabolic rate by up to 2 times the standard metabolic rate (SMR), and in laden locomotion, by as much as 4 times [117]. In closely related *Atta colombica*, which favour cutting leaves over grass, the laden cost of transport was found to raise SMR 10 times, largely due to the heavy fragments carried [101]. Terrain also influences the energetic cost of foraging; for instance, in carpenter ants (*Camponotus*), slope was found to increase metabolism to over 7 times SMR for unladen locomotion, and ants have been shown to favour paths that reduce energetic costs when traversing hilly terrain [103].

The metabolic cost of herbivory (i.e., cutting, harvesting, or feeding) is difficult to quantify, as reflected in the few studies available on the subject (but see [102]). Two main limitations contribute to this challenge: first, separating the physiological excitement that feeding induces from the cost of feeding itself requires careful experimental design and strict controls [97]. Second, reliably assessing the energetic cost of cutting natural substrates (e.g., leaves) is difficult, as the substrates themselves have their own metabolic rates, making it methodologically challenging to disentangle the two [97, 118]. Consequently, only one prior study on the metabolic cost of cutting exists, and it was conducted on a single substrate type — metabolically inert parafilm [118]. The findings were remarkable, with metabolic rates increasing over 30 times above SMR during cutting [118]. Given the significant energetic cost of cutting, it is likely a key determinant in the colony's overall energetic efficiency [119]. Since generalist herbivores forage on a variety of plants with differing mechanical properties, an open question remains as to how the metabolic cost of cutting varies with these mechanical demands. In the second experimental chapter of this thesis (Chapter 3), I aim to address this gap by measuring the metabolic cost of cutting metabolically inert Polydimethylsiloxane (PDMS) pseudoleaves with tuneable mechanical properties.

While the costs of cutting are high, they are dwarfed by the aerial cost of locomotion. During tethered flight, the metabolic rate of honey bees (*Apis mellifera*) reaches between 70 to 100 times their SMR [120]. During foraging, it is estimated that both bumblebees and honeybees carry close to 50% of their unladen body mass in either pollen or nectar [121]. However, the increase in mass due to the foraging load does not lead to a linear increase in metabolic rate [121, 122]. All metabolically costly activities have an upper limit, which is set by an individual's aerobic scope [106]. Aerobic scope is defined as

the difference between standard metabolic rate (SMR) and maximum metabolic rate (MMR) without resorting to anaerobic respiration [123].

The fact that insects can raise their metabolic rates to 30 times SMR during cutting and 100 times SMR during flight—while doing so aerobically—is a remarkable evolutionary adaptation. By comparison, vertebrates are capable of raising their metabolic rates only up to 12 times SMR, and even this is rare [124]. In fact, it is thought that if insects were limited in their aerobic scope in the same way as vertebrates, the face of this planet would be very different. Using leaf-cutter ants as an example Lighton postulated: "Had the gas exchange capabilities of the ants been similarly proscribed by their respiratory physiology, leaf-cutting as we know it would not exist; fungus-garden tending in the absence of a dependable, abundant substrate resource would not have evolved; and the evolutionary history of the Attine ants, and perhaps of neotropical forests, would have been profoundly different." [124]. But what enables such aerobic capacity?

1.2.2 The insect tracheal system

Thought to be key to such a range in aerobic scope is an insect's respiratory organs – the tracheal system [125]. There are several works that describe the structure, role and evolution of the insect tracheal system (see [126–129]); however, in brief, tracheal systems in insects generally consist of spiracles, tracheae, tracheoles and air sacs. Spiracles are valve like structures located in pairs on the thorax and abdomen of an insect. The thoracic spiracles are usually responsible for air moving into an individual and the abdominal spiracles facilitate the air expulsion. The spiracles connect to the tracheae – large air-filled tubes that run throughout an insect's body. Trachea are lined with taenidia, spiral ridges made of chitin which prevent the airways collapsing. The trachea then branches into tracheoles which are much thinner tubes with smaller diameters which penetrate active tissues such as muscle. Diffusion of gasses into the cells happens through the tracheole walls, which are very thin and contain fluid to further facilitate diffusion. The final parts of an insect's tracheal system are air sacs which run alongside the tracheae. They are balloon like structures which act as air reservoirs increasing the amount of oxygen available for metabolically costly activities; they also serve a dual purpose and help ventilate the system by moving air through the tracheal tubes when the sacs are compressed. By favouring oxygen supply directly to the active tissue over expensive circulatory systems, characteristic of vertebrate's, insects are able to achieve an over two-fold increase in aerobic scope [124].

1.2.3 Metabolic rates and how to measure them

In this section, I have introduced key concepts such as metabolic rates, energetic costs, and gas exchange. How do these elements interconnect? To recap, an individual's metabolic rate refers to the amount of energy expended over a specific period, typically measured in watts. At rest, this energy expenditure covers the minimum required to maintain essential physiological functions, known as SMR. However, during activities like walking, cutting, or flying, the metabolic rate increases above

SMR, resulting in additional energetic costs. These heightened energy demands are collectively referred to as the organism's active metabolic rate.

In all living organisms, energy conversion is facilitated through respiration [97, 130]. While the specifics of respiration vary among species, the fundamental components remain consistent: an energy source derived from food and an efficient gas exchange system [126–129].

Energy expenditure in insects can be directly measured by assessing the gases consumed and produced during aerobic respiration. In this process, nutrients such as fats and sugars are converted into chemical energy through reactions that require oxygen, resulting in carbon dioxide and water as by-products. Metabolic rate is typically measured using flow-through respirometry systems, which analyse gas concentrations in the air stream before (incurrent air) and after (excurrent air) passing through a chamber containing the insect [97, 131]. While various respirometry methods exist, flow-through respirometry offers the distinct advantage of continuous gas monitoring, enabling real-time assessments of metabolic activity and revealing fluctuations in metabolic rates during different activities [97].

Larger animals generally have higher baseline energy expenditures and therefore consume and produce greater volumes of gases during respiration. In contrast, insects have relatively low metabolic outputs due to their small size, making it technically challenging to detect small changes in oxygen levels against the atmospheric baseline of 21%. To address this challenge, most measurements of energy expenditure or metabolic rate in insects focus on carbon dioxide production, which can be measured more precisely from a lower baseline concentration of 0.5% [97] (hence referred to as CO_2 respirometry). This can be further refined to a zero baseline using chemical scrubbers (see [97] and Chapter 3 for specifics). While the methodology for measuring metabolic rates is discussed extensively in the second experimental chapter (Chaper 3) of this thesis, the underlying theory will be briefly outlined here.

In simplest terms a respirometry system allows careful measurement of gasses flowing into and out of a chamber at a given flow rate (FR_i). First, I consider the incurrent air stream, the air flowing into the chamber. Incurrent air is normally chemically scrubbed, removing select gasses to ensure a stable baseline. In CO_2 respirometry the incurrent air stream is dry, [11] CO_2 free air, meaning the fractional concentrations of CO_2 (F_iCO_2) and H_2O (F_iH_2O) will be close to zero, whilst the fractional concentration of O_2 (F_iO_2) will be at normal atmospheric levels. In the chamber is an insect, whose activity you want to measure, and which consumes O_2 and expires CO_2. In the chamber the incurrent airstream and the insect's respired gases mix, meaning the air that leaves the chamber (excurrent air) has different fractional concentrations of gasses (I now denote these as fraction concertration of excurrent air F_e: (F_eCO_2), (F_eH_2O), (F_eO_2), (F_eN_2)) than the incurrent air and contains the amount of CO_2 produced by the insect and thus the key to calculating its metabolic rate. So how do you calculate the amount of CO_2 produced?

[11] Water vapour leads to dilution effects and as such is always scrubbed from incurrent airstreams.

The key, as Lighton states, [97] is to think paradoxically about nitrogen. Nitrogen is a nonparticipant in respirometry: the fractional concentration of ($F_i N_2$) is the same in both incurrent and excurrent air. Being inert, it is not affected by the insect's metabolism. The gasses that the insect will affect are CO_2, O_2 and H_2O. As it is known that the flow rates of nitrogen are exactly equivalent coming into and out of the chamber, I can derive the following equation for the flow rates and fractional concentrations coming into and out of the respirometry chamber [97]:

$$FR_i\left(1 - F_iO_2 - F_iCO_2 - F_iH_2O\right) = FR_e\left(1 - F_eO_2 - F_eCO_2 - F_eH_2O\right) \tag{1.3}$$

The key to respirometry theory is that these equations are equivalent. In theory, if an animal large enough to generate sufficient metabolic signal and you had the right analysers you can measure the fractional concentrations of all these gasses. However in the case of CO_2, provided that the incurrent air is scrubbed, this equivalence permits a direct calculation of the concentration of CO_2 produced by the animal via [97]:

$$\dot{V}_{CO_2} = FR_e\left(F_eCO_2\right) - FR_i\left(F_iCO_2\right) \tag{1.4}$$

CO_2 production can be easily converted into metabolic rate, as detailed in Chapter 3. The metabolic rate provides a measure of metabolic power, which, in this thesis, is compared to mechanical power (Chapter 4) to begin addressing cutting efficiency.

1.3 Leaf-cutter ants — model insect herbivores

By this point in the introduction, I hope to have conveyed both the extensive diversity and specialisation within the class *Insecta*, and the ecological significance of understanding the mechanical and energetic factors that influence herbivory. While many insects could serve as excellent models for studying herbivory, none, in my view, rival the majesty of the leaf-cutter ants.

Leaf-cutter ants, belonging to the tribe *Attini*, are the dominant pest species of the Neotropics [68], causing millions of pounds worth of crop damage through their prolific foraging [69, 70, 132]. However, they are much more than their reputation as pests, as through their foraging, they shape the world around them. Their foraging behaviour begins at their nests, which are vast underground structures containing hundreds of chambers, each with a specific function. These nests are easily identifiable by the mounds of soil excavated to create the subterranean caverns below. In doing so, the ants aerate and bioturbate the soil, enhancing its fertility [68, 133, 134]. From the nest entrance, they venture out along pre-cleared trails, sometimes stretching up to 200 meters, in foraging columns up to 10 ants wide [68, 70, 133, 135]. When they reach a suitable food source, they perform the behaviour for which they are named—cutting semi-circular fragments from as many as 130 different plant species [135]. However, it is not the variety of plant species that gives them their name, but the

industrial rate at which they harvest—accounting for up to 15% of total defoliation in regions where they are endemic [68]. Such large-scale herbivory limits both food resources and habitat availability for other insects in the area [68, 70, 133].

A key factor that distinguishes leaf-cutter ants from other social herbivorous insects is that they do not feed on the leaf fragments directly. Instead, they transport them back to the nest to cultivate a mutualistic fungus [12] (Figure 1.4), marking the first known example of agriculture and earning them the reputation of being a superorganism [68]. The ability to conduct such vast herbivory and maintain fungal gardens is only possible through their polymorphic, eusocial colony structure.

Leaf-cutter ants display extreme continuous polymorphism with the mass increase between the smallest minim and the largest major being a factor of almost 300 (0.4-110 mg in *Atta cephalotes*) [137]. No matter an individual's size each worker has a job to do. Minims, the smallest worker caste, are responsible for tending to the fungal gardens as well as caring for immature individuals such as brood, pupae and larva [68, 134, 136] (Figure 1.4). Majors, or soldiers, as they are otherwise referred, have the primary role to defend the colony from potential attackers [68, 134, 136] (Figure 1.4). Mediae workers are deemed as the foraging caste and as such their main role is to cut, process and transport plant matter [68, 134, 136]. Polymorphism and its associated task specialisation are thought to increase ergonomic efficiency [68, 134, 138, 139].

To summarise, here I will outline the choice of leaf-cutter ants as a model species, with strict relevance to this thesis. First, they are both economically and ecologically significant: through their prolific foraging behaviour they act as ecosystem engineers, while also causing millions of pounds in crop loss [68–70, 132, 134, 140]. Second, their high polymorphism allows the experimental assessment of size effects across a 10-fold mass range within the foraging caste, without confounding inter-species effects [134, 137, 141]. Additionally, within this caste, worker mandibles change in size but maintain a consistent shape, further minimising confounding factors [142]. Third, regarding the energetics of herbivory, since leaf-cutter ants do not consume the food they cut, there are no confounding effects of metabolic excitement. This allows for the study of the true metabolic cost of cutting, using metabolically inert substrates [118]. Finally, leaf-cutter ants have long been studied for their foraging performance and ergonomic efficiency, providing a wealth of existing knowledge to build upon and use for comparison [59, 119, 134, 137, 139, 141, 143–147].

1.4 Thesis outline

Within this thesis I aim to study the beautifully complex foraging behaviour of leaf-cutter ants through a biomechanical and energetic lens. I aim to quantify the energetic and mechanical demands imposed on an individual ant during cutting – a key and underexplored aspect of their foraging behaviour. I also aim to quantify how these demands change across worker size and substrate properties. Through

[12] The fungus gardens of *Attine* ants don't just serve as a food source it also serves as a nursery to raise brood and an "external gut" to bypass plant chemical defences [68, 134, 136].



FIGURE 1.4: Leaf-cutter ant colonies consist of hundreds of thousands of polymorphic workers. Polymorphism, combined with task specialization, gives rise to different castes and roles within the colony. Minor and mediae workers comprise the foraging caste—individuals responsible for cutting and/or carrying leaf fragments back to the colony (top-left panel). Major workers, or soldiers, defend the colony from predators (top-right panel). Minims, the smallest caste, tend to the fungus gardens (bottom-left panel), and d) care for the growing brood and pupae (bottom-right panel). Photo credit: Dr Sam Fabian.

understanding the interplay of the mechanical and energetic demands at an individual level, I look to identify the determinants of optimal foraging strategy at a whole colony level.

In Chapter 2, I quantify the variation of mandibular cutting force with worker size, substrate properties and wear state, using both natural and pseduoleaves. I contextualise these findings with a mechanical model derived from linear elastic fracture mechanics. This study will allow me to quantify and predict the variation of cutting force across size and substrate.

In Chapter 3, I quantify the metabolic cost of cutting mechanically different substrates. Utilising highly sensitive flow through respirometry, I first measure the SMR of workers spanning the approximate foraging mass range. Using SMR as a baseline I then quantify the metabolic cost of cutting metabolically inert PDMS pseudoleaves, differing in toughness by a factor of two. This study will allow me to quantify the variation of metabolic power with increasing mechanical demand.

In Chapter 4, I quantify the variation in cutting speed. I first experimentally measure cutting speed for workers spanning the approximate foraging mass range on three natural substrates. I then outline a biomechanical model to explain the non-linear variation of cutting speed based on the relevant mechanical parameters. This study in combination with Chapter 2 will allow me to quantify the

variation in mechanical power with worker size and substrate.

In my concluding remarks I finally combine all aspects of my experimental chapters and evaluate the mechanical and physiological determinants of cutting efficiency, and finally humbly suggest an answer to a long-standing question within the field: do leaf-cutter ants assign workers to cutting according to ergonomic criteria?

2 The Biomechanics of Cutting

I acknowledge the contributions of Dilanka Deegala who conducted the FIB-SEM scans, Raphael Delattre, who conducted the mechanical characterisation of laurel and Dr. Frederik Püffel who provided R analysis scripts I later modified.

Summary

Insects and plants have been locked in an evolutionary arms race spanning over 350 million years. As a result of this competition, insects have evolved highly specialised tools to slice effectively into plant tissue and plants, in turn, developed both chemical and mechanical defences to counter these attacks. A significant body of research has been devoted to chemical deterrents to herbivory, but mechanical defences have received much less attention. Even less explored are the fundamental mechanical and morphological pressures on the insect feeding apparatus. How can plants best vary their mechanical properties to ward away herbivores, and how can insects best counter these mechanical challenges? In this work, I tested a simple physical model that related the force required to cut thin leaf-like tissues to their structural and mechanical properties, and the geometry of the cutting tool. To remove mandible shape variation while being able to investigate the effect of mandible size, I used leaf-cutter ants as a model system. Cutting forces were measured using a custom-built fibre optic setup, using either pristine or worn mandibles, as well as scalpel blades, and for homogenous pseudoleaves made from PDMS, and a small set of plant tissues. The results substantially support the simple model, so enabling a direct prediction of how leaf thickness, toughness and tool geometry jointly determine the cutting force. Perhaps surprisingly, wear emerges as a key modulator of the cutting force, elevating it by as much as a factor of five above a physical minimum. Thus, plants may be best served by implementing strategies that maximise wear, whereas insects should seek to minimise it.

2.1 Introduction

Insects and plants have co-existed for over 350 million years [18], and a variety of relationships have evolved between the two taxa. Some, such as pollination, are mutually beneficial [37]; others, however, are deleterious, and by far the most prevalent of such interactions is the predation of plants by insects [148]. The ecological impact of insect herbivores on plant species is vast: they directly affect plant selection, fitness, and geographic range, including the biological control of invasive plant species [149–154]; but they also have devastating economic effects: although only about 1% of insect species are classified as pests [155], they consume a staggering 13% of crops globally [156], and in the

United States alone account for damage worth an estimated 17.7 billion US dollars per year [157]. Despite the apparent success of insect herbivores, plant feeding is no trivial matter: it is mechanically challenging, and metabolically costly [118] . In order to minimise feeding time and the associated mechanical and energetic costs, large head muscles and specialised mouthparts evolved in insects [90]; and in order to keep them large, deterrence strategies evolved in plants. Chemical defences, such as the inclusion of flavonoids, terpenoids, tannins and alkaloids, or of secondary metabolites that can be poisonous, repellent or even trap herbivorous insects, are most well-studied [18, 158, 159]. However, because the efficacy of chemical defences is dictated by predator physiology, and because they are often only triggered through active insect attacks, it is increasingly held that mechanical defence strategies are more general, and a key line of first defence [76, 80, 160, 161]. Despite this broadening in perspective, it is not always clear which mechanical plant traits are most effective at deterring herbivores [61, 80], nor exactly how they should be measured—some have even suggested that the focus on leaf chemistry may have been partially due to the absence of reliable biomechanical assays [161]. Morphological structures such as waxy cuticles and thorns are examples of mechanical deterrents to herbivory [18]; but perhaps the most relevant mechanical factors are those that increase the physical barrier to herbivory, such as leaf toughening through cell wall thickening or lignification [18, 158, 162]. No matter the size of the animal, or the toughness of the plant, all herbivory involves a mechanical interaction between mouthpart and plant tissue, and this universal interaction imposes a number of shared physical constraints. A necessary condition for plant feeding is that the bite force—the maximum force an insect can generate—exceeds the force required to initiate and propagate a cut [55, 76, 80, 163]. The magnitude of the bite force is determined by the morphology and physiology of the musculoskeletal bite apparatus [e. g. 89, 90, 164, 165]; it is thus independent of the material being cut. The cutting force, in turn, depends both on the material properties of the substrate and the geometry of the "tool" that is used to make the cut . How do these factors come together to determine the total cutting force?

2.1.1 A biomechanical perspective on the cutting of thin leaves

Leaf cutting is a fracture process—it involves the creation of new surface area, and so the progression of each cut incurs an energetic cost dU_a. This cost must be supplied by doing work with an external load, $dU_{ext} = dU_a$, and from this simple energy balance, it follows that the force F required to cut a substrate of thickness t cannot drop below [56, 91, 166, 167]:

$$F \geq G_c t \tag{2.1}$$

where G_c is the critical surface energy per unit crack area. Notably absent from this expression are any contributions that reflect the tool used to make the cut—it states that the force is the same, whether the external work is supplied by a razorblade or a teaspoon. This unrealistic prediction arises because the simple energy balance $dU_{ext} = dU_a$ neglects additional energy sinks, arising from elastic bending, plasticity, or friction [56]. In thin sheets, contributions from bending are likely

negligible, but the cutting tool can demand additional energetic costs if it is insufficiently sharp. Assuming that cutting tool shape can be parametrised with one characteristic length scale, R, dimensional arguments suggest that the energetic cost associated with tool bluntness take the form $dU_{loss} \approx C\sigma_c R t dx$, where C is a dimensionless constant of order unity, and σ_c is a characteristic stress [55, 56, 167]. It follows that:

$$F_f = G_c t + C\sigma_c R t \tag{2.2}$$

The first term represents the unavoidable energetic cost arising from fracture alone; the second term accounts for additional costs incurred by interactions between mandible and plant material close to the crack tip. The importance of plant properties and mandible geometry in determining the cutting force thus depends on the relative magnitude of these two terms. An intuitive way to assess their relative contributions is to divide through with $G_c t$, to find a dimensionless form [55]:

$$\frac{F_f}{G_c t} = 1 + C\frac{\sigma_c R}{G_c} \tag{2.3}$$

This writing reveals that the relative importance of plant properties versus mandible geometry depend on the ratio between two length scales: the mandible length, R; and the material length scale, $G_c\sigma_c^{-1}$. If $R >> G_c\sigma_c^{-1}$, the cutting force is dominated by dissipative processes near the crack tip, and depends on mandible geometry; for $R << G_c\sigma_c^{-1}$, it is close to its physical minimum, and depends solely on plant properties—a mandible that satisfies this condition may thus be considered ideally sharp [55]. Although previous work provided preliminary evidence in support of this model, it was restricted to measurements with one simple model surface [55]; more robust and targeted testing thus remains outstanding. In this work I take this model as a starting point, and seek to systematically test two direct predictions:

i. Cutting force should be proportional to thickness and toughness for $R << G_c\sigma_c^{-1}$.

ii. Cutting force should be sensitive to tool geometry only if $R >> G_c\sigma_c^{-1}$.

In testing these predictions, I hope to ultimately determine some of the key factors that modulate herbivore efficacy. What makes insects most efficient and how can plants best mechanically defend themselves?

2.2 Materials & methods

2.2.1 Study animals

Atta cephalotes (Linnaeus, 1758) leaf-cutter ants were sampled from a mature laboratory colony kept in a climate-controlled chamber (FitoClima 12.000 PH, Aralab, Rio de Mouro, Portugal) at 25°C, 60 $\pm$ 5% relative humidity, and in a 12-hour day/night cycle. The colony was provided with bramble,

laurel, kibbled maize, and honey water *ad libitum*. To measure the force required to cut biological and synthetic substrates with ant mandibles, I collected mandibles from workers spanning the typical size range of foraging parties, 1–60 mg; workers with body masses below 1 mg (minims) and above 60 mg (majors) were excluded, as they do not usually partake in foraging, and have a distinctively different head and mandible morphology [89, 134, 142, 143]. Two sets of workers were collected: workers with "pristine" mandibles, allowing me to quantify the variation of mandible cutting forces with worker size independent of a possible covariation of mandible wear; and active foragers, to investigate the effect of mandible wear on cutting forces (See Figure 2.1A).

Pristine mandibles were collected from callows—recently eclosed workers distinguished from mature workers by their softer and lighter cuticle [88, 168]. Callows typically do not leave the colony nest, and are physically incapable of leaf cutting in the first few days after eclosion [168]; their mandibles are therefore likely pristine, i. e., unaffected by wear induced by repeated cutting [55, 88]. 12 pupae with a body mass above 10 mg were extracted from the fungal gardens of the colony, and placed in 50 ml centrifuge tubes (GMBH, Wertheim, Germany) with small amounts of fungus; a few minims were added to enable pupal maintenance [139]. The centrifuge tubes were fitted with custom 3D-printed lids, with holes large enough to allow minims to enter and leave, but small enough to prevent the escape of the developing workers upon eclosion. The tubes were then placed in the colony foraging area. A further 15 pupae with a body mass less than 10 mg were also collected from the fungus gardens, but then kept in larger isolated containers, again together with a small volume of fungus and some minims. All pupae were marked (Edding 4000 paint 120 marker, Edding AG, Ahrensburg, Germany), such that they could be distinguished from other mature workers of similar size [169]. The pupae were monitored daily to observe whether the legs had unfolded, at which point eclosion was considered complete [139]. A further 72 hours were allowed to pass, such that the incorporation of zinc into the mandible was completed [88]. At this point, both the shape and mechanical properties of the pristine mandibles corresponded to those of mature ants [88, 170].

Forager mandibles were collected from 20 mature workers, sampled from the foraging arena such that their body masses were approximately evenly spaced in $\log_{10}$-space within the foraging mass range. The mandibles of these individuals are likely worn to varying extent, due to repeated leaf cutting [55, 139]. For similar reports in other insects, see also [171–173].

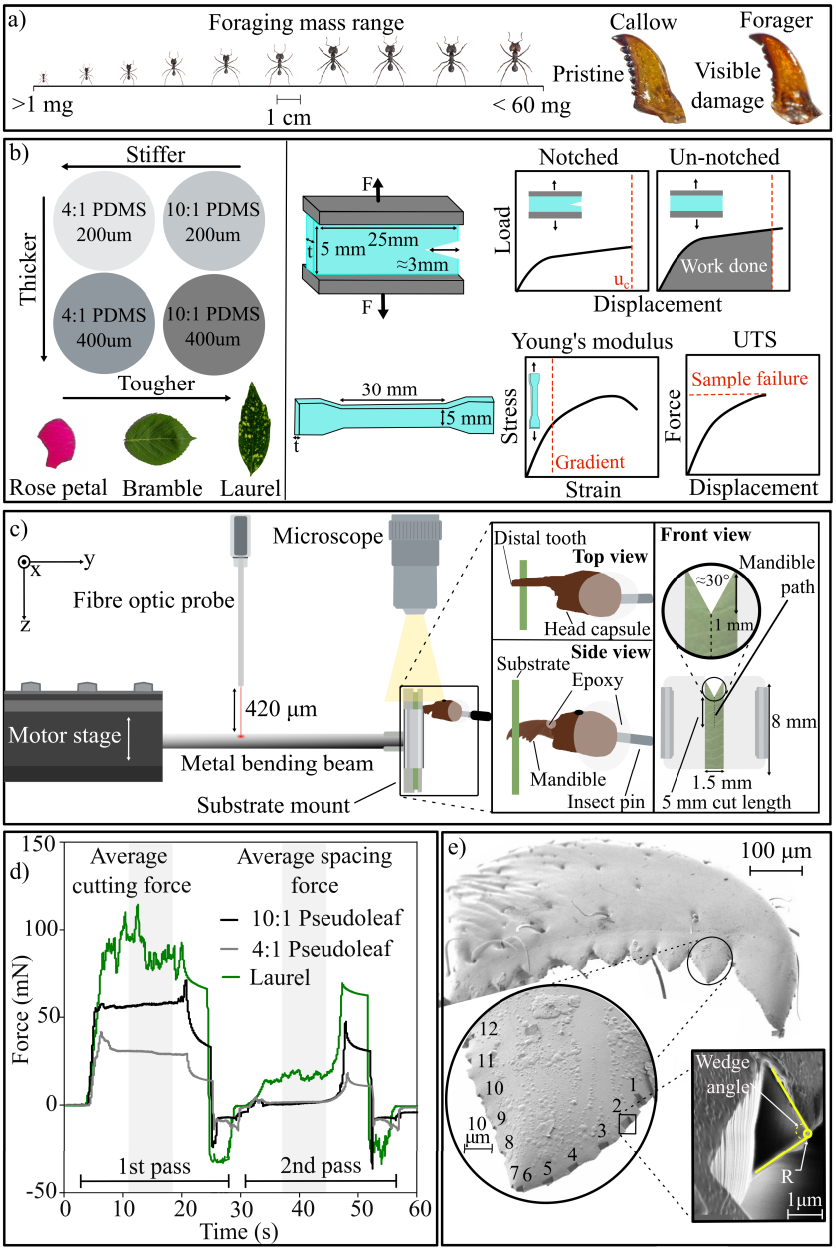


FIGURE 2.1: **(A)** In order to measure the force required to cut biological and synthetic substrates with ant mandibles, I collected mandibles from *Atta cephalotes* workers spanning the foraging size range (see main text). Both foragers (showing different degrees of mandibular wear) and callows (with pristine mandibles) were collected to quantify the effects of mandibular wear and worker size on cutting force, respectively. **(B)** Polydimethylsiloxane (PDMS) sheets were mechanically characterised via dogbone tensile tests to obtain Young's modulus and ultimate tensile stress; pure shear tests were used to measure the critical tearing energy (see main text for more details). **(C)** All forces were measured using a custom-built setup comprised of a fiber-optic displacement sensor and a bending beam, both connected to a piezo motor stage. Each substrate was fixed in place using a custom-designed holder, mounted at the free end of the beam, and the mandible was positioned above the substrate such that its cutting edge was perpendicular to the plane of the substrate. The motor then moved the beam mounting vertically against the mandible, causing the substrate to be cut and the beam to deflect. **(D)** Illustrative raw cutting force traces. The first pass was to measure the total cutting force, and a second pass through the cut was performed to extract the spacing forces which are due to side wall friction and elastic sheet bending. After cut initiation, a steady state cutting force was reached; the average across this area was used for further analysis. The force traces are from measurements for a callow mandible, extracted from a worker with body mass of 33.7 mg. **(E)** Mandible sharpness was assessed by measuring the radius and wedge angle of the cutting edge. Six mandibles and one scalpel blade were selected. Mandibles were fixed and positioned, and subsequently coated with chromium. FIB milling created 12 cuts on each mandible's second tooth, followed by SEM imaging to capture the cross-sections. Polymorphic colony rendering adapted from Dr. Fabian Plum.

2.2.2 Mandible preparation

All individuals were weighed to the nearest 0.1 mg (Explorer Analytical EX124, max. 120 g $\times$ 0.1 mg, 130 OHAUS Corp., Parsippany, NJ, USA). Body masses ranged between 1.9–55.5 mg for callows, and between 2.3–54.8 mg for foragers, representing the approximate size range that may partake in foraging activities [134, 174]. (See also [138] for the foraging size range in closely related *Atta colombica*). Ants were then sacrificed by freezing at -4°C for at least 12 hours, placed in a Petri dish, secured in place with Blutac (Bostik, Stafford, UK), and dissected under a light microscope (SAPO, Leica, Wetzlar, Germany). The head capsule was removed using micro scissors, and split in two along the sagittal plane, using fresh scalpel blades (No. 11 blades, Swann Morton, Sheffield, England). The head capsule of leaf-cutter ants is bilaterally symmetric [89], and ants do not appear to exhibit any obvious mandible laterality during cutting [175, 176]. I hence assume that there are no systematic differences between each head capsule half [55]. The left side of the head capsule was retained for cutting force measurements; the right side was used for imaging and mandible cutting edge radius measurements (see 2.2.6). To facilitate cutting force measurements, head halves were mounted on an insect pin (size '2' for ants $<$ 10 mg, size '4' for ants of 10-20 mg, and size '6' for ants $>$ 20 mg; Shigakontyu, Tokyo, Japan). The connections between pin and head, and head capsule and mandible, respectively, were immobilised with two-component epoxy (Araldite Rapid, Huntsman 143 Corp., The Woodlands, Texas, USA), taking great care that the epoxy did not cover the mandibular cutting edge, as confirmed via light microscopy. Nevertheless, some samples had to be discarded, reducing the sample size to n=15 for both pristine and forager mandibles.

2.2.3 Model substrates

PDMS pseudoleaves

Pseudoleaves were fabricated from PDMS, which brings the advantage that the structural and mechanical properties could be controlled and tuned through variation of four fabrication parameters: (i) the ratio of base and curing agent; (ii) "sandwich" thickness; (iii) curing temperature; and (iv) curing time [177–181].

PDMS pseudoleaves were synthesised from Sylgard184 ™ (Dow Inc., Midland, MI, USA) [182], a two component kit containing a vinyl-terminated base (A) and a curing agent (B) [177]. Pseudoleaves were fabricated with either a 10:1 or 4:1 mixing ratio. Parts A & B were weighed and carefully poured into a petri dish cleaned with isopropanol. The solution was thoroughly mixed with a pipette tip, and degassed at 1 ATM to remove air bubbles. The mixed but uncured PDMS was then poured onto a silanised glass plate (14 $\times$ 14 cm). To fabricate pseudoleaves with two different thicknesses, feeler gauges with a nominal thickness of either 200 or 400 μm were placed onto the plate such that they delineated a region of approximately 12 $\times$ 12 cm (Precision Brand, Downers Grove, IL, USA). A second silanised glass plate was then placed on top to create a PDMS-glass plate "sandwich",

held in place by two clamps. Two mixing ratios and two thicknesses provided four different PDMS pseudoleaves: 200 μm 4:1, 200 μm 10:1, 400 μm 4:1 and 400 μm 10:1 (see Figure 2.1B).

In order to tune the mechanical properties of the pseudoleaves further, the curing conditions differed across the mixing ratios. 10:1 PDMS pseudoleaves were cured at 65°C for 4 hours in a drying oven (Sanyo Electric Co., Ltd., Osaka, Japan) [183]; the 4:1 PDMS pseudoleaves were instead cured at 100°C for two hours. Both sandwich types were then removed from the oven, left to cool at room temperature, and gently peeled from the glass plates. The 4:1 pseudoleaves only were then placed on scrunched aluminium foil (reducing contact area and thus adhesion), and returned to the oven for a 48 h post-cure at 165°C [177]. Four pseudoleaf samples, each with a size of approximately 95 cm^2, were produced for each pseudoleaf type.

The thickness of each pseudoleaves was measured with a digital micrometre at six random locations (resolution 0.001 mm, Mitutoyo Corp, Kawasaki, Japan). The pseudoleaves had an average thickness of 210 $\pm$ 10 μm and 420 $\pm$ 15 μm, respectively, within 10% of the target thickness, and with a variation of less than 5% about the mean thickness. Rectangular test specimens (10 mm $\times$ 15 mm) were cut from each PDMS sheet using scalpel blades, and kept in labelled and closed petri dishes to avoid dust contamination until use. The thickness of each test specimen was additionally measured once in the centre of the sample before use in experiments to increase the accuracy of downstream calculations.

Plant leaves and petals

Leaves of bramble (*Rubus*) and laurel (*Aucuba japonica*) were collected from a private garden on Imperial College campus grounds (51.50078° N, -0.17242° W) between 8th February 2023 and 2nd May 2023. Leaves were harvested at 10am $\pm$ 2 hours on each experimental day, kept refrigerated in a sealed container, and wrapped in damp tissue to minimise water loss [184]; all leaves were tested within 4 hours of storage. Leaf mechanical properties may also vary with leaf age [62, 160, 184–187]. In an effort to reduce this covariation, leaves were collected from the same laurel bush, and from the same marked branches where possible. Within the same branch, leaf colour served as a qualitative proxy for leaf maturity [188]; only leaves with dark green colouration were used.

Rose petals were bought from local suppliers, used on the day of purchase, and stored as above. A thickness map for each leaf or petal was created by taking six thickness readings of the leaf lamina with a digital micrometre; the thickness of the mid vein and minor veins was also recorded as present. 10 mm $\times$ 15 mm rectangular test samples were cut from each biological substrate using scalpel blades, such that the sample long axis was perpendicular to the central leaf vein. Care was taken to select leaf areas free of minor or major veins, to maximise substrate homogeneity [189]. Leaf-cutter ants typically avoid cutting major veins [60, 190], so that measurements on more homogenous sections of the leaf laminas are likely representative [191, 192].

Mechanical characterisation

In order to test model predictions, three mechanical properties were determined for both pseudoleaves and real leaves where possible: (i) the Young's modulus, E; (ii) the ultimate tensile strength, σ (UTS); and (iii) the tearing energy, G_c.

The mechanical characterisation of homogenous materials such as PDMS is comparatively straightforward. Biological materials, however, pose a number of challenges. First, on smaller leaves and petals it is often impossible to cut samples with dimensions that comply with ISO/ASTM standards; miniaturised or non-standard geometries must be used instead out of necessity, which compromises comparability. Second, biological substrates such as leaves are often heterogeneous, so that standard assumptions such as those of linear elastic fracture mechanics may not hold [193, 194]. These difficulties prevented mechanical characterisation for rose petals and bramble leaves, which were either too small or too heterogeneous, respectively.

All tests described below were conducted with a uniaxial tensile testing machine, equipped with Mec277 double-action vice grips with diamond jaws (Multitest5-xt, Mecmesin Ltd., Slinfold, UK; 25 N load cell, $\pm$ 0.25 N resolution). For each material parameter, two test samples were taken from each of four pseudoleaf sheets (n=8 per pseudoleaf condition, n=32 total), unless stated otherwise. 20 laurel leaves were used across this study; three samples per leaf were taken for each test.

To determine the Young's modulus, ISO37 standard dog-bone shaped specimens were cut from each substrate using scalpels [Figure 2.1B, 195, 196]. Uniaxial tensile tests were conducted at 0.5mm s^{-1} , and terminated at sample failure. The Young's modulus was then obtained as the slope of the stress-strain curve in the 0-10% strain range [197, 198] for PDMS, and 0.25 – 2% for laurel leaves, restricted in both samples to a region that was approximately linearly elastic.

The ultimate tensile strength (UTS) was obtained by dividing the force at failure by the undeformed cross-sectional area of the sample. Samples that failed close to the clamping site were discarded; only ten samples failed in the central region of the specimen for synthetic substrates. To increase the sample size, further experiments were conducted, using an additional two PDMS sheets for each mixing ratio (200 μm); five samples were taken from each sheet (n=20).

The tearing energy was quantified via pure shear tests, following established protocols [199]. Two 25 mm $\times$ 5 mm paired rectangular samples (5:1 width-height ratio) were cut from each substrate using scalpel blades. One sample was left unnotched; a notch of about 3mm in length was introduced into the other sample with a pristine scalpel (Figure 2.1B). The unnotched sample was used to measure the load-displacement relationship. The notched sample was used to determine the critical displacement u_c at which the notch turned into a propagating crack, identified via time-synced video recordings (Logitech C920 HD Pro, 30fps). Both tests were conducted with a low strain rate

of 0.0067 s^{-1} to approximate quasi-static loading conditions. The tearing energy was then calculated via [199, 200]:

$$G_c = \frac{U_w(u_c)}{wt} \tag{2.4}$$

Here, G_c is the tearing energy of dimension force per length, U_w is the work done on the unnotched sample, $U_w(u_c)$ is defined as the integral of the force-displacement curve from zero to the critical displacement u_c, w is the width of the sample, and t is its thickness.

All pseudoleaf material properties were independent of thickness (two-way ANOVA; Young's modulus: $F_{1,28}$ = 0.164, p=0.689; UTS: $F_{1,20}$ = 0.003, p = 0.960; Tearing energy: $F_{1,28}$ = 0.787, p= 0.954) but varied significantly with mixing ratio (Young's modulus: $F_{1,28}$ = 609.1, $p < 0.001$; UTS: $F_{1,20}$ = 5.40 , p = 0.048; Tearing energy: $F_{1,28}$ = 222.6, $p < 0.001$). Results were thus pooled for each thickness (for a summary, see Table 2.1), and were consistent with independent reports in the literature [195, 199, 200].

TABLE 2.1: Cutting forces were expected to vary with the mechanical properties of the target material, which were thus characterised. Sample Young's modulus and ultimate tensile strength (UTS) were determined via tensile testing of dog-bone specimens, and tearing energy was measured via a pure shear test with rectangular specimens (see main text for further details). The Young's modulus - the ratio between stress and strain in the linearly elastic region – is a proxy for the material's resistance to elastic deformation. The UTS represents the maximum stress a material can withstand before breaking. The tearing energy denotes the energy required to propagate a crack through a unit length of material. The ratio between the tearing energy and the UTS yields a characteristic length scale, the influence of which depends on the characteristic length scale of the tool that is used for cutting. Each material parameter was independent of thickness.

Substrate	Young's modulus E (MPa)	Tearing energy G_c (Jm^{-2})	UTS σ_c (MPa)	Material length scale
4:1 PDMS pseudoleaf	4.1 ± 0.3	98 ± 9	6.0 ± 2	16.3 μm
10:1 PDMS pseudoleaf	1.6 ± 0.3	197 ± 25	5.5 ± 2	35.8 μm
Laurel	31 ± 4	746 ± 210	1.63 ± 0.3	449 μm

2.2.4 Cutting force set-up

The forces required to cut synthetic and biological substrates with mandibles were measured with a custom-built setup, based on a fibre-optic displacement sensor (μDMS-RC32 controlled via DMS Control v 3.015, Philtec Inc. Annapolis, MD, USA; see Figure 2.1C (for a similar setup see [55, 201]). The sensor was fixed in place with a custom mount attached to two micromanipulators that controlled its orientation, such that it was perpendicular to a stainless-steel bending beam placed below. Prior to all measurements, the sensor was set to record at 81.4 Hz, 30°C, 50% transmitted optical power, and was placed such that it remained within its linear range of 2.5 mm throughout the measurements - 420μm above the beam in its undeformed state (Figure 2.1C). The beam (114.7mm (L) × 10.4mm (W) × 0.35mm (T)) was held in place by a metal fixation plate, such that its free length was 28.7mm. The plate holding the beam was attached to a moveable motor stage (M-404.6PD controlled via PIMikroMove v 2.33.3.0, Physik Instrumente GmbH & Co. KG, Karlsruhe, Germany, maximum velocity 25mms^{-1}). At the free end of the beam, a custom-designed 3D printed mount was fitted, to

constrain the substrates during measurements. This mount consisted of two parts, clamped together using metal clips (Supaclip 40, Rapesco Office Products PLC, Sevenoaks, UK).

During measurements, the beam was deflected as a result of the force applied by the mandible to the clamped substrate. This deflection increased the distance between beam and sensor tip, and so altered the amount of light reflected back to the sensor. To relate this change to the applied force, the sensor was calibrated with known weights at the start of each experimental day. Calibration was conducted by hanging ten calibration weights, ranging from 10 – 245mN (1-25g Kern & Sohn GmbH, Balingen, Germany) onto the 3D mount, using strings with negligible mass. The weights were chosen such that they spanned the range of observed mandible cutting forces (17 – 199 mN; a larger range of weights was used to calibrate a stiffer beam for measurements with scalpel blades, see Appendix A). The sensor reading was averaged across 5s for each weight, and readings prior application and after removal of each weight were used to account for drift, which generally remained negligible (see [55] for further detail).

2.2.5 Cutting force measurements

Mandible cutting force measurements were conducted in randomised order to eliminate systematic effects of wear. Synthetic substrates were measured only once per sample, as previous work demonstrated minimal variation between repeats [55]; biological substrates, however, also bring material inhomogeneity, and were thus measured three times with each mandible. For each substrate, control measurements were conducted using pristine scalpel blades.

Before each experimental trial, substrates were "pre-cut" using a 3D printed template, resulting in a wedge with an opening angle of about 30°, and a depth of about 1mm (Figure 2.1C); this pre-cut decreases the propensity for leaf bending and buckling, and thus aids cut initiation [199, 202]. Samples were then clamped such that the pre-cut was central in a free region of 1.5mm (W) $\times$ 8mm (H). Prepared mandibles (see methods 2.2.2) were first clamped with an insect pin holder, which was then attached to a 3D micromanipulator (MM 33, Märzhäuser Wetzlar, Germany), positioned such that the apical tooth of the mandible was roughly perpendicular to the substrate, and just about extended over the sheet edge; mandible orientation was aided and verified with a custom-built top-down microscope. Previous work confirmed that the cutting force does not significantly vary between repeated mounts of the same sample, i. e., that this mounting procedure is repeatable [55]. Once substrate and mandible were aligned, the substrate was moved upwards against the mandible to initiate cutting. The stage movement proceeded at a speed of 0.3mm s^{-1} for 5mm during each trial, sufficient to initiate the cut and to achieve steady state cut propagation, as indicated by an approximately constant force reading (Figure 2.1D). The stage movement speed was chosen to be comparable to the cutting speed of larger foragers [55, 137, 143]. Cutting forces vary with motor stage speed, but this effect is small and thus not further evaluated here: an increase in cutting speed by a factor of three increases cutting forces by only about 20% [55, 203].

Each measurement consisted of two passes. The first pass was used to determine the total cutting force (F_c); the second pass through the now cut sheet was used to determine the contribution from spacing forces (F_s) due to elastic sheet deformation and sidewall friction (Figure 2.1D) [55, 204–206].

In all experiments, measurements were considered invalid and thus repeated if one of the following occurred: (i) contact between the head capsule/epoxy and the cutting substrates; (ii) failure of the epoxy fixation at the joint; (iii) damage/destruction of the mandible; (iv) the steady-state region was too short to extract a meaningful cutting force (less than 2 mm cutting length). In total, I conducted n = 390 cutting force measurements with mandibles: 30 mandibles for three natural substrates with three repeats and for four synthetic substrates with no repeats. Additionally, n = 65 control measurements with scalpel blades were completed; one measurement on synthetic substrates, and three repeats on natural leaves as outlined above.

2.2.6 Mandible "sharpness" measurements

To assess mandible sharpness, the radius and wedge angle of the mandibles cutting edge were measured using focused ion beam (FIB) milling and scanning electron microscopy (SEM) [21, 207, 208]. Six callow mandibles were selected from the dissected right head capsule halves (see methods 2.2.2) such that they spanned the forager size range and were distributed evenly in mass on log-log space. Additionally, one scalpel blade was imaged.

Mandibles were fixed onto atomic force microscopy (AFM) sample holders under a stereomicroscope using Everbuild high viscosity superglue (Sika, Baar, Switzerland). They were positioned at the edge of the AFM stub to prevent collisions with the FIB column and oriented such that the dorsal side of the mandible faced upwards and the mandible teeth were facing the edge of the stub. The samples were then sputter coated with 40 nm of chromium (Q150Tplus, Quorum, Sussex, UK).

To obtain a suitable section of the cutting edge, FIB milling was conducted using a Zeiss Auriga FIB-SEM at 30 KV acceleration voltage and 240 pA current. The voltage was fixed to reduce damage to the samples; the current was optimised via trial and error to obtain clean sections. A total of 12 trapezoidal cuts were milled on the second tooth of each mandible, counted from distal; six cuts were made on each edge (Figure 2.1E), distributed from the base to the tip of the tooth (Figure 2.1E). Of these six cuts, one was taken in the bottom 20% of the tooth height; the rest were distributed amongst the top 80%; the cuts were thus symmetric in their distribution from each edge, but not evenly distributed in height. All cuts were oriented such that the exposed section was roughly perpendicular to the cutting edge (Figure 2.1E). SEM imaging was conducted on the same machine at an acceleration voltage of 3 KV. Images of the exposed cross section were taken with the parallel sides of each milled cut horizontal in FIB view, such that an equivalent planar view was ensured across all milled areas.

Subsequent analysis was conducted in ImageJ cutting edge radius was measured as the radius of the smallest fitted circle wedge angle with wedge angle also measured at this point (Figure 2.1E) (see [209] for similar measurement methods).

2.2.7 Data curation and analysis

Raw data obtained from the fibre optic sensor (.txt file) was converted to a force time graph, for which F_c and F_s were extracted for a 2 mm steady state region after the initial peak (Figure 2.1D). Fracture force (F_f) was determined by removing the contribution of F_s from the F_c:

$$F_f = F_c - F_s \tag{2.5}$$

Cutting force measurements conducted on biological substrates were corrected $F_{c,c}$ for lamina thickness (t_1):

$$F_c = \frac{F_{c,c}\bar{t_1}}{t_1} \tag{2.6}$$

where $\bar{t_1}$ is corrected laminar thickness obtained by dividing sample thickness with average thickness [55]. Extraction of the average total cutting and spacing forces from raw data, calculation of fracture forces, and cutting force correction on biological substrates were conducted in Python (v. 3.9.7).

The relationship and interaction between worker body mass, pseudoleaf type, substrate thickness, and mandible group were analysed via a repeated measures analysis of covariance (RM ANCOVA). A nested RM ANCOVA was used to assess the relationship between worker body mass, mandible group and leaf type. Type II sum of squares permitted us to accurately assess main effects in the presence of possible interactions [210]. Log-transformed measured force (F_c, F_f, or F_s) was the continuous response variable, and body mass (continuous, log-transformed), group (categorical), mixing ratio (categorical), and thickness (categorical) or body mass (continuous, log-transformed), plant type (categorical) and group (categorical) were the predictor variables for pseudoleaves and plant tissues, respectively. Sample (Mandible ID) was included as a random effect to account for repeated measures across substrates in pseudoleaves; for measurements in plant tissues, sample (mandible ID) was treated as a nested random factor in a nested RM ANCOVA model to account for within substrate repeats. We verified that RM ANCOVA assumptions, including normality of residuals (Shapiro-Wilk test), sphericity and homoscedasticity (Mauchly's test, visual inspection) were met.

Ordinary least squares (OLS) regressions on $\log_{10}$-transformed data were performed to characterise scaling relationships between response variables and body mass. The assumptions of the linear model were verified as outlined above. Values stated in text and tables are mean ± standard deviation unless stated otherwise; boxplots presented show median and upper and lower quantiles. All statistical tests in this chapter and those that follow were performed with a significance threshold of $\alpha = 0.05$, as is the standard practice. All statistical analysis, data curation and plotting was conducted in R (v. 4.1.1).

2.3 Results

2.3.1 PDMS pseudoleaves

Substrate thickness affects force, independent of material or mandible length scale

F_c increased significantly with pseudoleaf thickness (RM ANCOVA: $F_{1,26}$ = 341.32, p < 0.001), an effect with no significant interaction with worker body mass, pseudoleaf type (4:1 vs 10:1) and mandible group (callow vs forager) (see Appendix A for full statistical analysis). F_c was directly proportional to pseudoleaf thickness for both mandible groups (see Appendix A and Figure 2.2A), but differed significantly between them (RM ANCOVA: $F_{1,26}$ = 386.6, p < 0.001). Forager mandibles, required about twice the cutting force of pristine mandibles for all pseudoleaf types, independent of worker body mass (Figure 2.2A). A forager thus cuts a 200 µm pseudoleaf with about the same force as a pristine mandible cuts a 400 µm pseudoleaf for each pseudoleaf type.

F_s accounted for up to 12% and 22% of the total cutting forces for thin and thick pseudoleaves, respectively. These values differ, for spacing forces did depend significantly on pseudoleaf thickness (RM ANCOVA, thickness: $F_{1,26}$ = 11.9, p = 0.001: they were 4 ± 2 mN and 16 ± 12 mN for 200 μm and 400 μm pseudoleaves respectively (Figure 2.2). F_f mirrored the results of total cutting forces, and increased significantly with pseudoleaf thickness (RM ANCOVA: $F_{1,26}$ = 306.2, p < 0.001), but again showed no significant interaction with worker body mass, pseudoleaf type, and mandible group (see Appendix A for detailed statistics).

F_c observed for scalpel blades always considerably exceeded the forces measured with callow and forager mandibles, by as much as a factor of 4 and 2, respectively, in the starkest cases. F_s indeed also differed significantly from both mandible groups being on average 13 ± 6 mN and 35 ± 20 mN for 200 μm and 400 μm pseudoleaves, respectively. Although the contribution of spacing forces (F_s) for scalpels was lower than each mandible group, contributing 10% and 13% for thin and thick films, respectively.

To test statistically whether the results indeed reflect solely an effect of thickness, I divided F_c and F_f of each sample by each test specimens' average thickness, and then compared the thickness corrected forces. A RM ANCOVA revealed an no significant difference between thickness corrected forces for 200 μm and 400 μm films (RM ANCOVA: F_c: $F_{1,26}$ = 0.455, p = 0.51, F_f: $F_{1,26}$ = 0.117, p = 0.74). However, the thickness corrected force still depended significantly on mandible group and pseudoleaf type (RM ANCOVA: mandible group F_c: $F_{1,26}$ = 138.26, p < 0.001, mandible group F_f: $F_{1,26}$ = 133.1, p < 0.001, pseudoleaf type F_c: $F_{1,26}$ = 192.82, p < 0.001, pseudoleaf type F_f: $F_{1,26}$ = 240.67, p < 0.001), and remained mass independent (See Appendix A for full statistical analysis).

In order to place the magnitude of the cutting force into perspective, an approximate theoretical prediction may be derived via a simple virtual work argument. The minimal steady-state cutting force then follows as:

$$F_f = G_c \cdot h \tag{2.7}$$

Where G_c is the tearing energy of PDMS calculated via pure shear testing (see methods) and h is the thickness of the cutting test specimen. Because these are experimental quantities associated with an error, the bounds of the theoretical minimum fracture force were calculated as propagated uncertainty following [211]. Fracture forces of callow mandibles consistently fall within the theoretical minimum bands for all substrates and thicknesses, indicating that they are ideally sharp (Figure 2.2).

Material length scale and its effect on cutting force scaling

When considering material length scale and its contribution to the scaling of cutting forces the key parameter is pseudoleaf type - with Young's modulus, UTS and tearing energy differing for the two pseudoleaf types (See methods 2.2.3 for full rationale and Table 2.1 for material characterisation).

F_c depended significantly on pseudoleaf type (RM ANCOVA: $F_{1,26} = 157.03$, $p < 0.001$), with a factor of two increase in toughness corresponding to a proportional increase in force between 4:1 and 10:1 leaves, respectively. Meaning for the same mandible group, it would take roughly the same force to cut a 400 μm 4:1 film and a 200 μm 10:1 film (see discussion for elaboration). There was no significant main effect of worker body mass on F_c meaning that mandibular cutting forces regardless of group, pseudoleaf type and thickness were independent of worker body mass. However there were statistically significant interaction terms for F_c which need to be considered. There was a significant interaction between pseudoleaf type and worker body mass (SI). Meaning that although F_c were independent of worker body mass the contribution of mass to cutting force did differ across the two pseudoleaf type. This significant interaction should be interpreted with caution, as F_f were also significantly dependent on pseudoleaf curing condition (RM ANCOVA: Pseudoleaf type $F_{1,26} = 181.5$, $p < 0.001$), and showed no significant interaction independent of substrate thickness, they did not co-vary with worker mass (see SI for full statistical analysis). F_f thus were independent of worker mass regardless of the substrate that was cut. Despite the main effect of worker body mass being statistically insignificant there were visual trends. For callows, F_c showed a small but statistically insignificant trend to increase with body mass for 4:1 pseudoleaves, but was almost perfectly size-invariant for 10:1 pseudoleaves. For forager mandibles, in turn, F_c were approximately constant with respect to worker body mass on 400 μm 4:1 pseudoleaves, but showed an insignificant trend to decrease with size on 200 μm 4:1 and all 10:1 pseudoleaves (Figure 2.2B). F_s again showed no significant main effect of body mass.

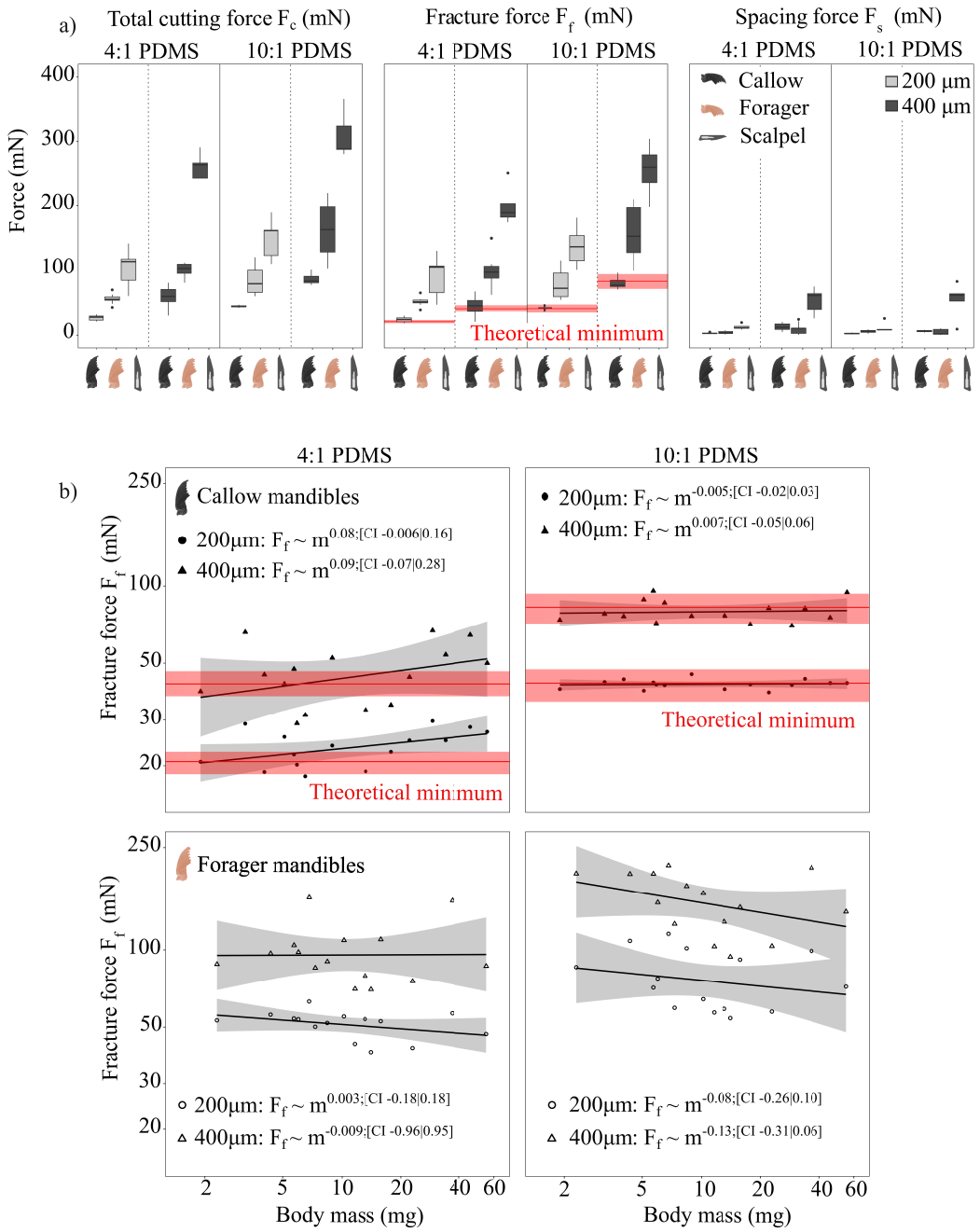


FIGURE 2.2: To investigate the relationship between mandibular cutting forces and factors such as body mass, wear state, substrate thickness, and pseudoleaf type, I measured total cutting, fracture, and spacing forces in two groups: callows (1.9-55.5 mg, n=15) with pristine mandibles and foragers (2.3-54.8 mg, n=15) with varying states of wear. Measurements were conducted on four synthetic substrates: 200 µm 4:1 PDMS, 400 µm 4:1 PDMS, 200 µm 10:1 PDMS, and 400 µm 10:1 PDMS. **(A)** Total cutting (F_c) and fracture forces (F_f) varied significantly with mandible group, thickness, and pseudoleaf type. On average, total cutting and fracture forces of callow mandibles were about half those of forager mandibles. A twofold increase in thickness corresponded to a proportional increase in force for both pseudoleaf types and mandible groups. Additionally, forces nearly doubled between 4:1 and 10:1 pseudoleaf types. Scalpel blade forces were consistently larger than those of both mandible groups. All boxplots display the median (centre line), the first and third quartiles (hinges), extended by 1.5 times the interquartile range (whiskers), and outliers (points) **(B)** All forces (F_c, F_f, F_s) were found to be independent of worker body mass, indicating size invariance. Although not statistically significant, there was a visible trend of forces increasing with body mass for callows and decreasing with body mass for foragers.

2.3.2 Biological substrates

Measurements were conducted across three biological substrates: Rose petals, bramble and laurel leaf laminas. To separate the influence of material properties and material thickness, the forces were re-scaled to the average leaf thickness (see methods).

F_c depended significantly on mandible group (RM ANCOVA (F_c): $F_{1,26}$= 43.51, p < 0.01), decreasing by a factor of about two between foragers (68 ± 20 mN) and callows (34 ± 11 mN) for rose petals, mirroring the results for synthetic substrates. However, this difference was smaller for bramble and laurel leaf laminas, and amounted to factors 1.6 and 1.3 respectively (Figure 2.3A) and Table 3) with F_c varying significantly with plant type (RM ANCOVA (F_c): $F_{1,26}$ = 404.7, p < 0.01). F_f also depended significantly on mandible group and plant type (RM ANCOVA mandible group F_f : $F_{1,26}$ = 40.34, p < 0.001, plant type F_f: $F_{1,26}$ = 125.5 p < 0.001), essentially mirroring the increases found in F_c. Within callow mandibles F_f ranged from a minimum of 31 ± 11 mN in rose petals to 46 ± 11 mN in bramble and a maximum of 78 ± 24 mN in laurel. A factor of 2.5 increase in force from rose petals to laurel. F_s did not differ significantly with mandible type, but varied across plant materials (RM ANCOVA (F_s) plant type: $F_{1,26}$ = 22.03, p < 0.001) although the absolute value of F_s differed the relative contribution of F_s across plant type remained relatively constant ranging from 9 to 14% across all plants and mandible groups. Scalpel blades again required significantly higher F_c than both callow and forager mandibles, respectively. With the largest observed difference being almost an increase of a factor of four, this trend was also observed in F_f. Scalpel F_s were consistently higher than those of mandibles, most prevalent in bramble and laurel, with observed differences being as large as an increase of a factor of 6.2 and 3, respectively.

None of the measured forces, (F_c), (F_f), (F_s), varied significantly with worker body mass and therefore mandible size (RM ANCOVA body mass: F_c, $F_{1,26}$ = 0.77, p = 0.39, F_f, $F_{1,26}$ = 0.34, p = 0.57, F_s, $F_{1,88}$ = 0.1, p = 0.8) (Figure 2.3B). The nested RM ANCOVA also failed to identify any significant two-way interactions between mandible group, plant and worker body mass nor any significant three-way interactions for both F_c and F_f. Despite no significant effect of worker body mass, the visible trends in rose petals mirrored those observed in the synthetic substrates. Where in synthetic substrates, there was a weak but insignificant trend for forces to increase with size for callow mandibles and decrease with size for foragers; the same can be observed in the rose petal mass scaling coefficients (Callows: $F_c \propto m^{0.15}$, $F_c \propto m^{0.12}$ Foragers: $F_c \propto m^{-0.02}$ $F_f \propto m^{0.0009}$). Visual trends with size in bramble and laurel did follow the same pattern but were more subtle with bramble being almost perfectly independent of body mass for callow mandibles. Despite an insignificant main interaction of mass on F_s, F_s did show a significant interaction between mass and plant (RM ANCOVA: Mass*Plant $F_{1,26}$ = 4.67, p = 0.008) meaning there was a different scaling relationship of the fracture forces between plants.

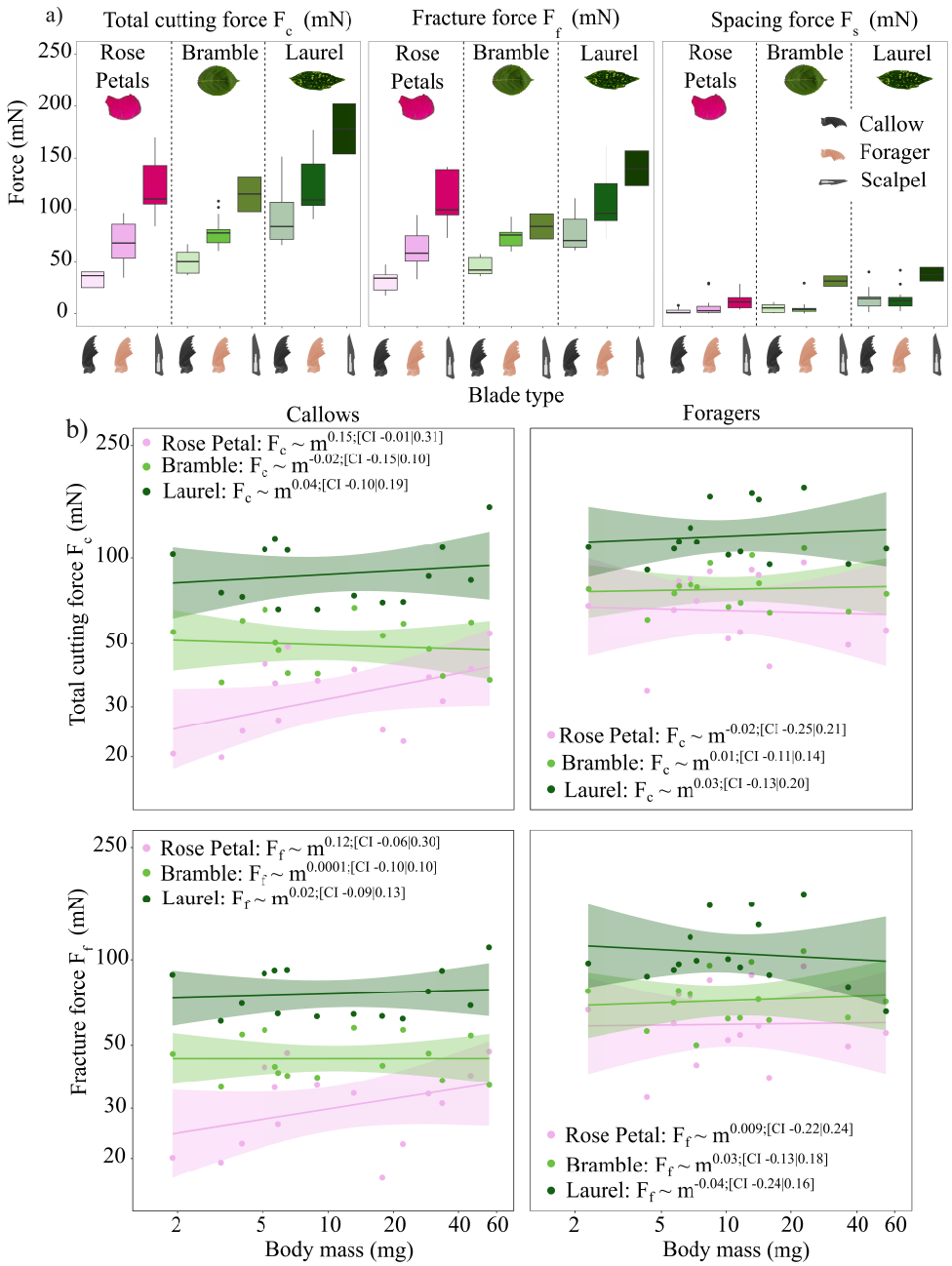


FIGURE 2.3: Total cutting (F_c), fracture (F_f), and spacing forces (F_s) were measured on three biological substrates: rose petals, and bramble and laurel leaf laminas. Forces were re-scaled to average leaf thickness. **(A)** Total cutting forces (F_c) depended significantly on mandible group and plant type, decreasing by about half from foragers (68 ± 20 mN) to callows (34 ± 11 mN) for rose petals, with smaller differences for bramble and laurel leaves. Fracture forces (F_f) showed similar patterns, ranging from 31 ± 11 mN in rose petals to 78 ± 24 mN in laurel. Spacing forces (F_s) did not vary significantly with mandible type but did vary across plant materials, contributing consistently 9-14% of total forces. Scalpel blades required significantly higher forces than mandibles, with the largest differences observed in bramble and laurel. **(B)** All forces (F_c, F_f, F_s) were independent of worker body mass, showing no significant variation with mandible size. However, visible trends suggested forces increased with body mass for callows and decreased for foragers in rose petals, with subtler patterns in bramble and laurel. Spacing forces showed a significant interaction between mass and plant type.

2.3.3 Mandible cutting edge radii are size invariant

A RM ANCOVA revealed a significant effect of mandible size (mass) on combined cutting edge radius for both callow and forager mandibles (RM ANCOVA: mass $F_{1,52}$ = 5.42, p = 0.02). However post hoc univariate ANOVAs revealed that callow mandible radii were not significantly dependant on mass (ANOVA: $F_{1,52}$ = 4.01, p = 0.09), forager mandible cutting edge radii were however mass dependant (ANOVA: $F_{1,52}$ = 15.01, p < 0.01). Across all mandible groups, tooth location had no significant effect on cutting edge radius (ANCOVA: location $F_{1,52}$ = 2.32 p = 0.08). Values were hence pooled, to determine the average cutting-edge radius for pristine mandibles as R_c = 162 $\pm$ 120 nm (Figure 2.4a). Forager mandible cutting edge radius R_f decreased significantly with worker body mass ($R_\mathrm{f} \propto m^{-0.87}$), dropping by almost one order of magnitude): smaller workers appear to have more worn mandibles (Figure 2.4b). The pooled average cutting-edge radius for forager mandibles was R_f = 2530 $\pm$ 3300 nm. From the most worn forager mandible to the smallest pristine cutting-edge radius, there was 200-fold decrease in cutting edge radius (Appendix A).

The cutting edge radius of scalpel blades was R_s = 115 $\pm$ 15 nm, comparable to that of callow mandibles.

The wedge angle of the mandible cutting edge did not vary significantly with worker body mass and tooth location (ANCOVA mass: $F_{1,46} = 2.55, p = 0.12$; ANCOVA location: $F_{1,46} = 0.74, p = 0.60$). It did, however, depend significantly on mandible group (ANCOVA mandible group: $F_{1,46} = 13.4, p < 0.01$). On average, the cutting edge wedge angle was $77 \pm 15^\circ$ and $93 \pm 9^\circ$ for callow and forager mandibles, respectively (Figure 2.4a)—a factor of two to three lower than for scalpel blades ($30 \pm 3^\circ$) (Appendix A).

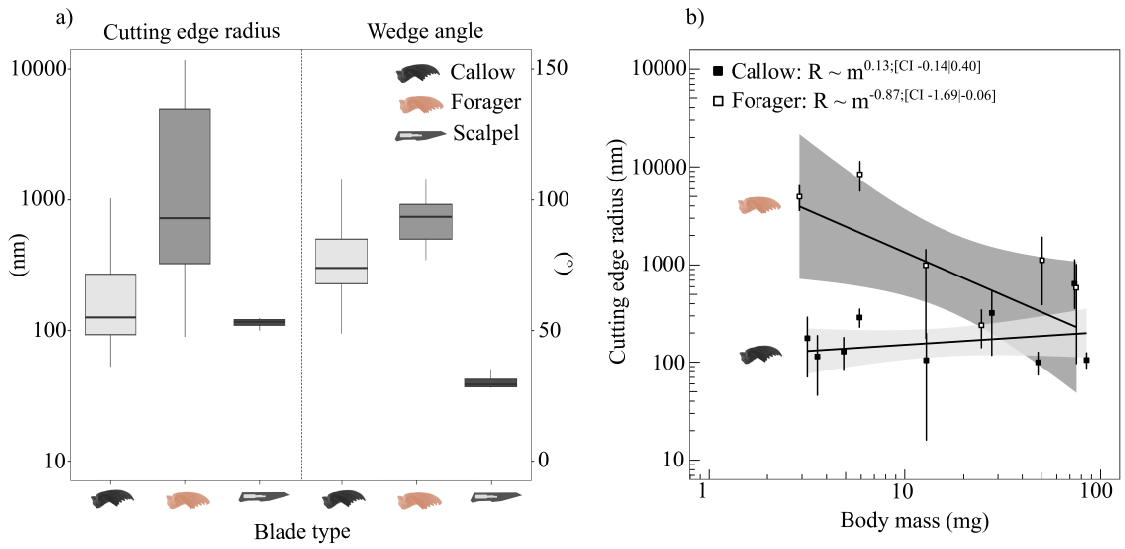


FIGURE 2.4: In order to assess the contributions of mandible geometry to cutting forces, we measured the cutting edge radius R and wedge angle of pristine and forager mandibles; scalpel blades served as reference (n=8, n=6 and n=1 respectively). **a)** Cutting edge radius varied significantly with mandible wear state—in the most extreme case, it differed by a factor of more than 200 (note the logarithmic y-axis on the left). The average cutting edge radii were R_c = 162 ± 120 nm, R_f = 2530 ± 3300 nm, and R_s = 115 ± 15 nm for pristine mandibles, forager mandibles, and scalpel blades, respectively. Pristine mandibles were thus about as sharp as scalpel blades. The wedge angle varied minimally but significantly between callow and forager mandibles and was substantially higher than for scalpel blades. Boxplots display the median (centre line), the first and third quartiles (hinges), extended by 1.5 times the interquartile range (whiskers). **b)** Callow cutting edge radii showed an insignificant trend to increase with worker size ($R_c \propto m^{0.13}$). In contrast, forager mandible cutting edge radii decreased significantly with mass ($R_f \propto m^{-0.87}$), suggesting that larger workers have less worn mandibles.

2.4 Discussion

Insects and plants have co-existed for over 350 million years [18]. The perhaps most consequential of their interactions is that many insects feed on plants [148]. So ubiquitous is this interaction that virtually every plant species is predated on by at least one insect species [212], leading to an ongoing and widespread evolutionary arms race in which specialised feeding "tools" evolved in insects, and specialised defence strategies evolved in plants. Much attention has been paid to chemical deterrents to herbivory [213–216], but only a much smaller number of studies discussed mechanical defences [for reviews, see 62, 80, 158, 217–220], and the fundamental mechanical and morphological pressures on the insect feeding apparatus remain less understood still [76, 78, 89–91, 139, 168, 221–225]. To learn more about some of the mechanical components of this ancient contest, I set out to test a simple physical model that relates the cutting force to the structural and mechanical properties of the cut material, and the geometry of the cutting tool. Because leaves are complex and inhomogeneous composite materials, I initially tested the model with homogenous pseudoleaves made from elastomers, handing us control over the relevant structural and mechanical properties; and because mandibles come in many complex shapes [e. g. 226], introducing variation that is difficult to account for, I used mandibles from leaf-cutter ant foragers as a model for blades that differ in size, but not in

shape [142]. In the following discussion, I inspect the evidence in support of and against the simple model, evaluate the extent to which it can be applied to more complex plant tissues, and then leverage these results to pinpoint strategies to make plant cutting as hard or as easy as possible, respectively.

2.4.1 The biomechanics of leaf cutting

Breaking up plant tissue involves the creation of new surface area; it may thus be conceptualised as a fracture process. Combining a simple virtual work argument with dimensional considerations yields a first-order prediction of the steady-state force required to blade-cut thin leaves [see 2.1 and 91, 167, 227, 228]:

$$F_f = G_c t + C\sigma_c R t \tag{2.8}$$

Here, the first term depends on the structural and mechanical properties of the cut material only, while the second term combines contributions from both cut material and cutting tool. This simple model thus, at once, identifies two relevant regimes, separated by the magnitude of the dimensionless group $\Omega = C\sigma_c R G_c^{-1}$ [91, 167]. For $\Omega << 1$, $F_f \approx G_c t$—the steady-state fracture force is unaffected by blade geometry, and determined solely by the properties of the cut material. Empirically, this scenario appears to apply to pristine mandibles [see also 91], for which fracture forces were statistically indistinguishable from this prediction, independent of whether pseudoleaf thickness, toughness, or both were varied (Figure 2.2). The fracture force corresponded to about 90% of the total cutting forces in all trials, indicating further that contributions from other energy sinks, subsumed in the spacing forces, are small enough to be neglected; these results justify the omission of other energy terms in the cutting energy balance *a posteriori*. Thus, all else being equal, the cutting forces for pristine mandibles are dominantly defined by pseudoleaf thickness and toughness. If Ω is comparable or much larger than unity, blade geometry comes into play [56, 91, 167, 227]. Three experimental treatments were implemented to manipulate the magnitude of Ω, and to thus probe the validity of the model: a variation in mixing ratio and curing conditions for the pseudoleaves, which altered the characteristic material length scale by about a factor of 2 (Table 2.1); a pristine mandible and forager mandible group, distinguished by a different likelihood of mandibular wear [91, 139]; and a variation in mandible size, realised by using mandibles from foragers that differed by more than two orders of magnitude in body mass. Empirically, it would appear that Ω is close to unity for both forager mandibles and scalpel blades, for their fracture forces were consistently and significantly higher than the lower bound (Figure 2.2). Two further observations are superficially consistent with this physical interpretation: the disparity between pristine, forager and scalpel blade fracture forces was independent of pseudoleaf thickness (Figure 2.2); and the disparity between pristine and forager mandibles was less pronounced for 10:1 than for 4:1 pseudoleaves, presumably because the larger material length scale of 10:1 pseudoleaves masked the effects of geometric differences (Figure 2.2). To render this qualitative discussion quantitative, I note that the fracture forces of pristine mandibles are within the uncertainty of the lower bound estimate $F_f = G_c t$ if $\Omega < 0.05$; and the results for forager mandibles demand $\Omega \approx 1$. A closer assessment of the quantities R, σ_C, and C is in order. R represents a characteristic length scale of the cutting tool. For a simple geometry such as a wire, the

choice is obvious, for there is only one length scale [167, 227, 229]. But for a more complex geometry such as an insect mandible, the case is much less clear cut . Using FIB milling, I measured the radius of the mandible cutting edge—not the only, but perhaps the most obvious choice for R. In contradiction with the parsimonious hypothesis of geometric similarity, $R \propto m^{1/3}$, R took a size-invariant mean value of 162 nm for pristine mandibles, and of about 3µm for forager mandibles (Figure 2.4). σ_c is a quantity of dimension force per area, and for PDMS pseudoleaves, $\sigma_c \approx 6$ MPa (see 2.1 Table 2.1). C is a dimensionless constant of order unity [56, 91, 167, 227, 230], which generally depends on the shape of the contact between blade and crack tip, the friction coefficient, and the strain stiffening characteristics of the cut material [56, 91, 167, 227, 230]. I follow Püffel et al. [91] and assume $C \approx 2$, so that $\Omega \approx 0.02 - 0.009$ for pristine, and $\Omega \approx 0.2 - 0.6$ for forager mandibles. Given the simplicity of the model, this order-of-magnitude agreement between prediction and observation is encouraging; but some uncertainty of course remains. For example, a weak trend for an increase of fracture force with mandible size persists in pristine mandibles. Two explanations may be put forward to account for this increase. First, it is possible that the technically challenging radius measurements carry so much uncertainty that they failed to uncover a true underlying scaling. Second, the tip radius may not be the relevant length scale [21, 205, 207, 208, 231]. It is clear that the mandibles of larger ants are, in fact, larger; so perhaps a different characteristic dimension comes into play, and is responsible for the small increase in fracture force with size. Further research is required to sharpen our understanding of the interaction between mandible geometry and material length scale.

2.4.2 From pseudoleaves to leaves

Having evaluated the predictive power of the simple model for a well-defined model material, we next turn to the more complex case of cutting heterogeneous plant materials. Do the same major physical effects dominate the cutting process? Two major difficulties stand in the way of answering this question: to obtain independent measures of G_c; and to determine the appropriate choice for σ_c. It has long been recognised that cutting tests—in form of a guillotine [206], shearing blades [67], scissors [232], or a single razorblade [161]—may well yield the best estimate for the fracture toughness of leaves, for they restrict failure to small regions close to the blade edge, so that extrinsic toughening mechanisms are circumvented [217–219, 232]. Traditional fracture assays, such as notched tensile tests and pure shear tests, will instead often return elevated toughness estimates, for they permit the crack to interact with material architecture, and so result in crack arresting, crack deflection, or crack bridging. Consistent with this expectation, laurel leaf lamina toughness estimated via pure shear tests was almost a factor of two larger than the estimate from cutting tests ($G_c = 746 \pm 210\,\mathrm{J\,m^{-2}}$ vs. $G_c = F_f t^{-1} = 223 \pm 70\,\mathrm{J\,m^{-2}}$, respectively) (Figure 2.3). This stands in contrast to experiments with pseudoleaves, where the two independent estimates were in excellent agreement. Physically, the fracture force cannot be lower than $F_f \leq G_c t$, which at once suggests that, even for relatively homogeneous laurel leaf laminas, tests that involve free running cracks do not provide reliable leaf fracture toughness estimates. Although extrinsic toughening mechanisms are not well-studied in plant leaves [e. g. 184, 217, 233], it appears they may be potent. A disparity

between toughness estimates from tensile and cutting tests is not universal for plant tissues: Vincent [217] reported a robust agreement for approximately isotropic parenchyma; in other cases still, notch tests yielded lower toughness estimates than cutting assays [184]. Intriguingly, leaf toughness estimated via cutting force data from forager mandibles appear to be in closer agreement with estimates from pure shear tests ($G_c = 746 \pm 210\,\mathrm{J\,m^{-2}}$ vs. $G_c = F_f t^{-1} = 580 \pm 180\,\mathrm{J\,m^{-2}}$, respectively) (Figure 2.3) —the effect of a blunt blade can evidently be just as large as the effect of extrinsic toughening arising from the deflection of free running cracks. The importance of blade sharpness is well recognised, but the associated discussion in the plant literature typically remains on qualitative terms [e. g. 161, 234]. Scissors used in previous work had edge radii of about 2-3 μm Choong [160], Lucas [184], Lucas and Pereira [232], and Lucas [235], comparable to those of forager mandibles. It is therefore plausible that the toughness estimates thus obtained were inflated, too. More recent work has sought to circumvent this problem by using razorblades, with smaller cutting edge radii [about 300 nm 161]. At what point is a blade sharp enough? The model studied in this work may be simple, but it has the advantage that it provides an explicit connection between blade geometry and cutting force, so permitting evaluation of conditions upon which blade geometry may be neglected altogether. For thin sheet cutting, I have recently argued that a cutting tool is ideally sharp if and if only $\Omega << 1$ [91]—making it sharper still will not result in a further noticeable decrease in the cutting force. This condition can be used to determine a critical radius below which a tool may be considered sharp, with the principal difficulty hidden in the non-trivial definition of the characteristic stress σ_c: depending on the material and the fracture process, σ_c may be a yield or failure stress [91, 227], a shear stress [167], an elastic modulus [56, 236], or the critical strain energy density [167, 236]. Using a large dataset to estimate the properties of the median tropical leaf [35] provides $\sigma_c = 3\mathrm{N\,mm^{-2}}$ and $G_c = 0.4\,\mathrm{N\,mm^{-1}}$, so that $\Omega \approx 23(0.4)^{-1} R\,\mathrm{mm}$; a blade with a radius $R < 10$ μm would thus return a toughness estimate within 5% of the true value. However, this calculation assumes that the tensile strength is an appropriate proxy for σ_c, and, more crucially, that the toughness data itself, measured dominantly via scissor cutting, was not inflated by the use of blunt blades. Both may well be incorrect. More detailed experiments are required to determine the appropriate choice for σ_c for leaf laminae; a suitable route are cutting measurements with wires of variable radii [229], combined with more detailed leaf material characterisation via tensile tests.

2.4.3 Mechanical strategies of an evolutionary arms race

There is a significant body of work seeking to determine the mechanical and structural traits of plants most effective at herbivore deterrence [e. g. 57, 62, 67, 158, 219]. Disentangling the effect of leaf structural and material properties on insect herbivores generally remains challenging, because they often appear to be cross-correlated [57, 67]. Although some leaf traits are more strongly correlated with herbivore deterrence than others [57, 67], a one-fits-all condition appears unlikely, and the relevant traits likely depend on animal size and feeding guild [57, 67, 232]. In fact, the existing evidence is so noisy that the leaf area density, $\zeta = m/A$ (sometimes also called leaf specific mass),

may often be about as good a predictor as any other mechanical or structural trait, but with the distinct advantage that it is easy, cheap and fast to measure [158]. ζ is a combined trait—it depends on both leaf thickness (t), a structural trait, and leaf density (ρ), a material property, $\zeta = \rho t$ [66]. In line with this observation, the cutting force model, put forward in this work, predicts that minimum cutting force is determined by the product between a structural and a material property: leaf thickness and toughness, respectively. Leaf toughness is likely strongly correlated with leaf density, for it is approximately proportional to the relative volume fraction of the composite cell wall, and thus the crude fibre content [62, 76, 237]. Leaf area density may thus well be a good proxy for cutting force, $F_f \approx \zeta$. But is increasing the cutting force via toughening or thickening equivalent in its deterrent effect [219]? Increasing the cutting force through changes in thickness vs toughness appears *mechanically* equivalent. However, there are good reasons to argue that this mechanical equivalence will not readily translate into equivalence of deterrence. Leaf thickness generally depends on the number of layers and length of palisade cells, the placements of veins, and the width of the mesophyll, epidermis, hypodermis and indumentum [66]. Thus, doubling the thickness may double the required cutting force, but it will likely also double the material gained per cut length—the net deterrent effect, then, may well be zero [larger leaf fragments may still be harder to digest, and so require more chewing, or may delay nutrient assimilation 76, 80]. Increasing leaf lamina toughness by increasing the volume fraction of the usually indigestible cell wall, in turn, would make cutting more energetically challenging and less rewarding both. From the perspective of the plant, increasing ζ via a high density and thus toughness may be preferable to an increase due to lamina thickness; and from the perspective of the insect, "sensing" toughness as opposed to absolute cutting force requirements may be advantageous. So can they? I am not aware of any evidence in support or defiance. Tough leaves are often described as scleromorphic [237, 238]. Although there is no universally agreed definition of scleromorphy, qualitative ranks provided by botanist are strongly correlated [238], suggesting that humans generally sense similar traits—but it is unclear which traits exactly. A possible experimental approach to this problem may be to observe herbivore feeding preferences on leaves with different magnitudes of Loveless's sclerophylly index [LSI, the ratio of crude fibre to crude protein, or the ratio of cell wall to cell content 237], which provides a measure of dilution of nutrients by the cell wall [238], and correlates well with fracture toughness measured via scissor tests [237]. Of course, scleromorphic features have evolved for reasons other than herbivore deterrence, including resistance to wilting, water and nutrient conservation, to enhance longevity, or to ensure efficient photosynthesis [158, 160]. Where leaf thickness or toughness are otherwise constrained, a suitable, and perhaps more effective, deterrent may then be to render cutting costly by inducing wear. In mammalian teeth, mild wear is sometimes seen as essential for tooth function [163, 239], but in insects, it can lead to reduced development and increased mortality rates, shifts in task-preferences, and even induce responses in mandible morphology and relative head size [139, 171, 221, 240–244]. So strong is the assumed impact of wear that some have speculated that frequent moulting may be a counter adaptation [245, 246]. Consistent with earlier work by Schofield et al. [139], my data shows that the effect of wear on leaf-cutting force can be substantial: it can cause an elevation over the minimum force by up to

a factor five (Figure 2.2). To achieve the same increase through a change in thickness would require substantially elevated material investment; and realising it through an increase in toughness may result in dysfunctional leaves made up dominantly by cell wall and crude fibre. The key question, then, is how plant leaves can go about rapidly inducing wear, and how insects should best avoid it. Two well-known strategies include the incorporation of exogenous grit or silica phytoliths in plants [80], or of transition metals in insect mandibles [88, 170, 247]. However, direct evidence for a positive or negative effect on wear rate is rare [247], and often ambiguous if not conflicting [e. g. 171, 241, 244, 248]. Understanding the biomechanics of mandibular wear both from the perspective of the plants and of the insects is a priority area for future work.

2.5 Conclusions and outlook

The efficacy of insect herbivory and plant mechanical defences is modulated by many factors. Within this study I utilised a simple mechanical model as a guide to test predictions on how thickness, toughness and cutting edge radius effect cutting force. When the cutting edge radius is sufficiently sharp, cutting forces are dominantly defined by substrate thickness and toughness equally. With an increase in either factor leading to a proportional change in cutting force. However, when tools are worn, cutting forces can increase to up to 5 times the theoretical minimum value.

Given that mandibular wear is found to be a dominating factor in the modulation of insect herbivory, a natural extension to this work would be to systematically assess the factors that modulate wear from both an insect's, and plant's, perspective. Nanoindentation provides insight into the material properties of mandibles showing that some insect species are more wear resistant than others [170] and may therefore be more effective herbivores. Previous studies have shown the deposition of silica within leaves significantly affects herbivore efficacy [249]. Perhaps most beneficial to the field would be a unifying study where wear-inducing structures within plants (silica depositions as one example) are systematically varied and the effects of wear and cutting force quantified. Before the addition of further experimental assays, I hope this study provides a foundation to asses the modulating factors of herbivory.

3 The Metabolic Cost of Cutting

I acknowledge the contribution of Dr. Fabian Plum who helped design the cutting respirometry chamber.

Summary

Cutting leaves is the second most metabolically costly activity ever measured in insects and is a core component of leaf-cutter ant foraging behaviour. Given its ecological importance, the determinants and variability of cutting energetics remain underexplored, with only one study that looked at costs for one material type only. To address this gap, I here measure the metabolic expenditure of ants of varying body size that cut metabolically inert pseduoleaves with different mechanical properties. The cutting metabolic rate (CMR) increases substantially with worker size (CMR $\propto m^{0.84}$), but appears unaffected by the different mechanical demands associated with cutting pseudoleaves of different toughness. Increasing the mechanical demands does however affect the speed at which workers cut fragments, which also increases with size but not as starkly ($v_c \propto m^{0.53}$). The diverging scaling of mechanical and metabolic power lead to a non-monotonous variation of mechanical efficiency with worker size, suggesting the existence of an optimal worker size that depends on leaf structural and mechanical properties.

3.1 Introduction

Attine leaf-cutter ants have a significant impact on most habitats in the Neotropics [134]. Through their prolific foraging behaviour, they shape their environment, affecting the distribution of nutrients in the soil, local fauna, and, most notably, flora [69, 70, 140]. During foraging, workers traverse hundreds of metres along well-established trails to reach food sources such as leaves, fruits, and petals. It is here they conduct their name-giving behaviour—cutting semicircular fragments, which are then transported back to the colony to feed a mutualistic fungus—their primary food source [124, 134, 174]. Given its ecological importance, several studies have sought to quantify different aspects of this iconic behaviour. In the first experimental chapter of this thesis, I investigated how substrate mechanical properties and mandible size together determine the force required to cut thin leaves and leaf-like sheets. Other work has focussed on the generation of the necessary forces by the insect bite apparatus [89, 90]; the effect of wear on cutting forces [55, 139]; or the mechanical constraints on leaf transport [119, 250, 251]. Foraging, however, is not only constrained by mechanics: it also incurs significant metabolic costs. The total metabolic cost of foraging can be split into three components: the cost of unladen locomotion associated with getting to the food source; the

cost of cutting a fragment; and finally, the cost of laden locomotion to transport the fragment back to the colony [119]. The metabolic cost of locomotion is well-explored in social insects, with previous studies quantifying the cost of unladen locomotion and its variation with insect body size and slope; as well as the effect of load size in laden locomotion [102, 103, 109, 117, 252, 253]. [13] By contrast, the energetic cost of leaf cutting is relatively underexplored, perhaps because it poses several challenges. First, leaves—the primary foraging substrate of leaf-cutter ants—are metabolically active, making it methodologically challenging to measure CMR on natural substrates [258] (see general introduction for a full rationale). Second, in insects that feed directly on leaves, it is difficult to disentangle the rise in metabolism due to the excitement of feeding from the cost of the feeding behaviour itself. Consequently, only one previous study has quantified the metabolic demand of cutting. The findings were remarkable: the metabolic rate was elevated to more than 30 times of the SMR—the energy needed to maintain basic physiological functions while at rest [118]—making cutting the one of the most energetically costly activity in insects, second only to flight.[14] However, this study was limited to just one substrate type. Much as the metabolic costs of transport varies with the load that is carried [119, 250, 251], it is reasonable to wonder if the metabolic costs of cutting vary with the difficulty of cutting, i. e., with the toughness and thickness of the leaf that is cut. Specifically, depending on substrate thickness, toughness, and tool geometry, cutting forces can easily vary by a factor five or more [55]. Does this translate into a fivefold increase in metabolic cost? To address this question, I fabricated metabolically inert PDMS pseudoleaves varying by a factor of two in toughness. I then used highly sensitive flow-through respirometry to measure two metabolic rates: first, the SMR, which provides a baseline; and second, the CMR exerted during cutting. To compare the metabolic power input with mechanical power output, I also measured the average cutting speed. By combining data on the metabolic and mechanical power, I ultimately seek to contribute to a quantitative theory of optimal foraging in leaf-cutter ants.

3.2 Materials & methods

3.2.1 Study animals

A sub-colony of approximately 10,000 *Atta cephalotes* (Linnaeus, 1758) leaf-cutter ant workers was isolated from a large laboratory colony comprising >200,000 workers, estimated from the fungal volume. The sub-colony was housed in an 18 $\times$ 18 $\times$ 20 cm (L $\times$ W $\times$ H) fungus box, connected to both a small foraging area and a waste box. The sub-colony was maintained in a climate-controlled environment at 25°C, with 60 $\pm$ 1% relative humidity, and a 12-hour light/dark cycle (Weiss Technik Fitotron, Type HGC, Loughborough, UK). The ants were provided with small amounts of bramble and kibbled maize at 8 pm daily; the food supply was limited to maintain foraging motivation [259]. Individuals across a mass range of 2-74 mg were selected at random for respirometry measurements.

[13] The energetic cost of locomotion has also been studied more widely across invertebrates and vertebrates. See [254] for studies in rats, [255] for studies in red squirrels, [256] for a general review of insect locomotion, and [110, 111, 257] for studies in humans.

[14] By contrast laden and unladen locomotion raise metabolic rate between 2 and 10 times above resting [103, 109, 252].

This mass range approximately covers the active forager mass range; it excludes minims (workers below 1 mg), which do not generally partake in foraging [55, 134, 142, 143].

3.2.2 PDMS pseudoleaves

PDMS pseudoleaves served as cutting substrates. PDMS was utilized as it is a homogenous substrate with adjustable structural and mechanical properties. It offers the further crucial benefit of being metabolically inert, so that all signal comes from ant metabolism alone. The use of PDMS pseudoleaves as a homogeneous, tuneable, and metabolically inert substrate is novel to this study. While parafilm has previously been used as a metabolically inert substrate [118], it presents distinct disadvantages: it is anisotropic and lacks the option for material tuneability. Two further observations suggest that some biological interpretability is retained, despite the use of a synthetic polymer substrate. First, the forces required to cut PDMS pseudoleaves are similar to those for leaf laminas and petals (see 2.2.3 and [35, 55]). Second, ants readily forage on synthetic materials (see also [118, 190, 260]), and cutting behavior is qualitatively and quantitatively similar to that exhibited when cutting biological materials.

Two primary pseudoleaf types were fabricated for this study, both with a nominal thickness of 200 μm but distinguished by the mixing ratio between base and curing agent and by the curing protocol. These differences altered the tearing energy, a proxy for pseudoleaf toughness, by a factor of about two (Table 3.1), allowing us to test whether different force requirements incur different metabolic costs during cutting. To further explore this idea, I supplemented a larger main dataset with a small set of measurements on 150 μm, 300 μm, and 500 μm 10:1 pseudoleaves (see Appendix B for characterisation). All pseudoleaves were fabricated using Sylgard184™; the base and curing agent were mixed in either a 10:1 or 4:1 ratio, followed by degassing and casting between silanised glass plates with 200 μm spacers. PDMS sandwiches were then oven-cured in different conditions, resulting in two pseudoleaf types that differed in mechanical properties.

Young's modulus, UTS, and tearing energy were characterized for each pseudoleaf type using ISO/ASTM standard tensile tests (Young's modulus and UTS: ISO37 and ISO5893 [177, 195, 196]; the tearing energy was extracted via pure shear tests, following [199, 200]). For a detailed account of the fabrication and mechanical characterisation, see 2.2.3, and [177–181, 195, 199, 200].

TABLE 3.1: The steady-state cutting force varies with the mechanical properties of the target material, and thus may induce differences in the metabolic expenditure during cutting. Three key material properties were measured for each pseudoleaf type: Young's modulus, ultimate tensile strength (UTS), and tearing energy. I also measured the average force required to cut each 200 μm pseudoleaf type with forager mandibles with varying degrees of wear. 4:1 pseudoleaves have a higher modulus, a lower tearing energy, and approximately equal UTS than 10:1 pseudoleaves; they thus are significantly easier to cut.

Substrate	Young's modulus E (MPa)	Tearing energy G_c (J m^{-2})	UTS σ_c (MPa)	Average steady state cutting force (mN)
4:1 PDMS pseudoleaf	4.1 ± 0.3	98 ± 9	6.0 ± 2	54 ± 6
10:1 PDMS pseudoleaf	1.6 ± 0.3	197 ± 25	5.5 ± 2	84 ± 20

3.2.3 Flow-through respirometry

Metabolic rate measurements were conducted using flow through respirometry. Two metabolic rates were measured: the SMR, i. e., the rate at which the ants consume energy to maintain basic physiological functions at rest [261–263]; and CMR, the rate at which energy is consumed during cutting. Ants are ectotherms, and as such rely on external heat sources to maintain body temperature. As a consequence, metabolic rates are intrinsically linked to environmental temperature, and hence temperature must always be tightly controlled and quoted when presenting metabolic data [97]. SMR is measured to serve as a baseline to which metabolically costly cutting is compared; the ratio between CMR and SMR is a proxy for the aerobic metabolic scope (MS)—a measure for the energy potential accessible to the ants to fuel activity.[15] Due to their small body size, leaf-cutter ants have a low absolute metabolic output and, as a consequence, it is technically challenging to measure the associated small changes in fractional oxygen concentration, relative to the high atmospheric baseline of 21% [97]. Hence the majority of flow through respirometry in small insects measures CO_2 production instead [265, 266]. CO_2 measurements have the crucial advantage over O_2 measurements that the incurrent air can be chemically scrubbed to have CO_2 concentrations as low as 0.5% [264]; I thus used CO_2 based respirometry to measure SMR and CMR. To convert CO_2 measurements into standard metabolic metrics, I follow previous work and assume that ants use lipids as primary metabolite [118]; CO_2 production can then be converted into O_2 consumption, and an individual's metabolic rate in Watts can be estimated [97] (for details, see 3.2.5).

The flow through respirometry system was set up in a pull configuration (Figure 3.1); all components were purchased from Sable Systems (Sable Systems International, Las Vegas, NE, USA). The setup comprised a flow meter and pump (SS4 Sub-Sampler) that pulled ambient air from a 50 cm $\times$ 50 cm $\times$ 30 cm (L $\times$ W $\times$ H) air reservoir, which acted as a low-pass filter for fluctuations in air consistency [97]. The flow rate was modulated by means of a calibrated mass flow control valve (0-500 SCCM Air, Alicat Scientific, Tucson, AZ, USA), connected to a mass flow controller (MFC-2). Incurrent air was chemically scrubbed of CO_2 and H_2O, using soda lime and DAD (Drierite/Ascarite/Drierite) scrubbing columns (Ascarite II 20–30 mesh; Thomas Scientific, Swedesboro, New Jersey, USA, Drierite 8 mesh; Sigma-Aldrich, St. Louis, Missouri, USA) [97, 104]. Baseline readings revealed that incurrent air had < 1 ppm CO_2 (resolution of approximately 0.1 ppm CO_2). CO_2 concentration of outcoming air was measured with a Licor LI7000 infrared CO_2 gas analyser in differential mode, at a sampling frequency of 10 Hz; the flow rate (MFC-2), temperature (Type-T thermocouple probe), and water vapor (RH-300) were recorded at the same frequency. The CO_2 sensor was calibrated and spanned using certified 1000 ppm CO_2 calibration gas in balance N_2 (BOC, certificate number: 21/005083, UK); pure N_2 was used to calibrate the system to true zero (BOC, 99.99% pure nitrogen, certificate number: 21/004497, UK). Calibration was performed at the start of

[15] In endothermic animals such as mammals, where body temperature is self-regulated, resting metabolism is referred to as basal metabolic rate (BMR). Comparing the allometry of SMR and BMR, is difficult even when data is collected in the same environmental conditions [264].

each experimental day, and the system was re-zeroed after each recording; re-calibration was conducted also whenever the flow rate was changed. All raw data were relayed to the data acquisition software Expedata (version 1.9.13), interfaced via a Sable Systems universal interface (UI-3), and all measurements were conducted in climate-controlled rooms (see above), at a constant temperature of 25 ± 0.1 °C.

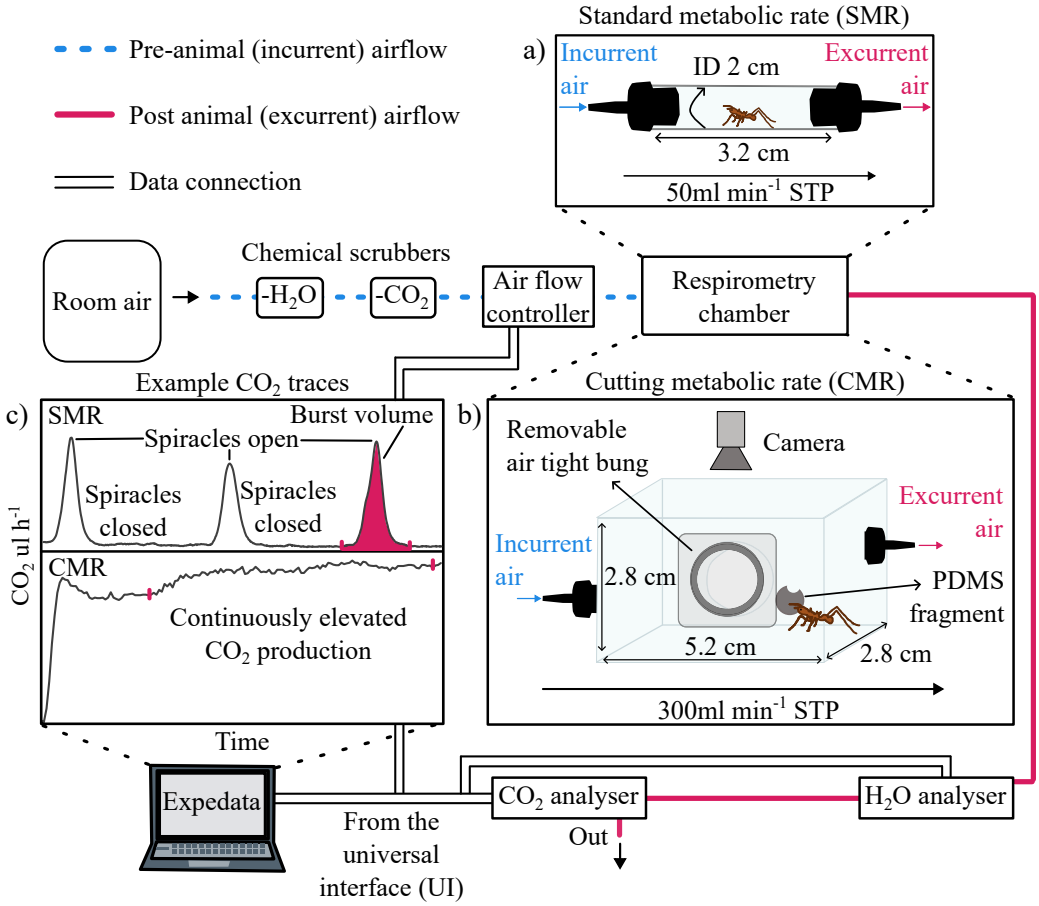


FIGURE 3.1: Simplified block diagram of the flow- through respirometry setup (not to scale). Blue dashed lines indicate air flow pre-animal (incurrent air), pink solid lines airflow post-animal (excurrent air), and black double lines data connections. The labels -CO_2 and -H_2O indicate that the ambient air is chemically scrubbed of carbon dioxide and water vapour by means of drierite/ascarite/drierite and soda lime scrubbing columns. To investigate the metabolic costs of leaf-cutting, two metabolic rates were measured for workers spanning the approximate foraging mass range (2-74mg): the standard metabolic rate (SMR) that characterises idle animals; and cutting metabolic rate (CMR) exhibited by animals cutting pseudoleaves of different material properties. **a)** SMR - Air was pulled through the system with a flow-rate of 50ml min^{-1}, chosen to achieve a time constant of 17 s for a cylindrical chamber with 14 ml volume. **b)** CMR – Air was pulled at 300ml min^{-1} through a larger rectangular cutting chamber (volume = 40.8ml), made from clear acrylic to facilitate filming with a top-down video camera. All distances represent working distance. **c)** Idle individuals exhibited discontinuous gas exchange cycles (DGC), characterised by a burst frequency and volume. In contrast, cutting workers exhibited a consistently elevated CO_2 emission. A representative metabolic rate is obtained by integrating the CO_2 emission with respect to time. All raw data from the gas analysers were stored and analysed in Expedata.

Standard metabolic rate measurements

SMR was measured using a small respirometry chamber [97] (Figure 3.1a)— a thin tube made from glass (RC inline chamber, Sable Systems ; ID 2 cm × 3.8 cm, internal volume = 14 ml). Two baselines were recorded prior to any animal measurements, each lasting 5 minutes [265, 266]. First, incurrent scrubbed air was directed straight into the CO_2 gas analyser to gauge the fractional concentration of gasses in absence of the chamber. Second, an empty chamber baseline was taken. Although this procedure is labour-intense, it helps ensure that chamber volume and flow rate are well matched, i. e., that there are no effects of gas dwelling and mixing [97]. Scrubbed air was pulled through the chamber at a rate of 50 ml min^{-1} standard temperature and pressure (STP), chosen to achieve a time constant of approximately 17 s—a resolution sufficient for SMR recordings in insects (see [97, 104, 105, 267] for similar time constants). The relatively high flow rate relative to the chamber volume further ensured that washout compensation was not necessary when calculating burst frequency (f_b) (see 3.2.5) [268]. Following baselining, idle individuals were extracted from the colony foraging area, placed into the chamber, and left for 30 minutes to acclimatise [267, 269]; the SMR was then measured over a 30-minute period. Measurements were considered invalid and discarded if anything but minor and short leg movements occurred during this period, as monitored via a camera (Supplementary video 1), and clearly identifiable from the metabolic traces (Appendix B) (see also [101, 267, 270]). Finally, a 5-minute baseline measurement was taken to remove drift downstream, which never exceeded 0.4 $ppmh^{-1}$ [267]. After each measurement, individuals were removed from the chamber, weighed to the nearest 0.1 mg (Kern ADB 100-4 120 g × 0.001 g, Kern analytical, Germany), and returned to the colony. SMR was measured for a total of n=21 individuals with body masses between 2.1 and 70.1 mg.

Cutting metabolic rate measurements

12 × 12 cm pseudoleaves were added to the foraging area, to trigger natural foraging behaviour. Once an individual worker initiated a cut, I carefully excised the area around the cutting worker using micro scissors, and placed both worker and pseudoleaf directly into a small custom made cutting chamber, inspired by the design reported in Schilman and Roces [102] (Internal dimensions: 2.8 × 5.2 × 2.8cm, Volume ≈ 40.8ml; Figure 3.1b). The chamber was sealed with a custom 3D printed bung made from resin, fitted with Viton O-rings, and the baselining protocol was as described for SMR measurements above. To purge the air introduced into the chamber during the opening period, I allowed a dwell time of one minute, well in excess of the about 40 s required to replace 99% of the gas in the chamber, given the flow rate of 300ml min^{-1} STP (see Appendix B). Subsequently, the CMR was measured over time periods that varied across individuals, but generally ranged from between 2 and 13 minutes. After an individuals ceased cutting, the metabolic rate was measured for a further 10 minutes to monitor the decay, if any, of the metabolic rate as a rough indicator for potential anaerobic metabolism [118]. Both fragment and worker were then removed from the chamber and weighed (as above). The workers were returned to the colony, and the fragment retained for further analysis (see 3.2.4). A synchronized video camera (Raspberry Pi HQ camera V1.0 2018, Raspberry Pi model 3, UK)

was used to monitor cutting activity at 15 frames per second (FPS) in top-down view; where possible, cutting speed was estimated from these recordings downstream (see 3.2.4). A total of n=15 workers were used for CMR measurements for each substrate (N=30), varying in body mass between 2.1 and 74.1 mg.

3.2.4 Cutting speed measurements

Measuring the cutting speed during CMR measurements proved difficult, due to the uncertainty in estimating the length cut before the individuals were placed into the chamber. To avoid this difficulty, I instead measured the average cutting speed directly in the foraging arena, where the start and end point were readily identifiable (n=50 individuals with body masses roughly evenly distributed in log-log space, for each substrate type).

Average cutting speed was determined as the ratio between cut distance and cutting time. Cutting time was extracted from the video recordings. To this end, I first identified the first and last frame where ants engaged in scissor cutting — a characteristic cutting technique used by ants to initiate and finish cuts [271]. By dividing the number of frames between first and final frame by the frame rate, the total cutting time in seconds follows. To estimate the distance cut, the cut fragment was retrieved from the chamber, dipped into ink to increase contrast, and scanned with a 1200dpi scanner (PageWide Managed Colour MFP E58650dn, HP, UK). Scanned fragments were then analysed in ImageJ [272]. First, the image was split into RBG channels, and blue was isolated for the highest contrast; this channel was then converted to a binary image using a greyscale threshold chosen to remove shadows and image artefacts. Pixels were converted to real-world distance using a conversion factor of 47.24 pixels per mm, determined from the dpi of the scanner. Cut distance was extracted from the thresholded images using a custom-written ImageJ macro (see [272] and 4.2.3).

3.2.5 Data curation and statistical analysis

All handling of the raw respirometry data was completed in Expedata (Sable systems, version 1.9.13), including conversions from ppm to mL CO_2 h^{-1}, marker and drift correction, digital filtration, baseline subtraction, automatic peak detection, and integration. Individuals at rest exclusively exhibited discontinuous gas exchange (DGC; Figure 3.1c). After conversions and corrections, the following parameters were extracted from the 30 min SMR recordings: (i) f_b, (ii) burst volume (V_b) and (iii) average SMR. To extract f_b, peaks in the CO_2 trace were automatically detected using native routines in Expedata; the burst frequency in mHz follows at once as the ratio between peak number and recording time. Average V_b was calculated by integrating the CO_2 with respect to time during each burst, and then averaged across all bursts (Figure 3.1c). A low long term drift of 0.22 ppm h^{-1} ensured that V_b calculations were not significantly affected by drift [267]. For a more detailed description of the involved procedures, see Appendix B. Average SMR was then extracted by integrating the entire CO_2 trace over the 30-minute measurement period. Average CMR was extracted accordingly as the integral of the CO_2 rate over the cutting time. CO_2 concentration was converted into a volume flow

rate by dividing ppm CO_2 by 1 million, multiplying by the air flow rate (in ml min^{-1}), and dividing by 60 min h^{-1}. Converting this CO_2 flow rate into a metabolic rate in μW (microwatts) requires an assumption on the metabolite. Previous work in *Attine* ants identified lipids as the primary metabolite, implying a respiratory quotient (RQ) of 0.7 [118]—for every 10 molecules of O_2 consumed, 7 CO_2 molecules are produced. Each mL of O_2 has a caloric value of 26.7 joules per mL [118]. Hence, to obtain the metabolic rate in μW, CO_2 (ml h^{-1}) was divided by 0.7 and then multiplied by this conversion factor. Subsequent conversions from CO_2 emission to metabolic rate (μW), as well as all statistical analysis, data curation and plotting were conducted in R (v. 4.1.1) [273]. Ordinary least squares (OLS) regressions on log10-transformed data were performed to characterise scaling relationships with respect to body mass. Comparative allometric analysis via analysis of covariance (ANCOVA) is widely considered best practice (for more details see [97, 210]). ANCOVA was thus used to assess if different groups (SMR and CMR for each substrate) share a common mass scaling exponent (slope), and, if so, the same pre-factor (intercept); it was used further to assess if cutting speed differs across body masses and pseudoleaf types. Analysis of variance (ANOVA) was used to investigate the effect of body mass on both V_b and f_b. Prior to conducting the ANOVA and ANCOVA,I verified that all underlying assumptions for each test were met: normality of residuals (via the Shapiro–Wilk test and visual inspection of Q–Q plots) and homoscedasticity (via the Breusch–Pagan test and visual inspection of a fitted vs. residuals plot).

3.3 Results

3.3.1 Standard metabolic rate

Idle *Atta cephalotes* leafcutter workers exclusively exhibited discontinuous CO_2 gas exchange cycles (DGC). The DGC is clearly identifiable by the distinct open (O phase) and closed phases (C phase) (Figure 3.2a, see [264]). Notably absent from the traces was an obvious flutter phase (F phase), reported in previous work on large ants (>30 mg in body mass) [264, 267, 274]. The CO_2 emission characteristics of 10 ants were determined with three repeats for each worker (n=10, N=30). Neither f_b nor V_b varied significantly across repeats (ANCOVA burst frequency: $F_{1,29}$ = 0.14, p = 0.649; burst volume: $F_{1,29}$ = 0.691, p = 0.413) and were hence pooled. CO_2 f_b decreased significantly with body mass m (ANCOVA: $F_{1,9}$ = 12.96, p = 0.007), ranging from a minimum of 3.5 to a maximum of 11.1 mHz (Figure 3.2b); this pattern can be satisfactorily described via the relation $f_b = 13.8m^{-0.29}$, where body mass is in mg and the frequency in mHz (95% CI: [7.41, 25.12] and [-0.49, -0.11] for the pre-factor and mass scaling exponent, respectively). CO_2 V_b increased significantly with body mass (ANCOVA: $F_{1,9}$ = 135.8, p < 0.001), $V_b = 5.37m^{1.12}$, where mass is in mg and the volume in nL (95% CI: [2.75, 10.96] and [0.87, 1.30] for the pre-factor and mass scaling exponent, respectively). The largest worker released, on average, 27 times more CO_2 per burst than the smallest worker (Figure 3.2c). The size-specific variation in V_b and f_b combined to a substantial increase of SMR with size SMR $\propto m^{0.83}$ CI: [0.78, 0.88] (Figure 3.3b), which varied between 2.96 and 51.06 μW across the worker mass range. The allometric equation relating body mass *m* in grams to SMR in microwatts

(μW) at 25 °C followed as:

$$\text{SMR} = 692m^{0.83} \tag{3.1}$$

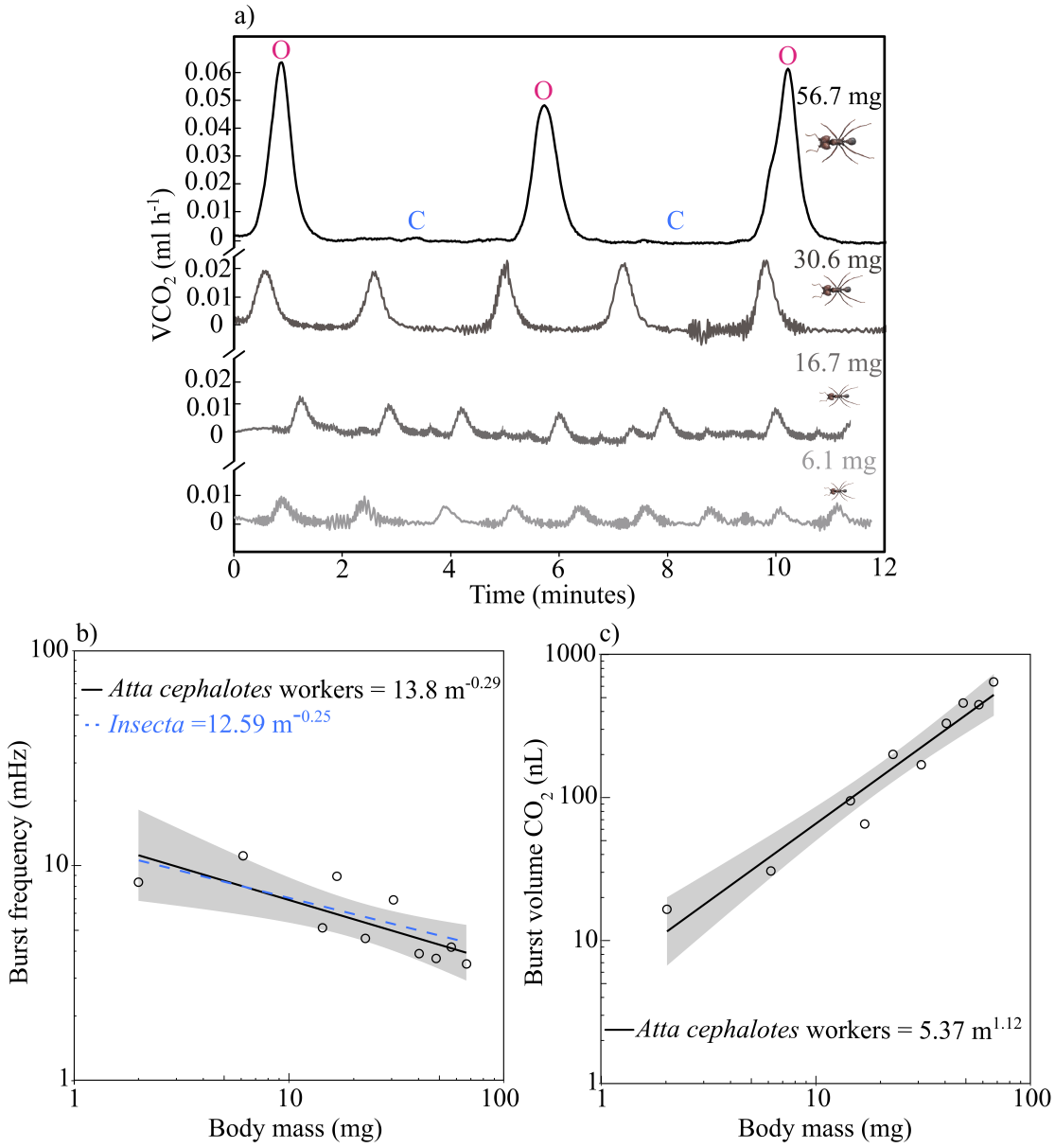


FIGURE 3.2: Standard metabolic rate (SMR) was measured across the approximate foraging mass range (2.0 – 74.0 mg) to gauge a baseline for comparison to metabolically costly leaf-cutting. a) Idle individuals exclusively exhibited discontinuous gas exchange cycles (DGC), readily identified by the clear opening (O) and closing (C) phase of the spiracles. Illustrative CO_2 emission traces at 25°C are shown for a selection of body masses; note the breaks in the y-axis scale. b) Burst frequency (f_b) showed a negative trend with body mass, $f_b \sim m^{-0.29}$, and ranged from 3.5 – 11.1 mHz. The trend for burst frequency across several insect species is indicated by the blue dashed line [275]. c) Burst volume (V_b) showed a positive trend with body mass; the largest worker released about 27 times more CO_2 than the smallest individual, $V_b \sim m^{1.12}$. Both burst frequency and volume are plotted in log-log space; lines indicate mass scaling exponents and shaded regions indicate the confidence intervals as estimated via ordinary least-squares regression.

3.3.2 Cutting metabolic rate

CO_2 emission traces obtained from workers that were actively cutting indicated a clear departure from discontinuous ventilation. Instead, CO_2 release was considerably elevated to an approximately constant level (Figure 3.3a). As observed for idle individuals, the metabolic rate increased with mass. Neither the pre-factor nor the mass scaling exponent of this relationship varied across the two pseudoleaves types, distinguished by the mechanical difficulty of cutting (ANCOVA – mass scaling exponent, Mass:Substrate: $F_{1,26}$ = 0.923, p = 0.346; ANCOVA – pre-factor: $F_{1,27}$ = 0.1, p = 0.806) (Figure 3.3b). Consequently, removing the interaction term made no significant difference to the fit (ANOVA: $F_{1,26}$ = 0.93, p = 0.35). Given the insignificant difference in CMR between the two substrates, the data were combined to estimate a single allometric equation relating body mass *m* in g to CMR in μW:

$$\text{CMR} = 21,380m^{0.87} \tag{3.2}$$

I additionally compared the CMR of workers cutting 150, 300, 500 μm 10:1 pseudoleaves (a smaller dataset collected in a previous preliminary study and so not included in the above allometric estimate). Although the measured cutting forces vary by more than a factor of three across these substrates, CMRs did not differ obviously in their magnitude, and instead were close to the confidence intervals of the combined CMR allometric regression. There was a small but statistically insignificant difference in mass scaling exponent between SMR and CMR (ANCOVA: $F_{1,42}$ = 3.725, p = 0.07). The metabolic scope—the ratio between CMR and SMR—is thus mass-independent, and follows as the ratio of the two pre-factors, 21,380/692 = 31.

3.3.3 Cutting force and cutting speed

Cutting force for the main substrate types and thicknesses are described in detail in chapter 1 (see 2.2.3). However, in brief, here I present F_c required to cut the two substrate types for each thickness with forager mandibles – showing different degrees of wear likely covering the range found naturally in workers in our cutting speed dataset. F_c depended significantly on mixing ratio and thickness (RM ANCOVA mixing ratio: $F_{1,26}$ = 157.03, p < 0.01, RM ANCOVA thickness: $F_{1,26}$ = 341.32, p < 0.01) (Figure 3.4a). F_c showed no significant variation with body mass (RM ANCOVA mass: $F_{1,\ 26}$ = 0.537, p = 0.47) therefore on average for the only comparable thickness between the two substrate types (200 μm) there was roughly a factor of 1.5 increase between 4:1 and 10:1 PDMS. See Appendix B for the characterisation of 150, 300 and 500 μm used in preliminary trails. Cutting speed varied significantly with worker body mass (ANCOVA mass: $F_{1,99}$ = 145.37, p < 0.01) with a mass scaling exponent that was statistically indistinguishable across pseudoleaf types (ANCOVA mass:substrate: $F_{1,98}$ = 1.89, p = 0.43) (Figure 3.4b); on average, larger workers cut almost 10 times faster than smaller workers, independent of substrate types. However, the cutting speed differed across substrates, as indicated by a significant difference in the pre-factors (ANCOVA substrate: $F_{1,99}$ = 18.9, p < 0.01). For 4:1 pseudoleafs, the scaling coefficient was 6.91 CI[5.70|8.12] compared to 5.05 CI[3.54|6.56] for

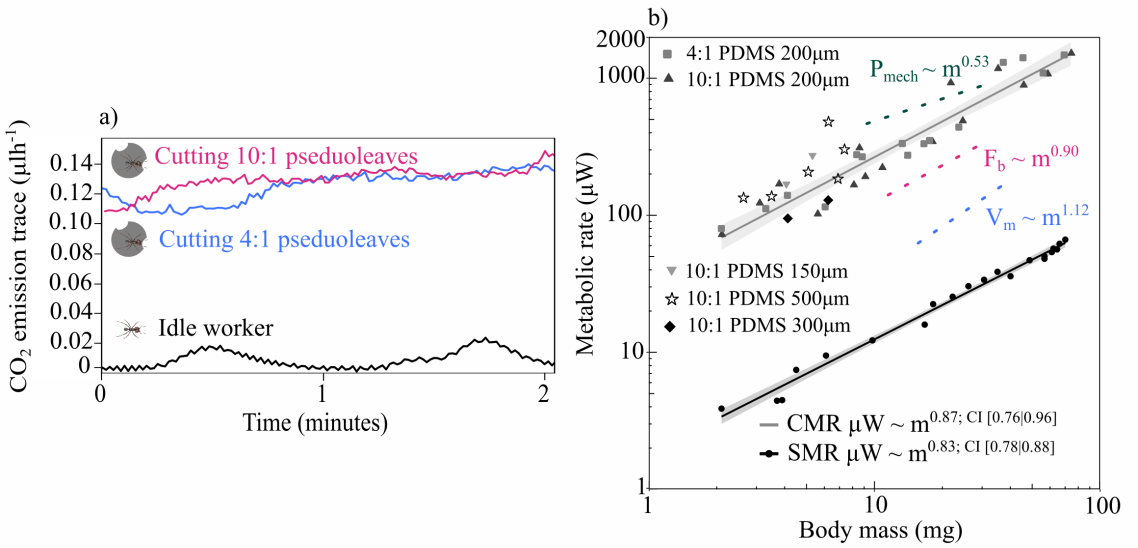


FIGURE 3.3: Cutting metabolic rate (CMR) was measured for two pseudoleaf types (4:1 and 10:1 200μm); these measurements were supplemented with data from preliminary experiments involving three additional thicknesses on the toughest pseudoleaf type 10:1 – 150, 300 and 500 μm. a) During cutting, CO_2 traces departed from the discontinuous gas exchange cycles observed in idle workers, and instead showed a constantly elevated CO_2 release. CO_2 traces were virtually indistinguishable for the two pseudoleaf types, as illustrated with two representative examples. b) Standard metabolic rate (SMR) was measured across the approximate forager body mass range (2.0 – 74.0mg) to provide a baseline for CMR. SMR scaled strongly with mass, as did CMR for both pseudoleaf types; the scaling exponents were statistically indistinguishable across pseudoleaves, indicating that the metabolic costs of cutting are not noticeably influenced by the mechanical costs of cutting. The data were thus combined to extract a common allometric relationship, CMR $\sim m^{0.87}$. CMR on 150, 300 and 500 μm 10:1 psuedoleaves sat close to the combined allometric regression line. CMR was on average 30 times higher than SMR across all body masses, as calculated by the ratio of the pre-factors. Data are presented in loglog space, and fitted lines (solid) and confidence intervals (shaded) were obtained with ordinary-least-squares regression.

10:1 pseudoleaves (Figure 3.4b). In other words, ants cut 4:1 pseudoleaves about 1.4 times faster on average – roughly mirroring the difference in cutting force between the two substrate types.

3.4 Discussion and conclusions

Leaf-cutter ants are well known in the Neotropics as the primary insect pest species. Harvesting plant matter on an industrial scale they account for 15% of the total defoliation in the region [276–278]. This not only significantly affects human agriculture, but also engineers the ecosystem around them [68–70, 140, 279]. At the heart of their herbivory is cutting — if workers can't cut or slice into plant tissue then their 100,000 strong colonies would fall apart. The cutting behaviour observed within *Attine* ants is in itself remarkable; during cutting gas exchange rates, and thus metabolic rate, rise to over 30 times resting [118]. This impressive aerobic scope is twice that of vertebrates [124, 280] and enables insects to achieve feats such as cutting and flight. As well as their aerobic scope, key to their successful herbivory is their large mandibular closer muscles, which account for 25% of their total body mass [124]. Such an adaptation has ensured that leaf-cutters can generate far in excess of the force required to cut most tropical leaves [35, 90]. The bite forces also show strong positive

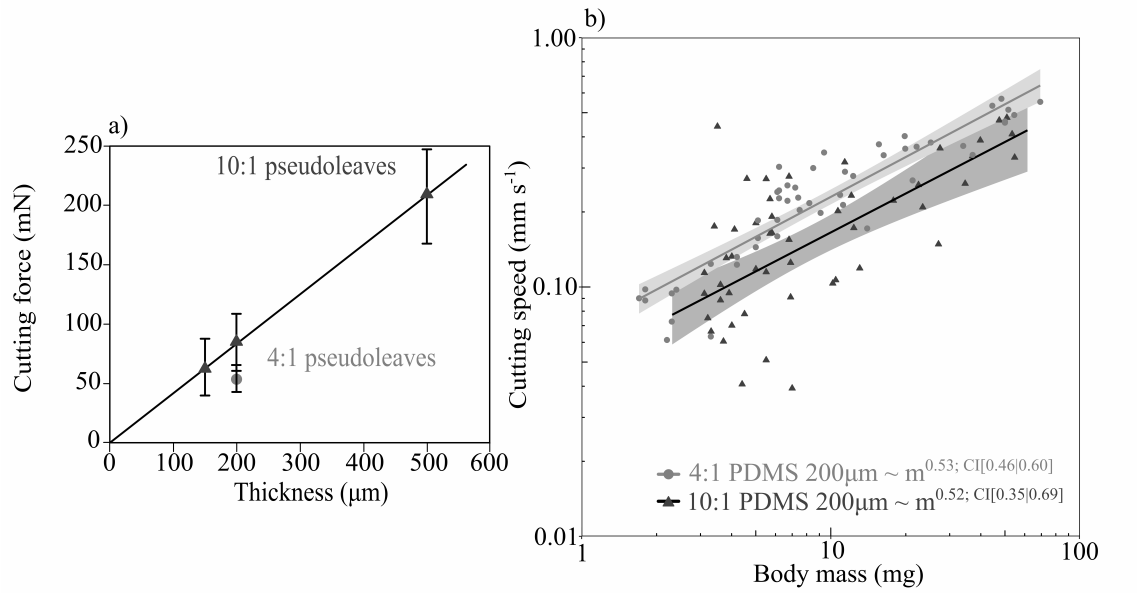


FIGURE 3.4: In order to estimate the mechanical power output during cutting, I measured a) mandible cutting forces and b) cutting speed. Cutting forces were measured with forager mandibles spanning the approximate foraging mass range for each pseudoleaf type and thickness; they did not vary significantly with mass and were hence pooled. Cutting forces did however vary significantly across both substrate type and thickness: 4:1 and 10:1 pseudoleaves with 200 μm thickness differed by about a factor of 1.5. b) Cutting speed was measured for n=50 workers spanning the approximate foraging mass range. Cutting speed varied significantly with worker body mass, and this relation was independent of pseudoleaf type. However, 4:1 leaves – which are cut with lower forces – were cut about 1.4 times faster on average.

allometry meaning that the mechanical demand will differ across size and substrate whilst foraging. Previous studies have looked at metabolic scaling with size for various aspects of foraging [101, 118], namely cutting and locomotion, but we still lack robust empirical evidence for the varying scaling of metabolic cost with changing mechanical demands, reducing our capacity to make informed efficiency estimations. Do the costs of cutting increase with mechanical power?

Within this work I address this question directly. I fabricated pseudoleaves with controllable and distinctively different mechanical properties; a factor of two difference in toughness and a factor of 1.5 in cutting force for forager mandibles between 4:1 and 10:1 pseduoleaves; and measured the metabolic cost of cutting for each pseudoleaf for workers spanning the approximate foraging mass range. I additionally measured the speed at which leaf-cutter ant workers cut each substrate, to fully characterise the mechanical power. To gauge the metabolic scope, I additionally measured the SMR of idle workers across the equivalent mass range and characterise their DGC.

Within the following discussion I look to address two main aspects of our results: the scaling of DGC, its origins and modulations, and the scaling of metabolic and mechanical power across substrates and its implications for the suitability of workers of different body sizes to cut leaves.

3.4.1 Discontinuous gas exchange; burst frequency, burst volume and their modulation of SMR

To address the tantalisingly unsolved question of the diverging scaling of mechanical and metabolic power we must first start with the base to which all activities are compared — SMR. SMR is defined as the minimum energy requirement for self-maintenance at rest [281] and these needs are met by respiration. Whether you're as large as a majestic blue whale or as tiny as a mite, respiration is the fire that fuels you [97, 130]. The process is different across scales but the main necessary components remain the same; an energy source —- lipids are assumed for leaf-cutter ants [118] and a method of effective gas exchange —- facilitated by the tracheal system in insects (see General introduction for an in depth description). Whilst all gas exchange in insects is facilitated by the tracheal system, the methods of gas exchange differ. The two main expulsion modes are either discontinuous gas exchange cycles (DGC) or as continuous gas exchange. In *Atta cephalotes* leaf-cutter ants I found distinctive DGC (see figure 3.2a) where CO_2 is released in discrete bursts. In all insects that display DGC, the average standard metabolic rate is defined by the combination of the frequency f_b at which gas emission occurs, and the volume V_b of each emission [97]. Whilst there are several studies that postulate the evolutionary origins of DGC (see [261, 267, 282–284]) the question of how frequency and volume combine to give SMR is relatively under explored. How do the two factors influence each other and combine to give SMR?

Several studies have consolidated the allometry of burst frequency f_b in insects [261, 285–288]. In a notable 2007 study Terblanche *et al* found that 49 insect species all share a frequency scaling relationship of $f_b \sim m^{0.25}$ [275] a finding that aligns with the ventilation frequency of endothermic vertebra [289], within our work we also find a similar and statistically insignificant variation $f_b \sim m^{0.29}$. The consistency in the allometry of burst frequency across species suggests that the burst volume V_b will need to change significantly to represent the variation in SMR we see across species (see Appendix B, Table B.3 for variation in *attine* ants and [106] for a thorough breakdown of SMR scaling across species and ecosystems).

Though the allometric scaling of burst frequency f_b is well described there are significantly less studies characterising the scaling of burst volume V_b in insects. Despite the obvious factor that this field could be underexplored, I postulate that there could be a distinct reason for the lack of comparative allometric data. Between small and large insects (as an example ants [252] vs locusts and beetles [287, 288]) the mechanism for gas exchange into and out of the tracheal system are different. Where ants primarily use diffusion and convection (depending on the phase of the DGC) larger insects use active ventilation (where the contraction of large air-filled sacs help move gasses throughout the body). This makes direct comparison tricky, as it likely changes the primary factor that modulates the expulsion of gas.

We find that in *Atta cephalotes* leaf-cutter ants burst volume scales hypermetrically with size $V_b \sim$

$m^{1.12}$ (Figure 3.2c). In order to expel CO_2 in large discrete bursts as seen in DGC, there needs to be a sufficiently steep concentration gradient. Within ants it has been shown the local CO_2 concentration rises to the maximal tolerable level before expulsion [124]. At this high internal level of CO_2 there is a significant partial pressure difference between intratracheal and external CO_2 levels allowing CO_2 to "burst" out. The spiracles then close and external gas exchange ceases and the process of build up begins. Due to the differing concentration of CO_2 and O_2 within the atmosphere and the way the two gasses are transported, it is likely the tracheal system evolved to favour the removal of CO_2 over the uptake of O_2 as this is the more difficult transport task [124, 261, 290].

This task is exacerbated with size due to distances increasing unfavourably, thus the tracheal system of larger insects faces growing demands [290]. Ant tracheal scaling follows Nunome's pattern—an area reducing hypothesis that suggests that tracheal branches get smaller and thinner further away from the body surface, providing more "options" for CO_2 to diffuse out of the tissue and be buffered by the haemolymph [291] [290]. A direct result of this adaptation is a hypermetric scaling of the tracheal volume, $V_{\text{tracheal}} \sim \text{m}^{1.02-1.24}$ [286, 290, 292–294]. [16]

To summarise the comparison of the above literature and our experimental findings in the highly polymorphic insect species *Atta cephalotes* leaf-cutter ants, I postulate that DGC in ants is primarily modulated by CO_2 burst volume. The main constraint in DGC is the removal of CO_2 from the tracheal system which is made increasingly difficult in larger insects due to the increased diffusion distance. To provide more gas diffusion pathways, the insect tracheal system scales hypermetrically with the same mass scaling exponent we find in the burst volume scaling.

3.4.2 The diverging scaling of metabolic and mechanical power during cutting

What determines the metabolic costs of cutting?

The allometry of SMR provides a basis to assess metabolically costly activities such as cutting. During cutting, gas exchange departed from DGC and was continuous instead (Figure 3.3a) in order to supply the active tissues with an abundant supply of O_2.[17] Despite this shift, the allometric slopes of SMR and CMR were statistically indistinguishable (see also [118]), regardless of the mechanical difficulty of cutting. What determines the scaling of the CMR? Three plausible hypotheses may be evaluated.

First, one may speculate that the CMR is proportional to the volume of metabolically active muscle tissue [296]. Leaf-cutter ants are capable of producing exceedingly large bite forces, allowing them to cut a large range of plant tissues [89] [90]. These forces are generated by large mandible closer muscles [90] which may account for as much as 25% of the total body mass in large workers [124]. Using semi-automatic segmentation of high-resolution μ-CT scans, Püffel et al quantified the allometry of the

[16] In larger insects such as locusts and beetles the scaling of V_b is less stark, likely due to active ventilation reducing the intensity of intratracheal gas concentration. [287, 288].

[17] Tangential note relating the shift between DGC and continuous CO_2 production. Hetz et al. hypothesise that an insect's respiratory system is designed to supply abundant oxygen during periods of high oxygen demand and DGC evolved to protect the muscle tissue from oxidative damage during rest [295].

mandible closer muscle in closely related *A. Vollenweideri* leaf-cutter ants, and found a strong positive allometry, $V_m \propto m^{1.12}$. This scaling far exceeds the scaling of CMR $\propto m^{0.84}$ (Figure 3.3b), suggesting that the volume of active muscle tissue is an unlikely determinant of the CMR.

A second plausible hypothesis is that the CMR is proportional to the mechanical power output of muscle . Although classic scaling theory assumes that muscle power capacity is proportional to muscle volume, recent work has argued that size-specific mechanical constraints can force departures from this prediction [95] [297] . The average mechanical power output during cutting is the product of average cutting speed v_c and the cutting force F_c:

$$P_{\text{Mech}} = F_c.v_c \tag{3.3}$$

Cutting forces are mass independent (see Chapter 1), and so the power output is directly proportional to the cutting speed, $P_{\text{Mech}} \propto v_c \propto m^{0.53}$—a significantly lower scaling than observed for the CMR, CMR $\propto m^{0.84}$. Thus, the CMR also does not seem to be directly related to the mechanical power output delivered by the muscle.

A third, and perhaps least obvious, hypothesis is that the metabolic costs are directly proportional to the maximum force generated. Perhaps most interestingly the scaling of the F_b scales similarly to CMR, $F_b \propto \text{m}^{0.9}$ (Figure 3.3b). Püffel noted that this is the measured maximum force an individual can apply [90] meaning that doing so the muscles maximally contract we also note the maximal contraction of the mandible closer muscles in the combined CMR – there was no significant difference in metabolic cost P_{Met} despite different mechanical demands (see below for full rationale). One could also draw the comparison of the similar scaling of maximum force production and CMR. A similar "energetic cost of maximum force production" has been presented before [298–300] in locomoting animals. Where the rate of O_2 consumption scaled with the force applied by the muscles. During cutting the mandible closer muscles have to contract frequently in close succession which also incurs additional energetic penalties [301].

The mechanical efficiency of leaf-cutting across worker sizes

Neither the mass scaling coefficient of the CMR nor of the average cutting speed differed significantly across two pseudoleaf types that differed in toughness and cutting force by a factor of 2 and 1.5, respectively. However, ants cut the less tough substrate about 1.5 more quickly. This difference in average speed closely resembles the difference in estimated cutting force, suggesting that ants cut with an approximately constant average mechanical power output (see also [139] for a similar finding related to mandibular wear). Because an increase in toughness affects cutting speed but not metabolic costs, cutting tougher substrates brings a considerable disadvantage. To illustrate this point, we take inspiration from the animal locomotion literature , and define a "metabolic costs of cutting": the metabolic energy required to cut a unit distance, $\hat{E}_{\text{Met}} = P_{\text{Met}}/(v_c)$. If metabolic power is independent of toughness, then $\hat{E}_{\text{Met}} \propto 1/v_c$—doubling the toughness makes it about twice as expensive to cut the same length of leaf. The scaling of metabolic power input and mechanical power output also

has consequences for size-specific task allocation in *Atta*. Consider the mechanical efficiency, η—the ratio of mechanical and metabolic power:

$$\eta = \frac{P_{met}}{P_{mech}} \tag{3.4}$$

From $P_{mech} \propto m^{0.53}$ and $P_{met} \propto m^{0.84}$, it follows that $\eta \propto m^{-0.31}$. In other words, larger workers are seemingly less efficient, and substantially so: a 40mg worker has an efficiency almost $40^{0.31} \approx 3$ times lower than a 1mg worker. So why should a colony ever produce large worker ants? One problem with a simple evaluation of efficiency on the basis of allometric power laws is the implicit assumption that the mechanical power output approaches zero only in the limit of a worker with zero body mass—but this is most certainly incorrect, for cutting requires the application of a minimum force F_c [56, 91, 166, 167]. Only ants above a certain size will be able to produce bite forces sufficient to cut a given material, and, for any smaller ant, the mechanical power output—and thus the efficiency—is zero. The allometry of bite forces has been measured for closely related *A. Vollenweider* [89], enabling a crude illustrative estimate: 10:1 pseudoleaves can be cut with a force as small as 43 mN, which can be generated by any workers larger than 2.4 mg. Thus, mechanical power out and efficiency should drop to zero for any workers lighter than 2.4 mg, whereas for very large ants, $\eta \propto m^{-0.31}$—there ought to be a local optimum of efficiency with respect to worker size. Predicting the variation of mechanical power and thus efficiency with worker size however requires a mechanical model that links cutting mechanics with the physiology and anatomy of the bite apparatus. This task exceeds the scope of this work, and will be addressed in follow-up work.

4 The Non-linear Variation of Cutting Speed

I acknowledge the contributions of Lina Rhmari Tlemcani and Finn Wagner-Douglas who collected the cutting speed data on laurel and rose petals. Matthias Fornefield for his preliminary work on establishing the macro used to obtain cut distance and area.

Summary

Cutting speed and its contributing factors are crucial performance metrics for assessing the efficiency of a leaf-cutter ant colony. In theory, the faster an ant cuts, the more resources it can harvest for the colony within a given time frame. However, the mechanical demands of cutting vary with both worker body mass and substrate mechanical properties, raising the question: how should the relationship between cutting speed and body mass be modelled? To answer this, I combine previously measured parameters—such as cutting and bite forces—with the force-velocity properties of muscle to derive a predictive model for cutting speed and its variation with worker size and substrate properties. This model outperforms linear models used in previous studies, whilst using only one fitted parameter. I then use this predictive model alongside previously measured cutting force (Chapter 2) to assess variation in mechanical power output. Finally, I combine mechanical and metabolic power (Chapter 3) to develop a tool that predicts the most efficient worker size for substrates with different mechanical demands.

4.1 Introduction

The foraging behaviour of insects is of significant ecological importance, as it actively shapes the environments they inhabit [68–70, 115, 140]. Social insects in particular are among the most significant foragers, despite representing only 2% of all insect species [68]. Insects are classified as eusocial if reproductive and non-reproductive members coexist, there is at least a two-generation overlap, and cooperative care for immature individuals is present [68, 113, 114]. These characteristics are thought to enable more efficient foraging strategies, further reflected in eusocial insects' advanced evolutionary adaptations, including distinct sterile castes and, in the most developed species, a sophisticated division of labour [68]. Perhaps the most well-known and extreme example for sophisticated division of labour can be found in the leaf-cutter ants of the tribe *Attini*, dominant throughout the Neotropics.

Leaf-cutter ants exhibit extreme continuous polymorphism, with workers varying by up to two orders of magnitude in body mass [68]. This variation in worker size is accompanied by other traits that likely evolved due to the importance of their foraging behaviour in maintaining the colony's fitness. For example, bite forces increase with strong positive allometry, allowing the foraging caste to generate enough force to cut approximately 90% of tropical leaves despite their small body size [35, 91], significantly enhancing their value to the colony. An important factor in foraging efficiency is how size variation within the colony affects task preference. Are certain sizes of workers more suitable to foraging on specific plants?

Previously, in Chapter 2, I argued that, despite biological complexity, the success of herbivory in leaf-cutter ants is constrained by the ratio of two key forces: the bite force (F_b) and the cutting force (F_c), which is the force required to drive a cut through a material (see also [55, 76, 80, 163]). However, this ratio merely determines the *ability* of an worker to cut, and previous work has suggested that this is a weak exclusion criterion: even workers as small as 5 mg can cut approximately 75% of tropical leaves [91]. So, among the large fraction of the workforce that can physically cut leaves, how does cutting performance vary?

It has long been hypothesised that leaf-cutter ants forage towards an ergonomic optimum [134], implying that workers should prefer activities they can conduct with maximum efficiency. Cutting is an important determinant of foraging efficiency, as the energetic demand associated with cutting is large (about 2 and 10 times higher than that of locomotion [118]).[18] The efficiency of a leaf-cutter ant during cutting may be defined just as the mechanical efficiency of any motor: it is the ratio of the energy output divided by the energy input. Or, concretely, the ratio between the mechanical power output, and the metabolic power consumption. The most suitable worker, therefore, may be defined as the worker that cuts with maximum efficiency.

Previous studies have investigated suitability from a mechanical efficiency perspective [55, 91, 119, 139], but two major limitations have hindered this approach. First, it remains unclear whether the metabolic costs of cutting vary across materials with different structural and mechanical properties. Second, although previous studies have calculated mechanical power [119, 134, 139], these findings remain correlational. Consequently, there is a need for a comprehensive study that can accurately predict changes in mechanical power output with size and across different substrates, enabling more precise efficiency calculations.

In the previous chapter, I addressed the gap concerning metabolic costs, discovering that metabolic power input appears independent of cutting difficulty. I now aim to fill the remaining gap: how does mechanical power output vary with both worker size and the properties of the substrate being cut? The aim of this chapter is to develop a predictive model for how mechanical power output varies across worker body size and substrate properties. To evaluate the model's predictive accuracy, I first experimentally measure the factors contributing to mechanical power. By combining such a model

[18] Several studies have also quantified locomotion efficiency in foraging behaviour from both an energetic and mechanical standpoint [101, 103, 119, 145, 302].

with measurements of metabolic rates, it becomes possible to directly estimate the worker size that cuts leaves most ergonomically, and thus to answer the question which worker size is best suited to cut different leaves— thus, a powerful predictive framework to study if leaf-cutter ants are optimal foragers emerges.

4.2 Materials & methods

4.2.1 Study organisms

Atta cephalotes leaf-cutter ants were sampled from a mature laboratory colony. From this main colony, a total of four sub-colonies were established. Each sub-colony was used for periods between 1 – 6 months, dependent on the time point at which foraging activity declined. The use of sub-colonies was essential, as they allow experimental manipulation without impacting the health of the main colony containing the queen (see also [303–307]). Each sub-colony consisted of an 18 $\times$ 18 $\times$ 20 cm (L $\times$ W $\times$ H) fungus box containing of the order of 1,000 of individuals. The box was connected to a small foraging area on one side (32 $\times$ 20 $\times$ 10 cm) and waste box on the other (13 $\times$ 7 $\times$ 5 cm) via PVC tubing (inner diameter 25 mm) (Figure 4.1a). Colonies were kept in a climate-controlled chamber (FitoClima 12.000 PH, Aralab, Rio de Mouro, Portugal) at 25°C, 60 $\pm$ 5% relative humidity, and in a 12-hour day/night cycle. They were fed each evening with small amounts of bramble, laurel, kibbled maize, and honey water—enough to maintain the fungus gardens and avoid starvation effects but not so that foragers lost their motivation [102, 308].

Worker size manipulation

Due to the task-specialisation within the polymorphic work force, there is a certain mass range that is more likely to forage [68, 134]. In an extremely polymorphic *Atta* species such as *Atta cephalotes*, body mass differences between the smallest and largest works span nearly two orders of magnitude [174]. In general, ants with a body mass between 1-50 mg may actively partake in foraging. However, individuals with a body mass between 3-9 mg dominate foraging parties, and comprise over 60% of all cutting speed measurements. To obtain representative measurements across the full size range, I hence manipulated the foraging party size-distribution (for a similar approach see [134]). To encourage workers with a body mass less than 3 mg, custom 3D printed gates were inserted at the connections to the foraging area and waste box. These gates had holes approximately 2 mm in diameter, such that only workers below 3 mg were able to pass through to forage, but larger workers were not. To obtain cutting measurements from the largest workers, custom 3D-printed sliding gates limited access to the foraging area and workers heavier than 9 mg, were selected from the sub-colony at random, and were added to the foraging arena. For workers heavier than 50 mg further manipulation was required. Using insect tweezers, I manipulated individuals such that they started

biting into a substrate, which eventually triggered cutting behaviour. At this point, the individual was released from the tweezer grip, and proceeded to cut a fragment.[19]

4.2.2 Cutting substrates

Cutting speed measurements were conducted on both natural and pseudoleaves. Leaves provide insight into realistic foraging behaviour in the wild, but introduce uncontrolled variability. Pseudoleaves, in contrast, are homogeneous and can be fully mechanically characterised, allowing precise control over key properties such as thickness and toughness. These factors make pseudoleaves valuable for directly linking cutting behaviour to mechanical power. Here I present cutting speed measurements on natural substrates; however, see Chapter 3 for pseudoleaf cutting speed results and concluding remarks for their conceptualisation.

I selected bramble, laurel and rose petals as natural cutting substrates, as they span a broad range of cutting forces (Table C.1), representing approximately 60% of tropical leaves [35]. Leaves of bramble (*Rubus fruticous*) and laurel (*Aucuba japonica*) were collected from a private garden on Imperial College campus grounds (51.50078° N, -0.17242° W). Leaves were harvested, wrapped in damp tissue to minimise water loss [184], and refrigerated in a sealed container until use on the same day. Leaf structural and mechanical properties typically vary with leaf age [62, 160, 184–187]. To minimise the influence of such covariation on our results, leaf colour served as a qualitative proxy for leaf maturity [188]: only laurel and bramble leaves with dark green colouration were used for experiments. Rose petals were bought from local suppliers, used on the day of purchase, and stored as above. Before each experimental trail, the leaf edges were trimmed using a scalpel blade such that they had straight edges; this process was necessary to aid automated image analysis downstream (see 4.2.3). A thickness map for each leaf or petal was created by taking six thickness readings at random positions with a digital micrometre; the thickness of the mid vein and minor veins was also recorded as present.

4.2.3 Cutting speed measurements

Experimental protocol

A Raspberry Pi HQ camera (V1.0 2018, Raspberry Pi model 3, UK) was positioned above the sub-colony foraging area to take recordings at 15 frames per second (FPS) in a top-down view (Figure 4.1a and 4.1b).[20] The camera was controlled via Raspicam (V2.1.2) using an ISO of 400, a shutter speed of 39 milliseconds, and a resolution of 1600×1200 px . Test substrates were placed on a small table in the foraging area of the sub-colony, to limit the number of ants that were cutting at any given time. This was necessary to ensure the successful paired retrieval of both the leaf fragment and the ant after each cut. Ants were left to forage naturally, and once a complete fragment had been cut, both the ant and fragment were collected and placed in a petri dish. Each ant was weighed to the

[19] In the cases of these "extreme" manipulations not all were conducted equally – in the case of rose petals it was especially hard to motivate the larger workers to cut.

[20] This frame rate was sufficient to resolve the relatively slow cutting speeds of 0.02 - 0.5 mms^{-1}.

nearest 0.1mg (Explorer Analytical EX124, max. 120 g × 0.1 mg, 130 OHAUS Corp., Parsippany, NJ, USA) and the fragment was filed in a fragment catalogue for further analysis.

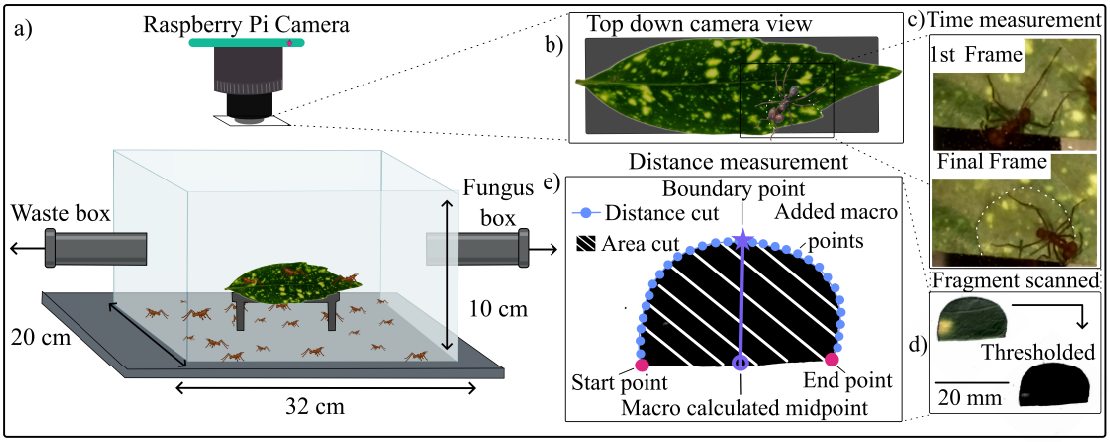


FIGURE 4.1: In order to quantify mechanical power output during cutting, I measured the cutting speed of *Atta cephalotes* workers on three natural substrates: laurel, bramble and rose. a) To measure cutting speeds, a RaspberryPI video camera was clamped above the foraging area. Substrates were placed on a small 3D printed table to limit access and thus the number of foragers that were cutting at any given time. b) The camera recorded a top-down view of the foraging area such that cutting behaviour could be observed, and cut time and distance obtained. c) Cutting time was extracted by manually identifying the beginning and end of cutting, facilitated by a characteristic "scissor cutting" technique used by the ants in these instances. By dividing the total number of frames with the camera frame rate, the total cutting time follows. d) Cutting distance was obtained by scanning each fragment harvested, fragment catalogues were then thresholded and pixels were converted to mm using a conversion factor obtained from the dpi of the scanner. e) A custom written macro was used to obtain the cut distance. First the user selects the cut arc's start and end points. The macro calculates the midpoint and sweeps orthogonally until detecting a colour change at the leaf-paper boundary, placing a boundary point. After the first three points the macro then iterates 5 times placing a total of 33 points along the fragment edge. The total distance of the arc is then calculated.

Cutting speed analysis

Average cutting speed was determined as the ratio between cut distance and cutting time. The cutting time I recorded included not only active cutting but other behaviours, such as head and body repositioning and pivoting – the average cutting speed is thus likely much slower than the actual speeds of mandible movement through the substrates. However, mandible movements are challenging to resolve due to their small size, and average cutting time is likely the more biologically relevant metric. The average cutting speed is likely proportional to the speed of mandible movement, because there is no obvious reason why the time to reposition the body should vary across substrates; it thus serves as a plausible and accessible proxy.

Cutting time was extracted from the video recordings; Raspicam videos were exported in .h264 format and converted to .HVI files via FFMPEG (V7.0.2) for analysis. HVI files were imported into ImageJ (ImageJ 1.54f, National Institutes of Health, New York, USA) as an image stack for analysis. I identified the frames where ants engaged in scissor cutting – a characteristic cutting technique used by ants to initiate and finish fragment cutting [271]. Scissor-cutting was clearly visible in the video

recordings, due to the orientation of the head capsule relative to the substrate plane (Figure 4.1c). The cutting time then follows as the ratio between the number of frames between cut initiation and cut completion and the frame rate.

To estimate the distance cut, the cut fragment was retrieved from the chamber and scanned with a 1200dpi scanner (PageWide Managed Colour MFP E58650dn, HP, UK). Scanned fragment sheets were analysed in ImageJ. First the sheets were split into RBG channels, and blue was isolated for the highest contrast. This channel was then converted to a binary image using a greyscale threshold of 141, chosen to remove shadows and image artefacts (Figure 4.1d). Pixels were converted to distance using a conversion factor of 47.24 pixels per mm determined from the dpi of the scanner. Cut distance was extracted from the thresholded images using a custom-written ImageJ macro (for similar see [272]). The start and end points of the cut arc are manually selected by the user, with the arc of the cut on the left with respect to the starting point. The macro then calculates the distance between the two points and places a midpoint. From this midpoint the macro sweeps orthogonally in increments until detecting a colour change which happens at the boundary between the black leaf fragment and white paper, here a boundary point is placed. The number of points (P) along the cut arc is given by:

$$P = 1 + 2^n \tag{4.1}$$

Where n is the number of iterations, after several preliminary trails 5 iterations was found to be optimum to sufficiently describe the shape, leading to 33 placed points (Figure 4.1e).

Measurements were deemed invalid if fragments were lost, the start and end time could not be easily identified, or if there was any uncertainty around if the collected ant was indeed the ant that cut the fragment. After exclusion in total, I obtained n=225 measurements of cutting speed for each leaf type giving a total sample size of N=675.

Fragment area, volume, and energy

I additionally measured fragment area using a custom macro. After thresholding the fragment and spatially calibrating the area with the pixel-to-mm conversion factor, the fitted points used to calculate cut distance were applied to mark the fragment parameters (Figure 4.1d, e). The significant pixel intensity contrast between the dark fragment perimeter and the white background allowed the "analyze particles" function in ImageJ to accurately calculate the area of the contrasting pixels. From the measured fragment area, I then calculated fragment volume by multiplying the area by each fragment's thickness.

To gauge the energy gained by the fungus per fragment harvested I converted fragment volume to mass using the leaf tissue area density value reported by Onoda [35] for our plant species: laurel (*Aucuba japonica*) - 0.3043 g cm^{-2}, bramble (*Rubus fruticous*) – 0.2123 g cm^{-2} and rose – 0.1897 g cm^{-2}. Having calculated the fragment mass I then calculated the energy gained by the fungus per

fragment via the method described by Burd [145] (see also [309] for first use):

$$G = mh(4500)(0.45)(4.19) \tag{4.2}$$

Where m is the mass of the leaf fragment in grams, h is the fraction of dry mass of the leaf species, 4500 is the conversion factor applied for calories to dry mass in grams, 0.45 relates to the percentage of energy obtained by the fungus and 4.19 is the joules to calorie conversion rate. Again, I used Onoda's tropical leaf dataset [35] to obtain the fractional concentration of dry mass for each substrate, laurel – 0.35874, for bramble and rose I assumed the same fractional concentration of dry mass as this data was not available. To calculate energy balance of cutting I additionally calculated energetic investment per fragment. I took the product of cutting time across worker size for each substrate with CMR given in μW or Js^{-1} to obtain energy invested per fragment in joules. In order to assess cutting strategy of the sub colony as a whole, I also calculated the worker size distribution frequency in percentage of total workers for each substrate to see if the distribution of workers changed with substrate.

4.2.4 Data curation and statistical analysis

Extraction of the total cutting time, cut distance, and cut area were completed in ImageJ (ImageJ 1.54f, National Institutes of Health, New York, USA). All subsequent handling of data including calculations of cutting time, fragment volume, fragment mass, and energy gained and invested calculations were conducted in RStudio (v. 4.1.1). I utilised analysis of covariance (ANCOVA) on log transformed data to compare the effect of mass, substrate, and the interaction of the two on the measured experimental factors (see above). I utilised ordinary least squares (OLS) regression on log-log space to characterise the mass scaling exponent and intercepts. Before conducting statistical tests, all assumptions were verified as outlined in section 3.2.5. All statistical analysis, data curation and plotting were conducted in R (v. 4.1.1). The implementation of the mechanical model to estimate cutting speed was conducted in Python (v. 3.9.7) using the SciPy package and optimise fit function. As, was the derivation of mechanical power to calculate efficiency.

4.3 Results

4.3.1 Cutting time, fragment size, and cutting speed vary with worker body mass and substrate

Total cutting time decreased significantly with worker body mass (ANCOVA mass: $F_{1,\,674} = 241.56$, $p < 0.001$, see Table 4.1 and Figure 4.2a). On average, larger workers (>20 mg) spent 45 seconds less per fragment than smaller workers (<20 mg), a relative increase of 55%. The strength of this size-effect varied across substrates (ANCOVA mass:substrate: $F_{1,673} = 31.91$, $p < 0.001$), as evident in the different allometric relationships (Table 4.1). The pre-factors indicate the parameter estimate for a worker of 1 mg, equal to 316 s, 191 s, and 174 s on laurel, bramble and rose, respectively (Figure 4.2a).

TABLE 4.1: Results of ordinary least squares (OLS) regressions describing the relationship of cutting time, fragment mass, and cutting speed for each biological substrate with body mass in milligrams. Parameters represent values in an equation of the form $y = am^b$ where the pre-factor represents a (the parameter estimate for a 1 mg body mass worker) and b is the mass scaling exponent. Subscripts indicate 95% confidence intervals. All regressions were conducted on $\log_{10}$-transformed data.

Cutting time			
Substrate	Pre-factor (sm^{-b})	Mass scaling exponent	R^2
Laurel	$_{281.84}$ 316.23 $_{346.74}$	$_{-0.47}$ -0.43 $_{-0.38}$	0.63
Bramble	$_{147.91}$ 190.55 $_{239.88}$	$_{-0.46}$ -0.40 $_{-0.23}$	0.48
Rose petals	$_{151.36}$ 173.78 $_{199.53}$	$_{-0.45}$ -0.37 $_{-0.29}$	0.42
Fragment mass			
Substrate	Pre-factor (mgm^{-b})	Mass scaling exponent	R^2
Laurel	$_{4.9}$ 5.75 $_{6.8}$	$_{0.25}$ 0.42 $_{0.59}$	0.42
Bramble	$_{3.84}$ 4.55 $_{6.25}$	$_{0.37}$ 0.46 $_{0.71}$	0.24
Rose petals	$_{3.72}$ 4.12 $_{5.05}$	$_{0.38}$ 0.48 $_{0.56}$	0.36
Cutting speed			
Substrate	Pre-factor (mm $s^{-1}m^{-b}$)	Mass scaling exponent	R^2
Laurel	$_{0.037}$ 0.042 $_{0.047}$	$_{0.52}$ 0.57 $_{0.61}$	0.61
Bramble	$_{0.048}$ 0.054 $_{0.059}$	$_{0.47}$ 0.54 $_{0.57}$	0.67
Rose petals	$_{0.058}$ 0.065 $_{0.078}$	$_{0.48}$ 0.54 $_{0.58}$	0.59

Fragment mass increased significantly with worker body mass (ANCOVA mass: $F_{1,674} = 370.03$, $p < 0.001$, see Table 4.1 and Figure 4.2b); large workers cut fragments approximately 2.5 times heavier than fragments cut by their smallest counterparts. Fragment mass and its variation with size also differed significantly across substrates (ANCOVA mass:substrate: $F_{1,673} = 0.038$, $p = 0.0439$, see Table 4.1); the pre-factors differed significantly across all three substrates (Table 4.1) (ANCOVA substrate: $F_{1,674} = 23.52$, $p < 0.001$), and the average fragment mass for a 1mg worker was 5.75 mg, 4.55 mg and 4.12 mg for laurel, bramble and rose respectively (Figure 4.2b). Cutting speed increased significantly with worker body mass (Figure 4.3a) (ANCOVA mass: $F_{1,674} = 1358.99$, $p < 0.001$; see Table 4.1). On average, larger workers cut almost 10 times faster than smaller workers across all substrates. The effect of worker body mass on speed did not depend significantly on substrate type (ANCOVA mass:substrate $F_{1,673} = 1.105$, $p = 0.332$). However, the pre-factors differed significantly (ANCOVA substrate: $F_{1,674} = 62.148$, $p < 0.001$); a worker of 1 mg body mass cut with a speed of 0.04 mms^{-1}, 0.05 mms^{-1}, and 0.07 mms^{-1}, for laurel, bramble and rose, respectively.

A complete statistical analysis for all three parameters is presented in Appendix C.

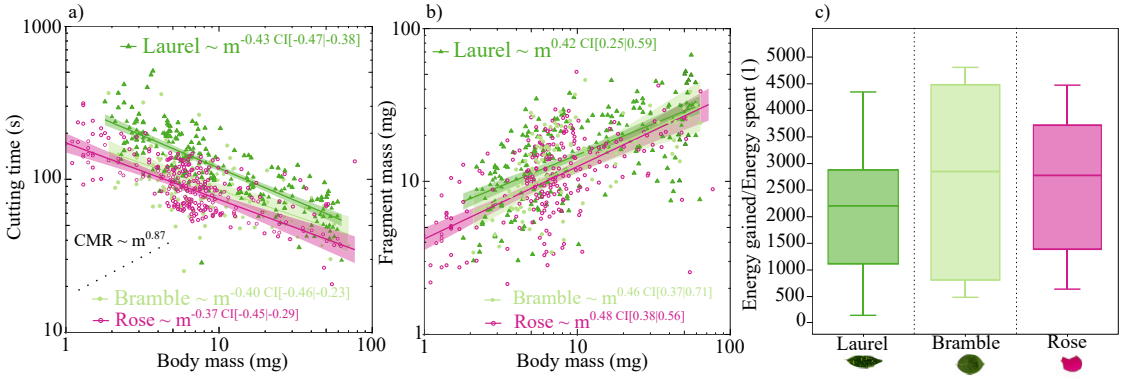


FIGURE 4.2: To investigate how the energetic gain varies across worker size and substrate type, I estimate the energy invested in cutting a leaf fragment and compare it to a rough estimate of the energy returned. (a) The total time spent cutting decreased with body mass across all substrates, but the exact allometric relationships varied across substrates. In general, ants spend longer cutting tougher plant tissues. (b) The fragment mass increased significantly with worker body mass; the mass scaling coefficient was roughly the inverse of the scaling coefficient for the total cutting time. Fragment mass decreased slightly but significantly with substrate toughness, with larger fragments harvested on tougher substrates. (c) To gauge the energetic cost invested per fragment, the total cutting time was multiplied by the metabolic costs of cutting, which are independent of tissue toughness (Chapter 2). Following Burd [145], I estimated the energetic gain per unit fragment mass to obtain the energy gain as a function of worker body mass. The ratio of energy gained vs invested was larger in bramble (2824) and rose (2805) compared to laurel (2275), and thus lowest in the toughest leaf.

4.3.2 Energy gained vs energy invested scale with the same mass scaling exponent but differ by a factor of over 2000

To gauge the total metabolic energy each worker invested per fragment, the total cutting time was multiplied with the CMR, (see Chapter 3). Due to the strong allometry of the CMR, CMR $\propto m^{0.87}$, the energy investment per fragment significantly increased with body mass (ANCOVA mass: $F_{1,674}$ = 677.725, p < 0.001), but less starkly, due to reduction in cutting time with body mass (Table 4.2). The mass scaling exponents varied significantly across substrates (ANCOVA mass:substrate: $F_{1,673}$ = 4.319, p = 0.0137): the largest workers spent about 3.5 times less energy than the smallest worker when cutting rose petals, and about 3 times less energy when cutting laurel. The pre-factors also differed significantly across the three substrates (Table 4.2): a worker of 1 mg body mass invests 0.008 J, 0.005 J and 0.004 J into cutting laurel, rose and bramble fragments, respectively. Where energy invested is a simple product of metabolic power and time, the energetic gain is somewhat more complex: it strictly depends on the energetic content per leaf fragment that the colony fungus can convert, which is challenging to estimate [145]. I follow previous work in the reasonable assumption that this energy is generally proportional to fragment mass and estimate an approximate proportionality constant [145]. Because the energetic content is likely proportional to fragment mass, the estimated energetic gain varies with worker mass in the same way as the fragment mass. The absolute values of the pre-factors, however, change (see table 4.2). This change is a direct function of the assumed energy density of each leaf mass and is thus subject to uncertainty (see 4.2). A worker of 1 mg body mass gains 18.2 J, 14.12 J and 11.22 J per fragment on cutting laurel, rose and bramble,

respectively For all three substrates, energy gained and invested shared statistically indistinguishable scaling exponent; the intercepts, however, differed (see Appendix C). The ratio between energy gained and invested accordingly differed significantly across substrates, and was lower for tougher leaves; this effect, however, was small (Figure 4.2c). The ratio of energy gained vs invested for a 1 mg worker was 2275, 2824 and 2805 for laurel, bramble and rose respectively.

TABLE 4.2: Results of ordinary least squares (OLS) regressions describing the relationship of energy invested and energy gained per fragment for each substrate with body mass in milligrams. Parameters represent values in an equation of the form $y = am^b$ where the pre-factor represents a, which is the parameter estimate for a 1 mg body mass worker, and b is the mass scaling exponent. Subscripts indicate 95% confidence intervals. All regressions were conducted on $\log_{10}$-transformed data.

Energy invested			
Substrate	Pre-factor (sm^{-b})	Mass scaling exponent	R^2
Laurel	$_{0.007}$ 0.008 $_{0.009}$	$_{0.32}$ 0.44 $_{0.50}$	0.59
Bramble	$_{0.004}$ 0.005 $_{0.006}$	$_{0.40}$ 0.50 $_{0.56}$	0.39
Rose petals	$_{0.003}$ 0.004 $_{0.005}$	$_{0.36}$ 0.47 $_{0.59}$	0.34
Energy gained			
Substrate	Pre-factor (mgm^{-b})	Mass scaling exponent	R^2
Laurel	$_{12.02}$ 18.2 $_{27.54}$	$_{0.25}$ 0.42 $_{0.59}$	0.42
Bramble	$_{7.41}$ 14.12 $_{16.98}$	$_{0.37}$ 0.46 $_{0.71}$	0.30
Rose petals	$_{9.46}$ 11.22 $_{13.49}$	$_{0.38}$ 0.48 $_{0.56}$	0.36

4.3.3 Worker size-frequency distribution

To assess whether tougher substrates are cut by larger workers, I inspect the size-frequency distribution across substrates (Figure 4.3b). All distributions had a large right tail, which makes statistical characterisation challenging. Workers cutting laurel, the toughest leaf, had a body mass mode of 6.1mg (minimum 2.1 mg, median 7.3 mg, mean 15.7 mg); the equivalent masses for bramble and rose were 5.0 mg and 3.9 mg (minimum 1.4 mg and <1 mg, median 6.4 mg and 6.2 mg, mean 10.6 mg and 8.4 mg respectively). The percentage of workers heavier than 50 mg was about 15% for laurel - three times higher than for rose (Figure 4.3b). Thus, tougher leaves tend to be cut by larger workers.

4.4 Discussion

4.4.1 A biomechanical model to rationalise the variation in cutting speed

Cutting speed, cutting time and cut distance are significant metrics in the foraging performance of an attine ant colony. Cutting time and speed combine to define the total length cut, and so the fragment size and thus resource intake. The longer the time invested per fragment, the more energy it costs;

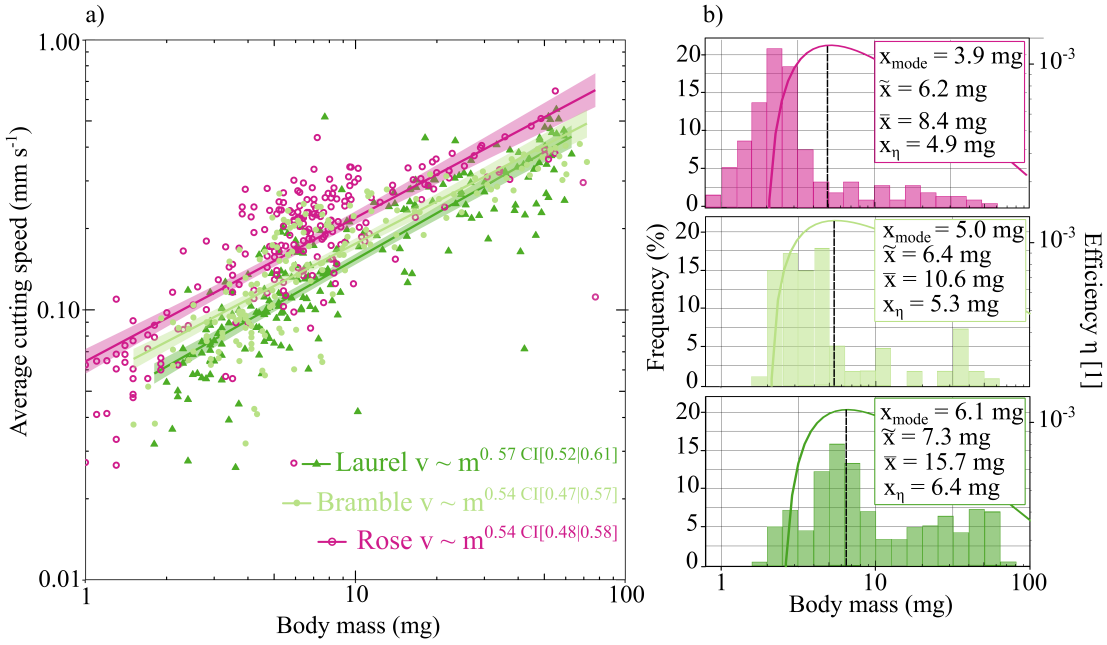


FIGURE 4.3: a) Cutting speed varied significantly with both worker body mass and substrate type. Large workers cut almost ten times faster than small workers independent of substrate type (ANCOVA mass:substrate: $F_{1,673}$ = 1.105, p = 0.332); the intercepts, however, differed significantly: workers cut rose petals about 1.5 faster than laurel leaves (Table 2). b) Tougher leaves were cut by larger workers, as indicated by the size-frequency distribution obtained from the cutting speed trials. x_{mode} denotes modal worker mass, $\tilde{x}$ denotes the median worker mass and $\bar{x}$ denotes the arithmetic average worker mass. Note that the x-axis is logarithmic, and that all distributions have a right tail, which tends to be heavier for tougher substrates. Overlayed behind each frequency plot is the calculated efficiency curve for each substrate, where x_η denotes the most efficent worker size (see 4.4)

the larger the fragment mass gained per time, the larger the resource gain for the colony. However, the mechanical demands of cutting are not alike across individuals and substrates. Although I initially followed the typical process in allometric studies and described the variation of cutting speed with body mass as a simple power law (Figure 4.3a), it brings with it several problems, and the quality of the model fit may be deceiving.[21] Firstly, it implicitly assumes that the cutting speed only drops to zero in the limit of vanishing worker mass, which is non-physical. Instead, speed should drop to zero below the critical worker size that is just about able to cut the leaf, i.e., produce a bite force larger than the required cutting force. One way to avoid this problem is to follow previous work [134, 139], and instead fit a linear relationship with intercept in linear space. However, such fits indicate that the observed relationship violates assumptions of linear regression, and indeed yields positive and not negative y-intercepts, again physically inconsistent. How should the relationship between cutting speed and body mass be modelled?

Within the three experimental chapters of my thesis sits a common theme: even a superorganism cannot escape the laws of physics, and leaf-cutter ant performance must be bound by mechanics. I take the same approach to rationalise the variation of cutting speed with size. In Chapter 2 of this

[21] Reminiscent of the classic example of "a line to guide the eye" [310].

thesis, I noted that a necessary criterion for cutting is that the cutting force (F_c), the minimum force required to cut a material must be smaller than the maximum bite force (F_b) an ant can produce. But if this condition is met, what determines cutting speed? In the introduction of this thesis, I explain how bite force and cutting force relate to cutting speed through the muscle's force velocity properties, as described by the Hill relation (see section 1.1.2). Given the uncertainty surrounding the appropriate K value for invertebrate muscle, I adopt the linear form of the Hill model as a parsimonious starting point:

$$F = F_{max}(1 - v_{\text{rel}}) \tag{4.3}$$

In order to retain relation from the model to the experimental data I note here we are interested in the speed of the mandible. Muscle actuates the mandible via a joint that has a gear ratio G; therefore, the maximum speed of the mandible v_{man} is given by (adapted from [95]) :

$$v_{\text{man}} = v_{\text{max}} G^{-1}$$

It then follows that the bite force, F_b, applied by the mandible on the leaf, will equal the generated force F, multiplied by the gear ratio G:

$$F_b = FG$$

An immediate implication of the co-variation of force and velocity encoded in the Hill relation is that there exists a maximum speed, at which muscle can actuate the mandible against an opposing force (P). This speed, $v_{\text{man},\kappa}$, can be derived by setting the Hill equation equal to the external force, which yields:

$$v_{\text{man},\kappa} = v_{\text{man}} \left(1 - \kappa\right) \tag{4.4}$$

where $\kappa = P \left(F_{\text{max}} G\right)^{-1}$ is the ratio between the opposing force (equal to the cutting force F_c) and the maximum driving force (equal to the bite force F_b) exerted by the mandible.

Empirical estimates for both cutting and bite force exist: within Chapter 2 of this thesis, mandibular cutting forces were measured as a function of ant worker size (see also [55]). Püffel et al. [90] characterised the strong positive allometry of bite forces in closely related *Atta vollenweideri*. v_{man} may first be defined in terms of morphological parameters, $v_{\text{man}} = l_f \dot{\varepsilon}_{\text{max}} G^{-1}$; here, l_f is the muscle fibre length, G is the gear ratio, and $\dot{\varepsilon}_{\text{max}}$ is the maximum muscle strain rate. Both fibre length and gear ratio may again be estimated from scaling data in closely related *A. vollenweideri* [89], but there exist no measurements for muscle strain rate (although see [311] for mandible closing speeds).

To deal with this problem, I note that equation 4.4 predicts the maximum *instantaneous* speed, but the quantity of interest is the *average* cutting speed (see methods); thus, the cutting speed should not be equal but proportional to $\dot{\varepsilon}_{\max}$. I hence parametrise the model such that I fit a pre-factor, and replace all other quantities with their empirical estimates, yielding:

$$v_c = am^{0.25}\left[1 - \frac{F_c}{F_b}\right] = am^{0.25}\left[1 - \frac{F_c}{7501}m^{-0.9}\right] \tag{4.5}$$

where I assumed, in keeping with the classic scaling literature, that the strain rate is size invariant and used $G \propto m^{0.05}$, $l_f \propto m^{0.29}$ and $F_b \propto m^{0.90}$ from [89].

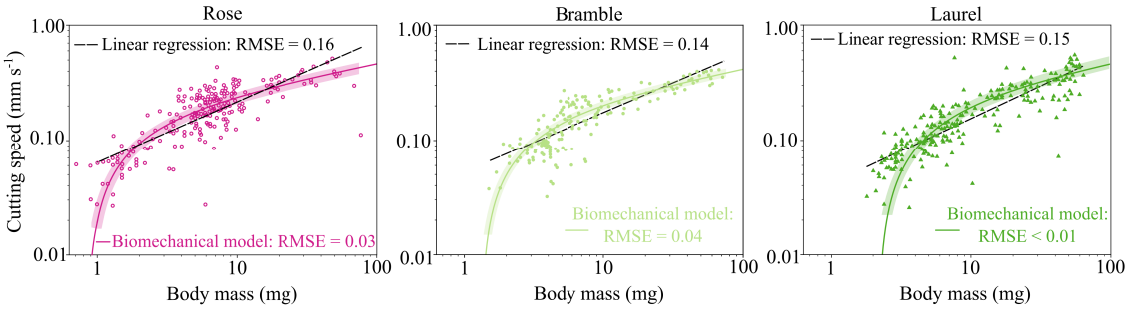


FIGURE 4.4: The variation of cutting speed with worker size may be characterised with a simple power law. Though consistent with classic scaling literature, this approach predicts nonphysically that even the tiniest workers can cut leaves. To overcome this limitation, cutting and biting mechanics may be combined with musculoskeletal modelling to directly predict cutting speed (Equation 4.5). Applying the model to our dataset requires knowledge of relevant physical parameters. In the first chapter of this thesis, I measure directly the cutting force F_c, which is the minimum force needed to fracture a material with forager mandibles. From previous work by Püffel *et al* I obtain the scaling of bite forces and relevant morphological parameters [89, 91]. I find that the model I derive to quantify the non-linear variation of cutting speed produces the best fit to the experimental data both visually and statistically (Appendix C).

The derived mechanical model appears to fit the experimental data well visually (Figure 4.4); however, to assess the "trueness" of the fit, I employed three model robustness metrics: R^2, Root Mean Squared Error (RMSE), and Akaike Information Criterion (AIC). For comparison, I also evaluated linear regressions in both log-log and Cartesian space, serving as a null hypothesis of sorts (see above for rationale). Across all metrics, the mechanical model outperformed both linear fits (see Appendix C, Table C.5). As an final model test, I compared the performance of the biomechanical model derived from the linear Hill relation ($K = 0$) to one based on a more physiologically realistic force–velocity curve ($K = 4$), commonly used for invertebrate muscle (See C.2). This allowed me to test whether incorporating a more realistic curvature improves the fit. However, the $K = 4$ model required an implausibly low value of κ to match the data and was outperformed by the $K = 0$ model in terms of RMSE (See C.3).

Importantly, the linear Hill model also benefits from greater simplicity. It uses fewer fitted parameters than a typical power-law or curved Hill fit, with its sole free parameter controlling only the magnitude, not the shape, of the curve.

4.4.2 Mechanical power and efficiency

To pivot the results towards a final estimation of worker efficiency, I combine our cutting speed equation with cutting force to calculate mechanical power:

$$P_{mech} = F_c v_c \tag{4.6}$$

Noting that cutting force F_c acts solely as a pre-factor after finding it has no mass scaling component (see Chapter 2), meaning the shape of the fit from the speed relation will not change. The mechanical power then follows as:

$$P_{\text{Mech}} = F_c v_{\text{c}} = F_c a m^{0.25} \left[1 - \frac{F_c}{7501} m^{-0.9}\right] \tag{4.7}$$

Where F_c is the cutting force as measured in Chapter 2 with forager mandibles, all other parameters have been previously defined. In Chapter 3 of this thesis I define efficiency as the ratio of mechanical and metabolic power:

$$\eta = \frac{P_{mech}}{P_{met}} \tag{4.8}$$

By measuring the metabolic cost of cutting pseudoleaves differing in mechanical power I converge on the finding that metabolic power is constant regardless of mechanical demands, and was empirically found to be described accurately by:

$$P_{met} = cm^{0.87} = 3534m^{0.87} \tag{4.9}$$

Having defined both mechanical and metabolic power can combine the two and look to address aspects of efficiency:

$$\eta = F_c \frac{a}{c} m^{-0.62} \left[1 - \frac{F_c}{7501} m^{-0.9}\right] \tag{4.10}$$

From Equation 4.10 there are three key features of the resultant efficiency curves that must be considered carefully (see Figure 4.3b). First, the vertical asymptote found on the right-hand side of the graph. This arises as cutting speed and thus mechanical power output drops to zero when the bite force $F_b \leq F_c$ — this is a physical limit of which workers below this size cannot cut. As a result cutting speed, mechanical power and thus efficiency drop to zero. Second, the existence of a (local) maxima. Initially, the scaling of cutting speed outpaces the rise in metabolic cost with size but then drops below it. It is at this peak we find the worker size most efficient for cutting the given substrate given by η (see Figure 4.3). Finally to the right of the maxima, efficiency begins to decrease. Cutting speed continues to increase with size but not as starkly as the increase in metabolic costs. Within

this region (to the right of the maxima) of the efficiency curve workers have the *ability* to cut but are not the most *suitable*.

After developing a predictive tool to estimate efficiency variations based on size and substrate, the final step is to evaluate whether these predictions align with observed patterns (Figure 4.3b). I begin with a basic comparison to the measured worker size frequency distribution plots (Figure 4.3b): Are the produced optimal worker sizes (x_η) within the correct order of magnitude? Finding that across all three substrates, x_η falls between 4.9 and 6.4 mg, which is within the mass range of media workers commonly observed foraging [68, 134–136], providing a reassuring first comparison. Next, the worker size frequency distribution plots reveal that foraging patterns shift with substrate mechanical demand, with larger workers more likely to forage on mechanically demanding substrates (Figure 4.3b). Specifically, more large workers forage on laurel than on rose. These findings mirror those of Wilson, who also noted a similar shift while observing natural foraging behaviour in the Neotropics [134]. The efficiency curves also mirror this shift with increasing mechanical demand, aligning with the observed experimental data. The most efficient worker mass (x_η) is identified as 3.9 mg on rose petals, the softest vegetation, and 6.1 mg on laurel, the toughest vegetation. When comparing the modal worker mass (x_{mode}) to the calculated optimal worker mass (x_η) I find a percentage difference of 4.8%, 5.8% and 22.7% for laurel, bramble and rose respectively, representing a reassuring first agreement of dynamic efficiency modelling and experimental observations.

4.5 Conclusions and outlook

Cutting speed has long been a determinate for the foraging performance of an insect colony [134, 139]. Previous studies have taken a correlative approach using experimental data to define a relation to body mass, using linear regressions. However, linear fits can be deceiving and give unphysical values, namely the cutting speed only drops to zero in the limit of vanishing worker mass. In this chapter I address the need for a predictive tool grounded in physical parameters to assess the variation of cutting speed.

In this chapter I derive a predictive mechanical model for the variation in cutting speed from measured experimental and morphological parameters. In combination with cutting force (Chapter 2) I derived an equation for mechanical power output. Finally in combination with metabolic power (Chapter 3) I synthesise the results from all my experimental chapters of my thesis to generate a model that allows dynamic prediction of efficiency variations across worker size and substrate properties. I then compare the optimal predicted worker mass (x_η) to the modal experimental size found foraging finding a reassuring first comparison between experimental and predicted values. This model provides a strong basis to test other modulating factors of efficiency, such as mandibular wear and can serve as a guide allowing larger scale predictions of efficiency from field work.

5 Concluding remarks

Herbivorous insects are ecosystem engineers, physically and structurally altering plants as they feed [10, 15]. Their activities result in millions of pounds in crop damage annually [69, 74]. Regardless of insect size or plant type, herbivory cannot occur without the ability to fracture plant tissue. Cutting is therefore a key modulating factor in the efficacy of herbivory. The efficiency of cutting can be studied conceptually the same way a mechanic would study the efficiency of a motor, as a ratio of useful power output over power input:

$$\eta = \frac{P_{out}}{P_{in}} \tag{5.1}$$

Within all living organisms the power input will always be an individual's metabolic rate.[22] In the specific case of cutting efficiency, this is the metabolic rate during cutting (denoted previously as (P_{met}, Chapter 4). Here, I define useful power output as P_{mech} which is the product of F_c and v_c. Including all terms, the general equation for cutting efficiency is thus given by:

$$\eta = \frac{F_c v_c}{P_{met}} \tag{5.2}$$

From this simple equation, I have identified the three key factors required to build a predictive model for efficiency.

By conceptualising leaf cutting as a fracture process, I assessed the modulating factors of F_c — the force required to initiate and propagate a cut in plant tissue. Given the importance of F_c in constraining herbivory (see Introduction 1.1.2 and Chapter 2), studies that establish a concrete biomechanical link between size-specific and substrate-specific foraging constraints remain rare (but see [91, 311, 312]). Prior efforts to experimentally measure F_c have been limited by reliance on natural substrates, which are inherently inhomogeneous and anisotropic. For example, Schofield used *O. macrantha* leaves that were later shown to be significantly anisotropic, necessitating complex force corrections and precluding direct comparisons between cutting force and foraging performance [139].

Recognising these limitations, I developed a predictive biomechanical model linking F_c to both substrate mechanics and tool morphology [168] (see Chapter 2 for full derivation), thereby providing a concrete link between cutting performance and the underlying mechanical constraints. To enable

[22] Respiration is of course the fire of life [97].

meaningful and novel progress beyond prior work, I tested this framework using standardised, homogeneous pseudoleaves — a key methodological advance[23]. This approach allowed me to isolate the key determinants of cutting performance without the confounding effects of natural substrate heterogeneity. Guided by the validated mechanical model, I was then able to replicate my findings on real leaves, providing for the first time a concrete link between mechanical constraints and foraging performance on natural substrates.

While much of the study focused on how variation in material properties modulates F_c, tool length scale also emerged as a critical factor — with mandibular wear alone increasing F_c by up to a factor of five. A limitation of this thesis is that I reviewed arbitrary effects of wear (i.e. using mandibles from foragers at different life stages and thus showing different levels of wear). I did not assess mandibular wear level systematically. This is also a limitation of past studies where direct evidence for a positive or negative effect on wear rate is rare [247] and often ambiguous if not conflicting [e. g. [171, 244, 248]]. A natural extension would be to assess the effects of wear systematically. Cutting force measurements could be conducted on abrasive substrates such as fine sandpaper. Then, wear per unit distance cut could be quantified using pristine mandibles as a control. In combination with synthetic substrates, these measurements could also be conducted on plant leaves rich in wearing structures such as abrasive silica [313]. Systematically quantifying wear per unit distance would provide insights into how mandibles perform as cutting tools over an individual's lifetime. These results could potentially inspire better solution for engineering plants than can better resist damage from herbivory.

Finally, one might question how predictive is a biomechanical model of F_c, derived from leaf-cutter ants alone, for other herbivorous insects? Leaf-cutter ants are atypical folivores: they neither chew nor directly consume the plant material they harvest. It is therefore important to consider the extent to which insights from a simplified blade-cutting model can be generalised to other biting-chewing insects. This is challenging because the kinematics of chewing involve two opposing mandibles, and are thus harder to replicate ex vivo. The choice of the relevant tool length scale is also less obvious for larger mandible surface areas involved in chewing. However, neither a variation in chewing kinematics nor in mandible geometry influence the minimal energetic cost that determines the lower bound for the fracture force. Therefore, the general energetic picture derived from fracture mechanics and the insights it affords remain valid [56]. Indeed, first-order mechanical models of scissor cutting, perhaps the closest simple analogue to leaf processing by chewing, yield essentially the same equations [61]. Further research is required to sharpen the understanding of the interaction between mandible geometry, material length scale, mandible kinematics, and mechanical effort across insects with biting-chewing mouthparts.

Having established a predictive model for how F_c varies with material properties and thus mechanical demand, the next missing piece in developing a predictive framework for efficiency is understanding how changes in mechanical demand translate into shifts in metabolic cost whilst cutting.

[23] Cutting force results using this methodology have been previously published, with my contributions noted [91, 92].

The energetics of cutting is a significantly underexplored field, with only one prior study quantifying the increase in metabolic costs above resting metabolism [118]. One reason for the scarcity of such studies is that leaves, the primary food source of herbivorous insects, are metabolically active, producing gas at rates comparable to insect metabolism [144, 314]. I addressed this challenge by using metabolically inert PDMS pseudoleaves to limit all metabolic signal measured to insect metabolism alone. A similar approach was previously taken by Roces and Lighton, who used parafilm pseudoleaves [118]. The use of PDMS as an inert substrate has some further benefit over parafilm: it is both mechanically tuneable and isotropic (where parafilm is anisotropic). Isotropy is crucial, as ants cut semicircular fragments and change direction multiple times during a cut [190], so to meaningfully link metabolic cost with material properties, the substrate used must have the same material properties throughout. My use of PDMS pseudoleaves therefore enables the first study directly linking increased mechanical demand to metabolic cost.

In line with Roces and Lighton, I find that cutting metabolic costs increase standard metabolic rate (SMR) by over a factor of 30 [118] (I find a factor of 31). Adding to this work, I present the novel finding that despite increasing mechanical demands, metabolic costs appear to remain constant. Even between substrates that differ by a factor of 5 in cutting force, metabolic costs do not change. I found that increasing mechanical demand does not increase metabolic power. These results support a previous hypothesis by Püffel [89, 168] which proposed that ants always maximally activate their mandible closer muscles during cutting and biting.

To what extent has the invariance of P_{met} with changing mechanical demand been confirmed? Given the limitation of having tested only five substrates, further measurements of cutting P_{met} would more robustly support this key assumption of the cutting efficiency model. However, the substrates used, though few, span over 75% of the force range reported for Neotropical leaves [35] -—the types leafcutters naturally forage on. Additional substrate measurements are unlikely to change the conclusions presented here. Given that the metabolic costs of cutting are so underexplored, there are several exciting avenues for future studies. Using previously measured bite force data [91], one could tailor the mechanical properties of pseudoleaves to approach the maximum limit of a worker's bite force within a selective size range. This would allow for the measurement of the metabolic cost of cutting near an individual's physiological limits, potentially providing additional validation to the hypothesis of non-varying metabolic costs of cutting. A logical next factor to consider is whether there are any elements that might reduce the metabolic cost of cutting. By rearing a sub-colony of callow workers with pristine mandibles, one could quantify the metabolic cost of cutting using ideally sharp tools. This could reveal whether the wear resistance of insect tools not only reduces mechanical demands but also might lower energetic costs.

Having provided evidence that ants maximally activate their mandible closer muscles during cutting, I now look to rationalise how this translates into a key aspect of mechanical power - v_c. v_c has long been a performance metric used in foraging studies. Early pioneering studies by Wilson characterised cutting speed across worker size by fitting a linear relationship with intercept in linear space

and showed for the first time that there is a clear decrease in cutting speed for tougher substrates [134]. A finding later confirmed qualitatively by Scofield [139].[24] Whilst both studies meaningfully contributed to understanding cutting speed as a modulating factor of foraging performance, they also both share a common flaw. The fits used to characterise cutting speed are correlational, not predictive, and violate physical assumptions. To fill an important gap in foraging performance studies, I produced a predictive mechanical model that accounts for the non-linear variation in cutting speed based on measured experimental parameters. Specifically, (F_c), (F_b), and muscle morphological parameters obtained from previous work [91]. Additionally, I introduce the force-velocity properties of muscle using the empirical Hill model (1.1.2). The resulting predictive model for cutting speed is grounded in realistic physical limits and offers the advantage of having only one free parameter that solely determines the magnitude of cutting speed whilst outperforming previously used linear regressions. I present the first fully predictive model for cutting speed – a novel contribution.

The cumulation of my three experimental chapters generates a predictive biomechanical model for cutting efficiency (derived mathematically in Chapter 4). This allows the prediction of an optimal worker size distribution that can be changed with plant material properties – a finding that is unique in foraging performance literature. An initial cursory assessment of the model vs experimentally measured worker size frequency distribution plots show successful predictions in the shift of worker size to substrate properties. Additionally, predicted (x_η) and observed (x_{mode}) differ by less than 23%. The development and first reassuring assessment of this predictive model is just the start, discussing exciting future avenues on the application of this model is how I would like to conclude this thesis.

Here I only begin to scratch the surface of the models predictive power assessing trends of body size and substrate. In reality, there are many factors that influence efficiency. A first use of the model should be to use the vast worn mandible cutting force dataset obtained in Chapter 2, to predict how the model will shift with effects of wear. Within this thesis we assess cutting in confined and sterile laboratory conditions, but shows reassuring similarity with field measurements [134]. Perhaps the most powerful use of this predictive model is in conjunction with deep learning-driven computer vision methods for animal behavioural research. Automated tracking and reference free weight estimation of leaf-cutter ant workers (developed in a previous thesis [315]) enable large scale foraging studies in an organism's natural habits that were not possible when foraging efficiency was first assessed [134]. The combination of automated tracking and a predictive efficiency model will enable large, long-term field studies allowing the dynamic study of foraging efficiency over a colony lifetime.

[24] Findings could not be confirmed quantitively due to confounding factors arising from substrate heterogeneity as discussed above.

I conclude this thesis with optimism that future researchers, fortunate enough to study the wondrous foraging behaviour of leaf-cutter ants, will be as captivated as I was, and will be able to use my predictive tool for future cutting efficiency experimental assays. I end this thesis with the following (humbling) quote as a reminder to enjoy the process.

"And at the end of the day lovely girl it's just ants, so don't get too stressed. "

Words of wisdom from my beloved nana, Olive.

A The Biomechanics of Cutting

A.1 Beam calibration co-efficient calculation

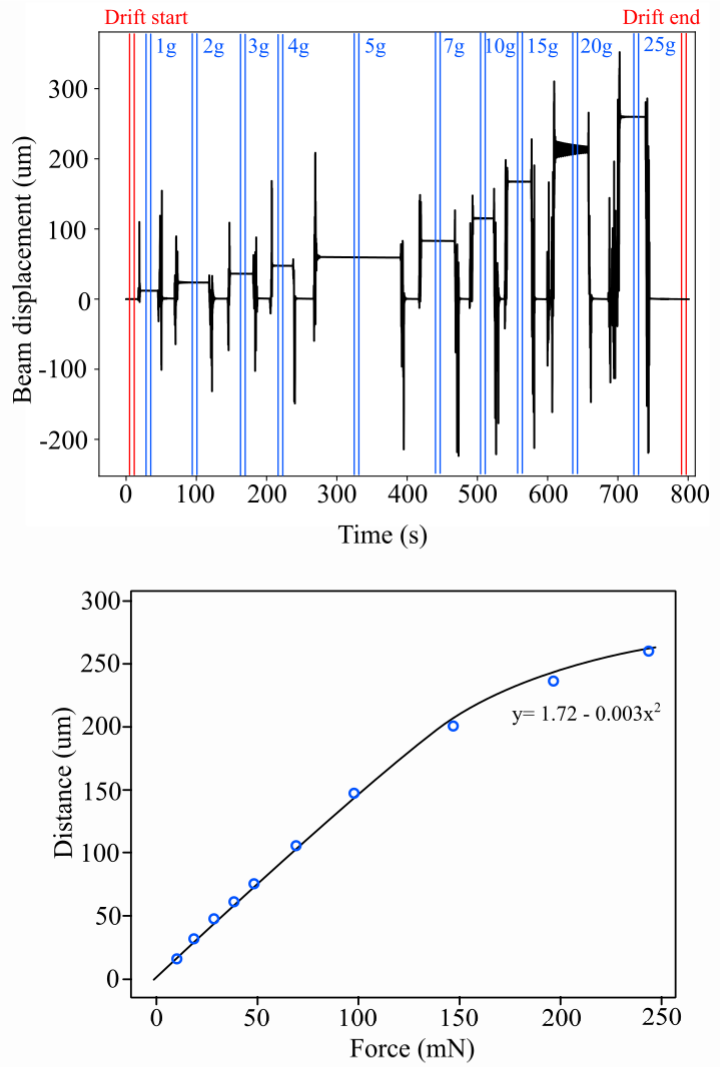


FIGURE A.1: In order to convert beam displacement into cutting force, I used a series of calibration weights. Weights were suspended in series from the polymer mount at the free end of the beam. I averaged the beam deflection over 5 seconds for each weight and calculated linear sensor drift over the total measurement time. The beam displacement was then converted to force using a quadratic regression.

A.2 The mass insignificant variation of cutting and spacing forces in pseudoleaves.

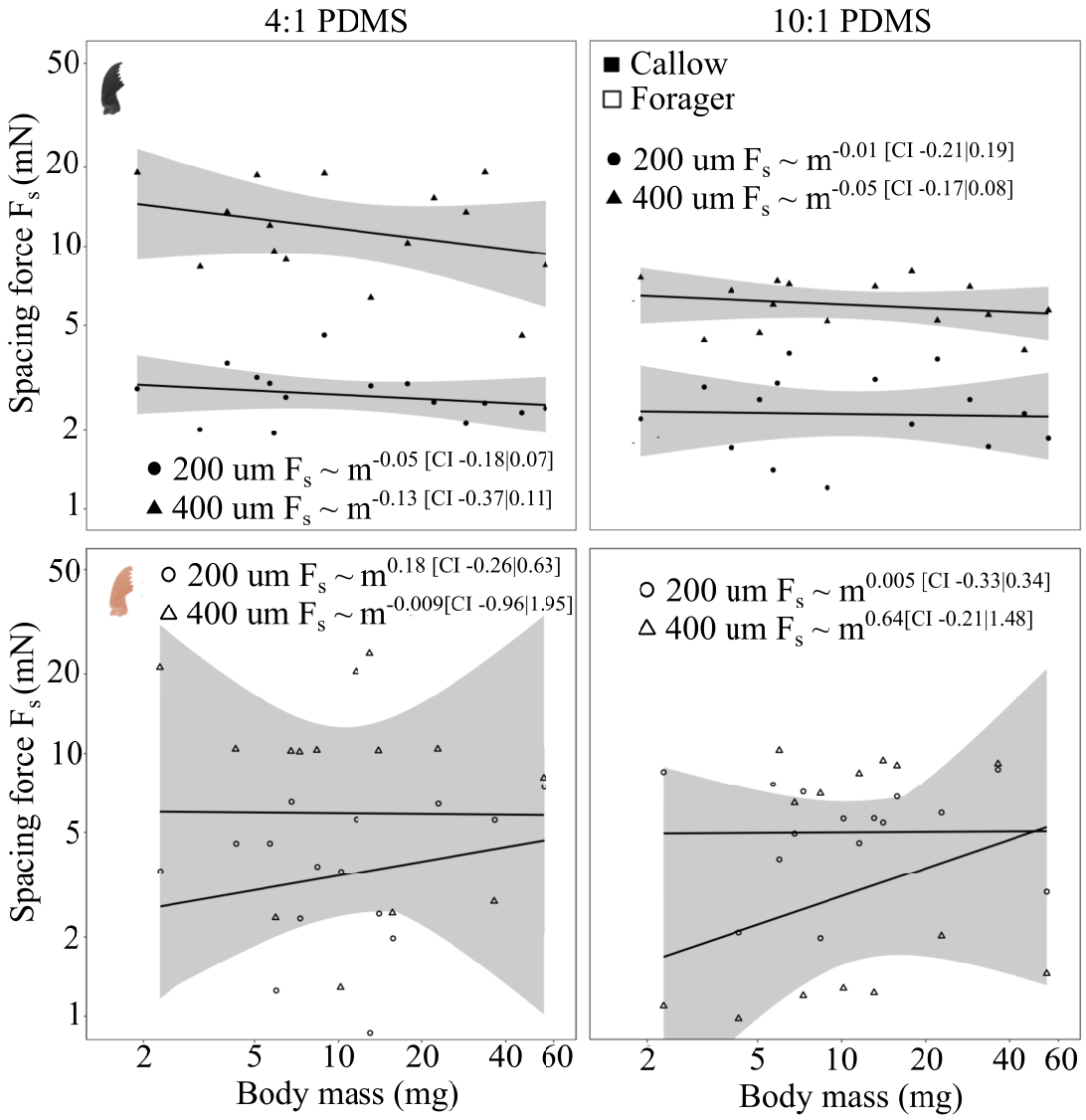


FIGURE A.2: Spacing forces showed no significant variation with worker body mass but did vary with pseudoleaf thickness accounting for 12% of total cutting forces and 22% in thin and thick pseudoleaves respectively.

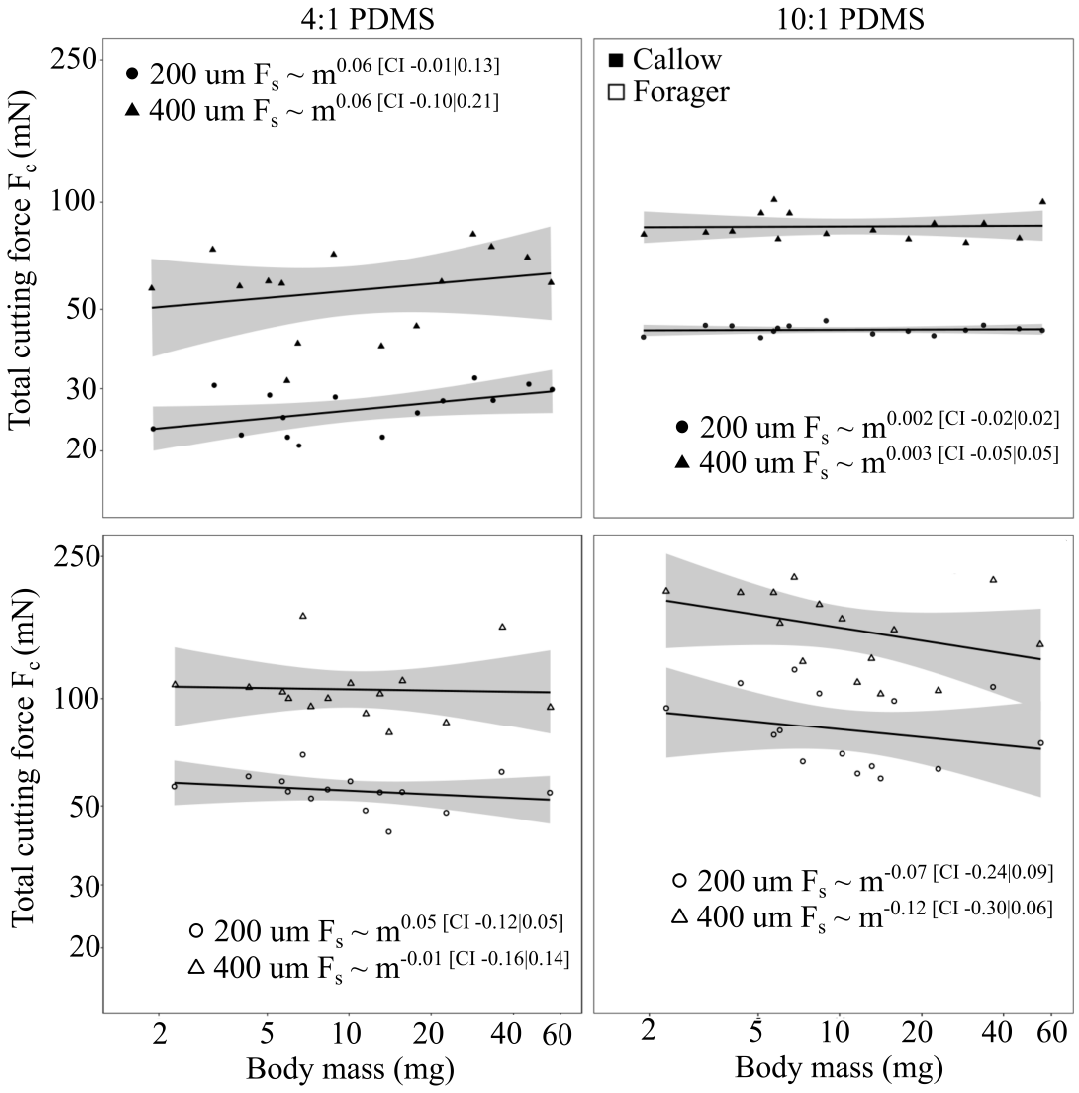


Figure A.3: Cutting forces showed no significant variation with worker body mass and varied in direct proportion to pseudoleaf thickness.

A.3 RM ANCOVA examining the effects of various modulating factors on cutting forces in pseudoleaves

TABLE A.1: RM ANCOVA results for mass, mandible group, pseudoleaf type and substrate thickness and their effect on cutting force F_c in PDMS pseudoleaves. Within the RM ANCOVA, the response variable was the measured force (cutting force in mN, continuous variable), and the predictor variables were mass (continuous variable), group (categorical variable), mixing ratio (categorical variable), and thickness (categorical variable). Sample (Mandible ID) was a random effect as the same mandibles were used across different substrates.

Variable	SS	df	F	p-value
Mass	0.018	1	0.537	0.47
Mandible group	12.89	1	386.6	<0.001
Pseudoleaf type	5.32	1	157.03	<0.001
Thickness	14.46	1	341.32	<0.001
Mass × Mandible group	0.004	1	0.115	0.737
Mass × Pseudoleaf type	0.216	1	5.78	0.02
Mandible group × Pseudoleaf type	0.027	1	0.793	0.381
Mass × Thickness	0.001	1	0.031	0.861
Mandible group× Thickness	0.046	1	1.08	0.308
Pseudoleaf type × Thickness	0.01	1	0.287	0.596
Mass × Mandible group × Pseudoleaf type	0.005	1	0.142	0.709
Mass × Mandible group × Thickness	0.002	1	0.053	0.82
Mass × Pseudoleaf type × Thickness	0.005	1	0.1100	0.7408
Mandible group × Pseudoleaf type × Thickness	0.009	1	0.036	0.856
Mass × Mandible group × Pseudoleaf type × Thickness	0.002	1	0.056	0.814

TABLE A.2: RM ANCOVA results for mass, mandible group, pseudoleaf type and substrate thickness and their effect on fracture force F_f in PDMS pseudoleaves. Within the RM ANCOVA, the response variable was the measured force (fracture force in mN, continuous variable), and the predictor variables were mass (continuous variable), group (categorical variable), mixing ratio (categorical variable), and thickness (categorical variable). Sample (Mandible ID) was a random effect as the same mandibles were used across different substrates.

Variable	SS	df	F	p-value
Mass	0.03	1	0.632	0.434
Mandible group	15.43	1	324.34	<0.001
Pseudoleaf type	7.23	1	181.5	<0.001
Thickness	13.33	1	306.2	<0.001
Mass × Mandible group	0.002	1	0.033	0.856
Mass × Pseudoleaf type	0.008	1	0.194	0.66
Mandible group × Pseudoleaf type	0.123	1	3.087	0.091
Mass × Thickness	0.003	1	0.064	0.80
Mandible group× Thickness	0.001	1	0.005	0.94
Pseudoleaf type × Thickness	0.004	1	0.86	0.36
Mass × Mandible group × Pseudoleaf type	0.006	1	0.144	0.71
Mass × Mandible group × Thickness	0.085	1	2.54	0.10
Mass × Pseudoleaf type × Thickness	0.02	1	0.319	0.58
Mandible group × Pseudoleaf type × Thickness	0.0002	1	0.004	0.95
Mass × Mandible group × Pseudoleaf type × Thickness	0.0001	1	0.003	0.96

TABLE A.3: RM ANCOVA results for mass, mandible group, pseudoleaf type and substrate thickness and their effect on spacing force F_s in PDMS pseudoleaves. Within the RM ANCOVA, the response variable was the measured force (spacing force in mN, continuous variable), and the predictor variables were mass (continuous variable), group (categorical variable), mixing ratio (categorical variable), and thickness (categorical variable). Sample (Mandible ID) was a random effect as the same mandibles were used across different substrates.

Variable	Sum Sq	df	F-value	p-value
Mass	0.0001	1	0.00036	0.99
Mandible group	0.275	1	3.6	0.55
Pseudoleaf type	2.83	1	3.31	0.08
Thickness	9.53	1	11.9	0.001
Mass × Mandible group	2.37	1	3.10	0.09
Mass × Pseudoleaf type	0.28	1	0.033	0.86
Mandible group × Pseudoleaf type	0.39	1	0.47	0.50
Mass × Thickness	1.53	1	1.91	0.18
Mandible group × Thickness	12.45	1	15.67	<0.001
Pseudoleaf type × Thickness	1.49	1	2.42	0.22
Mass × Mandible group × Thickness	0.014	1	0.018	0.89
Mass × Pseudoleaf type × Thickness	2.13	1	3.27	0.08
Mandible group × Pseudoleaf type × Thickness	1.04	1	1.51	0.23
Mass × Mandible group × Pseudoleaf type × Thickness	0.18	1	0.28	0.60

A.4 RM ANCOVA examining the effects of various modulating factors on thickness corrected cutting forces in pseudoleaves

TABLE A.4: RM ANCOVA Results for mass, mandible group, pseudoleaf type, and *corrected* substrate thickness and their effect on cutting force F_c in PDMS pseudoleaves.

Variable	SS	df	F	p-value
Mass	0.005	1	0.052	0.82
Mandible group	12.67	1	138.26	$<$0.001
Pseudoleaf type	5.49	1	192.82	$<$0.001
Corrected thickness	0.004	1	0.455	0.51
Mass $\times$ Mandible group	0.211	1	2.30	0.14
Mass $\times$ Pseudoleaf type	0.097	1	3.40	0.08
Mandible group $\times$ Pseudoleaf type	0.042	1	1.48	0.23
Mass $\times$ Corrected thickness	0.014	1	1.43	0.26
Mandible group $\times$ Corrected thickness	0.035	1	3.758	0.07
Pseudoleaf type $\times$ Corrected thickness	0.019	1	1.909	0.18
Mass $\times$ Mandible group $\times$ Pseudoleaf type	0.002	1	0.056	0.81
Mass $\times$ Mandible group $\times$ Corrected thickness	0.007	1	0.752	0.38
Mass $\times$ Pseudoleaf type $\times$ Corrected thickness	0.003	1	0.320	0.58
Mandible group $\times$ Pseudoleaf type $\times$ Corrected thickness	0.018	1	1.781	0.19
Mass $\times$ Mandible group $\times$ Pseudoleaf type $\times$ Corrected thickness	0.008	1	0.79	0.38

TABLE A.5: RM ANCOVA Results for mass, mandible group, pseudoleaf type, and *corrected* substrate thickness and their effect on fracture force F_f in PDMS pseudoleaves.

Variable	SS	df	F	p-value
Mass	0.003	1	0.001	0.98
Mandible group	14.84	1	133.1	<0.001
Pseudoleaf type	7.67	1	240.67	<0.001
Corrected thickness	0.007	1	0.117	0.74
Mass × Mandible group	0.301	1	2.78	0.11
Mass × Pseudoleaf type	0.153	1	4.79	0.07
Mandible group × Pseudoleaf type	0.18	1	5.66	0.03
Mass × Corrected thickness	0.002	1	0.117	0.74
Mandible group × Corrected thickness	0.002	1	0.143	0.71
Pseudoleaf type × Corrected thickness	0.02	1	1.038	0.32
Mass × Mandible group × Pseudoleaf type	0.001	1	0.019	0.89
Mass × Mandible group × Corrected thickness	0.0078	1	0.533	0.47
Mass × Pseudoleaf type × Corrected thickness	0.019	1	1.33	0.26
Mandible group × Pseudoleaf type × Corrected thickness	0.003	1	0.234	0.63
Mass × Mandible group × Pseudoleaf type × Corrected thickness	0.011	1	0.767	0.39

A.5 The mass insignificant variation of spacing forces in natural leaves.

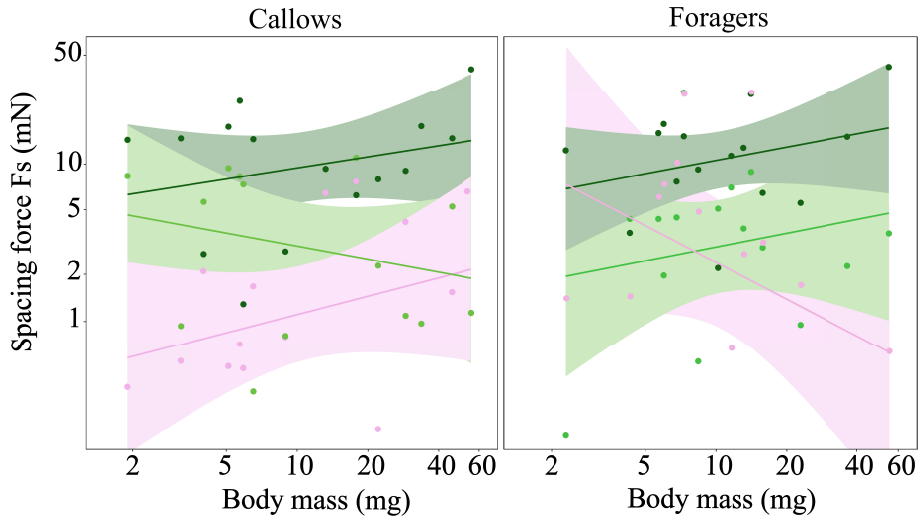


FIGURE A.4: Plant spacing forces showed no significant variation with body mass but did vary with plant type being on average increasing with substrate toughness (from rose to laurel).

A.6 Nested RM ANCOVA examining the effects of various modulating factors on cutting forces in natural leaves

TABLE A.6: Nested RM ANCOVA results for mass, mandible group and plant type and their effect on cutting force F_c in natural substrates. Within the RM ANCOVA, the response variable was the measured force (cutting force in mN, continuous variable), and the predictor variables were mass (continuous variable), plant type (categorical variable) and group (categorical variable). Sample (Mandible ID) and repeat were treated as random effects, as the same mandibles were used across different substrates with repeated measurements taken within each sample.

Variable	SS	df	F	p-value
Mass	0.29	1	0.774	0.39
Mandible group	16.31	1	43.51	<0.001
Plant	28.72	1	404.68	<0.001
Mass × Mandible group	0.168	2	0.448	0.51
Mass × Plant	0.213	2	0.3001	0.07
Mandible group × Plant	1.917	2	2.018	0.17
Mass × Mandible group × Plant	0.304	2	4.29	0.10

TABLE A.7: Nested RM ANCOVA results for mass, mandible group and plant type and their effect on fracture force F_f in natural substrates. Within the RM ANCOVA, the response variable was the measured force (fracture force in mN, continuous variable), and the predictor variables were mass (continuous variable), plant type (categorical variable) and group (categorical variable). Sample (Mandible ID) and repeat were treated as random effects, as the same mandibles were used across different substrates with repeated measurements taken within each sample.

Variable	SS	df	F	p-value
Mass	0.046	1	0.341	0.57
Mandible group	5.414	1	40.34	<0.001
Plant	8.612	1	125.468	<0.001
Mass × Mandible group	0.041	2	0.305	0.59
Mass × Plant	0.085	2	1.244	0.30
Mandible group × Plant	0.476	2	6.936	0.09
Mass × Mandible group × Plant	0.055	2	0.805	0.45

TABLE A.8: Nested RM ANCOVA results for mass, mandible group and plant type and their effect on spacing force F_s in natural substrates. Within the RM ANCOVA, the response variable was the measured force (spacing force in mN, continuous variable), and the predictor variables were mass (continuous variable), plant type (categorical variable) and group (categorical variable). Sample (Mandible ID) and repeat were treated as random effects, as the same mandibles were used across different substrates with repeated measurements taken within each sample.

Variable	SS	df	F	p-value
Mass	0.13	1	0.068	0.80
Mandible group	1.72	1	0.889	0.36
Plant	52.68	1	22.03	<0.001
Mass × Mandible group	0.59	2	0.303	0.59
Mass × Plant	9.59	2	4.665	0.008
Mandible group × Plant	1.99	2	0.834	0.44
Mass × Mandible group × Plant	1.09	2	0.832	0.52

A.7 RM ANCOVA examining the effects of modulating factors on mandible cutting edge radii and wedge angle

TABLE A.9: RM ANCOVA results for mass, mandible group and location and their effect on mandible cutting edge radii.

Variable	SS	df	F	p-value
Mass	4.34	1	5.42	0.02
Mandible group	61.18	1	76.35	$<$0.001
Location	4.35	5	2.32	0.08
Mass $\times$ Mandible group	33.42	1	41.70	$<$0.001
Mass $\times$ Location	1.58	5	0.394	0.85
Mandible group $\times$ Location	0.72	5	0.18	0.97
Mass $\times$ Mandible group $\times$ Location	3.13	5	0.78	0.57

TABLE A.10: RM ANCOVA Results for mass, mandible group and location and their effect on mandible cutting edge wedge angle.

Variable	SS	df	F	p-value
Mass	0.091	1	2.55	0.12
Mandible group	0.48	1	13.4	$<$0.001
Location	0.13	5	0.74	0.60
Mass $\times$ Mandible group	0.002	1	0.0006	0.99
Mass $\times$ Location	0.032	5	0.181	0.97
Mandible group $\times$ Location	0.124	5	0.694	0.63
Mass $\times$ Mandible group $\times$ Location	0.024	5	0.171	0.95

B The Metabolic Cost of Cutting

B.1 Time constant calculations

The time constant T of a respirometry chamber is:

$$\mathrm{T} = \frac{V}{FR} \tag{B.1}$$

where V is the respirometry chamber volume, and FR is the flow rate.

The time constant indicates the time over which $1 - \frac{1}{e}$ (63%) of the air is replaced within the chamber. It then follows that the time required to replace a given percentage $F\%$ of air is:

$$\mathrm{T} = \frac{V}{FR} \ln\left(1 - \frac{(100 - F)}{100}\right) \tag{B.2}$$

B.2 Automated peak detection and burst frequency and volume validation

The automated peak detection function implemented in Expedata is a well-tested solution to identify the start and end of peaks, and is in widespread use [104, 252, 261, 268, 316]. Users can select a normal or derivative method to find the peaks. The derivative method works best on clean or smoothed data, whereas the normal method is more suited to noisier traces – although both employ the same technique. Due to the use of chemical scrubber and the minor system drift, I decided to use the derivative method. This method identifies burst peaks from a derivative-frequency histogram. Once this trigger level is reached, the macro scans on both sides to identify a peak, defined by a local gradient of zero. The width of this scan is user-defined, and varied with the mass of the individual—larger individuals exhibit peaks of a longer duration.

In order to verify that the macro obtained satisfactory results, we selected a small subset of traces (n=10), and hand marked the start and the end of each peak by eye, and then integrated to find the burst volume. The two methods did not differ significantly (ANOVA method type: $F_{1,9}$ = 10.34, p = 0.345), and the macro is therefore a quick, user friendly and efficient way to calculate burst volume and automatically mark peaks.

B.3 Activity affects discontinuous gas exchange cycles

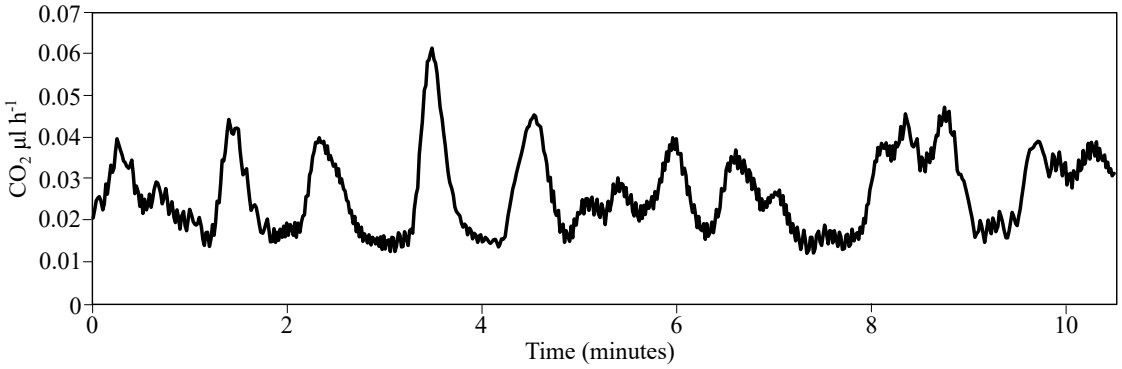


FIGURE B.1: Even minor movements can have a significant effect on the discontinuous gas exchange pattern of idle workers. The example here shows the metabolic trace of a 43.0mg worker that slowly rotated during the measurement. Note the elevated trace that does not return to zero, suggesting the spiracles never fully close. In addition, burst peaks are irregular.

B.4 Preliminary study on 150, 300 and 500 μm PDMS

Before conducting the full study as presented in this thesis I conducted a small subset of preliminary trials on 10:1 pseudoleaves. Here they serve as additional evidence that cutting metabolic cost is constant with changing mechanical demands.

Cutting force

TABLE B.1: The steady-state cutting force varies with the mechanical properties of the target material, and this difference may induce differences in the metabolic expenditure during cutting. To test initial substrates and how they vary metabolic cost I fabricated 150, 300 and 500 µm 10:1 pseudoleaves. Three key parameters were measured: Young's modulus, tearing energy and average steady state cutting force. The steady state cutting force was measured using a custom built fibre optic force set-up and using forager mandibles with varying degrees of wear. Whilst the Young's modulus and tearing energy remain constant for the same pseduoleaf type the steady state cutting force increases significantly with thickness

Thickness	Young's modulus E (MPa)	Tearing energy G_c (J m^{-2})	Average steady state cutting force (mN)
150 μm	1.5 ± 0.5	196 ± 25	63 ± 12
300 μm	1.5 ± 0.5	196 ± 25	128 ± 20
500 μm	1.5 ± 0.5	196 ± 25	215 ± 25

Cutting metabolic rate

In contrast to the main study SMR and CMR were measured over a very small mass range — between 2.6 and 6.8 mg. As during preliminary trials this was the mass range that was most likely to initiate cutting freely. Both SMR and CMR measurements were taken in ambient lab conditions and during summer and as such temperature was not as tightly controlled. Across all studies the average temperature during measurements was 27 ± 3 °C.

Table B.2: Standard and cutting metabolic rates for workers used in the preliminary metabolic cost of cutting trail. Both SMR and CMR are on average slightly higher than those obtained in the main study, this is likely due to the lack of temperature control and slightly elevated temperature conditions.

150 μm		
Worker body mass (mg)	Standard metabolic rate (μW)	Cutting metabolic rate (μW)
4.1	5.3	176.2
5.3	5.6	364.7
300 μm		
Worker body mass (mg)	Standard metabolic rate	Cutting metabolic rate
4.3	6.0	94.9
6.1	10.2	133.6
500 μm		
Worker body mass (mg)	Standard metabolic rate	Cutting metabolic rate
2.6	4.8	151.2
3.4	5.6	138.2
5.1	8.1	201.0
6.2	12.7	489.4
7.0	10.7	198.1
7.4	11.2	264.9

B.5 Mass scaling exponents across *Atta* species

Table B.3: Scaling of standard metabolic rate in *Atta* ant species. * denotes values obtained from the literature [118][261]. Size range refers to the orders of magnitude difference between the largest and smallest individuals measured. Subscript values represent CI.

Species	n	Size range	Mass scaling exponent
Atta cephalotes	21	1.52	$_{0.78}0.83_{0.88}$
Atta vollenweideri	8	0.95	$_{0.80}0.88_{0.96}$
*Atta columbica**	27	0.97	$_{0.44}0.64_{0.84}$
*Atta sexdens**	18	0.91	$_{0.87}0.89_{0.92}$

B.6 ANCOVA to discern the effects of repeats and mass on burst volume and frequency

Table B.4: ANCOVA to discern the effects of repeats and mass on burst volume.

Variable	SS	df	F	p-value
Mass	6.533	1	324.015	$<$0.001
Repeat	0.014	1	0.691	0.41
Mass $\times$ Repeat	0.016	1	0.82	0.38

Table B.5: ANCOVA to discern the effects of repeats and mass on burst frequency.

Variable	SS	df	F	p-value
Mass	2.41	1	12.96	0.007
Repeat	0.111	1	0.14	0.65
Mass $\times$ Repeat	0.0139	1	0.61	0.47

C The non-linear variation of cutting speed

C.1 Cutting speed model substrates

Table C.1: In order to assess cutting speed and strategy and its variation with worker size and substrate, I selected 3 substrates on which *Atta cephalotes* would naturally forage with a range of toughness that fall within those of tropical leaves [35]. I characterize the force required to cut each leaf type using forager mandibles with different states of wear for each.

Substrate	Average cutting force (mN)
Laurel	123 ± 30
Bramble	79 ± 13
Rose	68 ± 20

TABLE C.2: The effect of body mass and substrate type on cutting time, fragment mass, and cutting speed was analysed using ANCOVAs with type II sum of squares, performed on $\log_{10}$-transformed data.

Cutting time					
Factor	DF	SS	MS	F	p-value
Mass	1	7.296	7.296	241.56	< 0.001
Substrate	2	3.986	1.993	65.99	< 0.001
Mass $\times$ Substrate	2	1.928	0.964	31.91	< 0.001
Residuals	669	20.205	0.030		
Fragment mass					
Factor	DF	SS	MS	F	p-value
Mass	1	22.782	22.782	370.028	< 0.001
Substrate	2	2.900	1.448	23.519	< 0.001
Mass $\times$ Substrate	2	0.080	0.038	0.619	0.0439
Residuals	669	41.190	0.062		
Cutting speed					
Factor	DF	SS	MS	F	p-value
Mass	1	29.710	29.710	1358.993	< 0.001
Substrate	2	2.717	1.359	62.148	< 0.001
Mass $\times$ Substrate	2	0.048	0.024	1.105	0.332
Residuals	669	14.626	0.022		

TABLE C.3: The effect of body mass and substrate type on energy invested and energy gained per fragment was analysed using ANCOVAs with type II sum of squares, performed on $\log_{10}$-transformed data.

Energy invested					
Factor	DF	SS	MS	F	p-value
Mass	1	21.754	21.754	677.725	< 0.001
Substrate	2	4.687	2.343	73.004	< 0.001
Mass $\times$ Substrate	2	0.277	0.139	4.319	0.0137
Residuals	669	21.474	0.032		
Energy gained					
Factor	DF	SS	MS	F	p-value
Mass	1	23.303	23.303	152.653	< 0.001
Substrate	2	5.900	2.950	19.328	< 0.001
Mass $\times$ Substrate	2	0.100	0.051	0.336	0.0044
Residuals	669	102.100	0.153		

C.2 Analysis of Covariance (ANCOVA) full statistical analysis

TABLE C.4: The effect of body mass and substrate type on cut distance, fragment area, and fragment volume was analysed using ANCOVAs with type II sum of squares, performed on log10-transformed data.

Distance cut					
Factor	DF	SS	MS	F	p-value
Mass	1	3.627	3.627	202.826	< 0.001
Substrate	2	0.637	0.319	17.826	< 0.001
Mass $\times$ Substrate	2	0.233	0.117	6.525	0.0016
Residuals	669	11.962	0.018		
Fragment area					
Factor	DF	SS	MS	F	p-value
Mass	1	0.453	0.453	23.63	< 0.001
Substrate	2	1.086	0.5432	28.36	< 0.001
Mass $\times$ Substrate	2	0.786	0.3930	20.52	< 0.001
Residuals	669	12.184	0.0192		
Fragment volume					
Factor	DF	SS	MS	F	p-value
Mass	1	27.87	27.87	164.43	< 0.001
Substrate	2	6.15	3.18	24.04	< 0.001
Mass $\times$ Substrate	2	0.3	0.153	0.432	< 0.001
Residuals	669	110.27	0.202		

C.3 Statistically testing the "goodness-of-fit" of three models for cutting speed

Table C.5: In order to assess the quality of the biomechanical model, I evaluate three goodness-of-fit metrics: R^2, the root mean squared error (RMSE), and the Akaike Information Criterion (AIC). For comparison, I conducted an ordinary least-squares linear regression in log- and linear-space. The biomechanical prediction outperforms both linear regressions in each metric.

Laurel			
Statistical model	R^2	RMSE	AIC
Linear regression log-space	0.42	0.15	156.8
Linear regression linear-space	0.37	0.10	419.1
Biomechanical prediction	0.73	< 0.01	87.1
Bramble			
Statistical model	R^2	RMSE	AIC
Linear regression log-space	0.67	0.14	126.7
Linear regression linear-space	-0.32	0.10	338.8
Biomechanical prediction	0.46	0.04	112.4
Rose petals			
Statistical model	R^2	RMSE	AIC
Linear regression log-space	0.59	0.16	177.0
Linear regression linear-space	-1.20	0.14	242.4
Biomechanical prediction	0.64	0.03	95.4

C.4 "Null hypothesis" models examples in Laurel

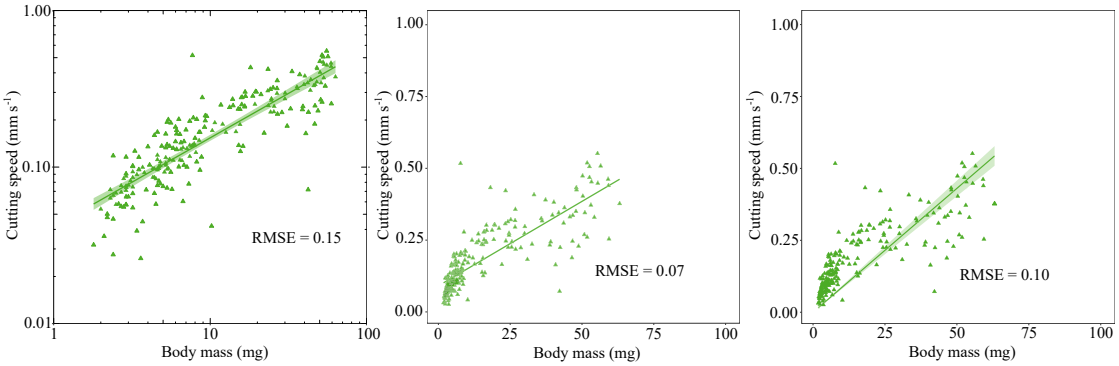


FIGURE C.1: I compared the fit of the biomechanical model to linear regressions on linear and log-log space finding, that both visually and statistically the biomechanical model rationalising the non-linear variation in cutting speed out performs both null hypotheses.

C.5 Comparison of linear (K=0) and non-linear hill model (K=4) biomechanical models for cutting speed.

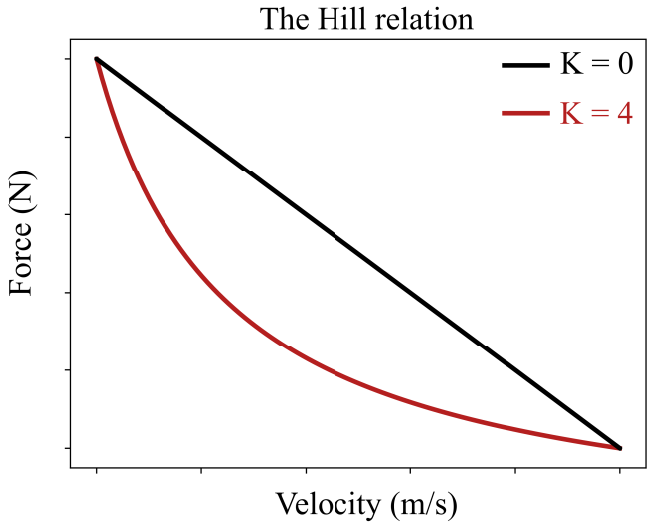


FIGURE C.2: Visual representation of the Hill force velocity properties of muscle for two values of the dimensionless constant K. The linear model (K=0, black line) assumes a direct inverse relationship between force and velocity. In contrast, the non-linear model with (K=4, red line) shows a more pronounced curvature, typical of invertebrate muscle, where force drops steeply with increasing velocity. These curves visually represent the assumptions used in the biomechanical models of cutting speed.

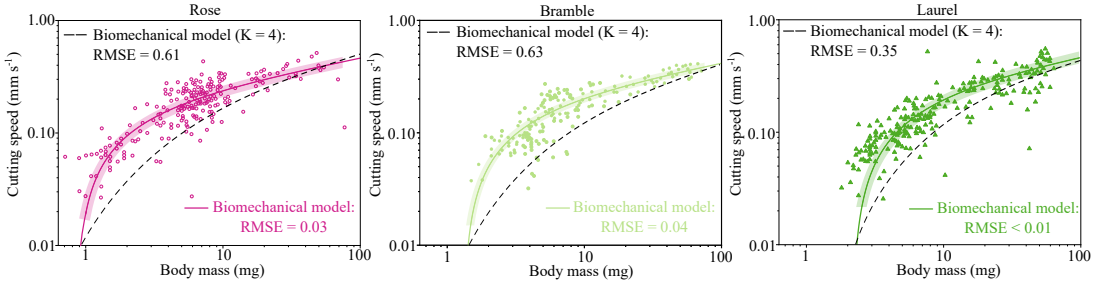


FIGURE C.3: Comparison of biomechanical models based on the linear Hill relation (K=0, coloured lines) and the non-linear Hill relation (K=4, black lines) for predicting cutting speed across three substrates. RMSE values are shown for each model. In all cases, the linear Hill model (with fewer parameters) provides a better fit to the data, particularly at lower body masses.

Bibliography

[1] R. E. Society. *Understanding Insects*. Accessed: 18 Sept 2024. 2024. URL: https://www.royensoc.co.uk/understanding-insects/.

[2] Z. Zhang. "Phylum Arthropoda". In: *Zootaxa* 3703.1 (Aug. 2013), pp. 17–26. ISSN: 1175-5326. DOI: 10.11646/zootaxa.3703.1.6.

[3] Z. Zhang. "Animal biodiversity: An update of classification and diversity in 2013*". In: *Zootaxa* 3703.1 (Aug. 2013), pp. 5–11. ISSN: 1175-5326. DOI: 10.11646/zootaxa.3703.1.3.

[4] R. W. A. M. S. Wehner. "Desert ants on a thermal tightrope". In: *Nature* 357 (1992), pp. 586–587.

[5] I. Kozeretska et al. "Belgica antarctica (Diptera: Chironomidae): A natural model organism for extreme environments". In: *Insect Science* 29.1 (Apr. 2021), pp. 2–20. ISSN: 1744-7917. DOI: 10.1111/1744-7917.12925.

[6] B. Misof et al. "Phylogenomics resolves the timing and pattern of insect evolution". In: *Science* 346.6210 (Nov. 2014), pp. 763–767. ISSN: 1095-9203. DOI: 10.1126/science.1257570.

[7] S. E. Pfeffer et al. "High-speed locomotion in the Saharan silver ant, Cataglyphis bombycina". In: *Journal of Experimental Biology* 222.20 (Oct. 2019). ISSN: 0022-0949. DOI: 10.1242/jeb.198705.

[8] A. F. Pomerantz et al. "Developmental, cellular, and biochemical basis of transparency in clearwing butterflies". In: *Journal of Experimental Biology* (May 2021). ISSN: 1477-9145. DOI: 10.1242/jeb.237917.

[9] R. J. Bomphrey et al. "Flight of the dragonflies and damselflies". In: *Philosophical Transactions of the Royal Society B: Biological Sciences* 371.1704 (Sept. 2016), p. 20150389. ISSN: 1471-2970. DOI: 10.1098/rstb.2015.0389.

[10] J. C. F. Cardoso et al. "Pollinators and plants as ecosystem engineers: post-dispersal fruits provide new habitats for other organisms". In: *Oikos* 2023.9 (May 2023). ISSN: 1600-0706. DOI: 10.1111/oik.09819.

[11] N. Calderón-Cortés. "Ecosystem Engineering by Insect Herbivores: Non-trophic Interactions in Terrestrial Ecosystems". In: *Evolutionary Ecology of Plant-Herbivore Interaction*. Springer International Publishing, 2020, pp. 147–172. ISBN: 9783030460129. DOI: 10.1007/978-3-030-46012-9_8.

[12] C. Darwin. *The formation of vegetable mould, through the action of worms, with observations on their habits.* J. Murray, 1881.

[13] B. J. Enagbonma and O. O. Babalola. "Potentials of termite mound soil bacteria in ecosystem engineering for sustainable agriculture". In: *Annals of Microbiology* 69.3 (Jan. 2019), pp. 211–219. ISSN: 1869-2044. DOI: 10.1007/s13213-019-1439-2.

[14] G. D. Martinsen et al. "Positive interactions between leafrollers and other arthropods enhance biodiversity on hybrid cottonwoods". In: *Oecologia* 123.1 (Apr. 2000), pp. 82–89. ISSN: 1432-1939. DOI: 10.1007/s004420050992.

[15] J. T. Lill and R. J. Marquis. "Ecosystem engineering by caterpillars increases insect herbivore diversity on white oak". In: *Ecology* 84.3 (Mar. 2003), pp. 682–690. ISSN: 0012-9658. DOI: 10.1890/0012-9658(2003)084[0682:eebcii]2.0.co;2.

[16] S. N. Johnson et al. "Insects as leaf engineers: can leaf-miners alter leaf structure for birch aphids?" In: *Functional Ecology* 16.5 (Sept. 2002), pp. 575–584. ISSN: 1365-2435. DOI: 10.1046/j.1365-2435.2002.00654.x.

[17] D. M. Kahn and H. V. Cornell. "Leafminers, early leaf abscission, and parasitoids: a tritrophic interaction". In: *Ecology* 70.5 (Oct. 1989), pp. 1219–1226. ISSN: 1939-9170. DOI: 10.2307/1938179.

[18] A. R. War et al. "Mechanisms of plant defense against insect herbivores". In: *Plant Signaling & Behavior* 7.10 (Oct. 2012), pp. 1306–1320. DOI: 10.4161/psb.21663.

[19] J. Fürstenberg-Hägg, M. Zagrobelny, and S. Bak. "Plant defense against insect herbivores". In: *International Journal of Molecular Sciences* 14.5 (May 2013), pp. 10242–10297. ISSN: 1422-0067. DOI: 10.3390/ijms140510242.

[20] P. R. Ehrlich. "Some Axioms of Taxonomy". In: *Systematic Zoology* 13.3 (Sept. 1964), p. 109. ISSN: 0039-7989. DOI: 10.2307/2411485.

[21] P. S. L. Anderson. "Making a point: shared mechanics underlying the diversity of biological puncture". In: *Journal of Experimental Biology* 221.22 (Nov. 2018), jeb187294. DOI: 10.1242/jeb.187294.

[22] R. Chapman. "Mouthparts". In: *Encyclopedia of Insects*. Elsevier, 2009, pp. 663–668. ISBN: 9780123741448. DOI: 10.1016/b978-0-12-374144-8.00182-x.

[23] L. Khadempour et al. "The fungal cultivar of leaf-cutter ants produces specific enzymes in response to different plant substrates". In: *Molecular Ecology* 25.22 (Oct. 2016), pp. 5795–5805. ISSN: 1365-294X. DOI: 10.1111/mec.13872.

[24] A. M. Nico Blüthgen. "Contrasting leaf age preferences of specialist and generalist stick insects (phasmida)". In: *Oikos* 116.11 (2007), pp. 1853–1862.

[25] S. Zlotnik and C. W. Miller. "Adult presence does not ameliorate juvenile feeding challenges in a leaf-footed bug". In: *Royal Society Open Science* 10.8 (Aug. 2023). ISSN: 2054-5703. DOI: 10.1098/rsos.221291.

[26] Q.-Q. Deng et al. "Damage of brown planthopper (BPH) Nilaparvata lugens and rice leaf folder (LF) Cnaphalocrocis medinalis in parent plants lead to distinct resistance in ratoon rice". In: *Plant Signaling & Behavior* 17.1 (July 2022). ISSN: 1559-2324. DOI: 10.1080/15592324.2022.2096790.

[27] S. Dobler, G. Petschenka, and H. Pankoke. "Coping with toxic plant compounds – The insect's perspective on iridoid glycosides and cardenolides". In: *Phytochemistry* 72.13 (Sept. 2011), pp. 1593–1604. ISSN: 0031-9422. DOI: 10.1016/j.phytochem.2011.04.015.

[28] S. C. Groen and N. K. Whiteman. "Convergent evolution of cardiac-glycoside resistance in predators and parasites of milkweed herbivores". In: *Current Biology* 31.22 (Nov. 2021), R1465–R1466. ISSN: 0960-9822. DOI: 10.1016/j.cub.2021.10.025.

[29] E. Bernays and M. Graham. "On the evolution of host specificity in phytophagous arthropods". In: *Ecology* 69.4 (Aug. 1988), pp. 886–892. ISSN: 1939-9170. DOI: 10.2307/1941237.

[30] G. M. Douglas J. Futuyma. "The Evolution of ecological specialization". In: *Annual Review of Ecology and Systematics* 19 (1988), pp. 207–33.

[31] A. J.G. "Specialist versus generalist insect herbivores and plant defense". In: *Trends in plant science* 17.5 (2012), pp. 293–302.

[32] E. A. Bernays and O. P. J. M. Minkenberg. "Insect herbivores: different reasons for being a generalist". In: *Ecology* 78.4 (June 1997), pp. 1157–1169. ISSN: 0012-9658. DOI: 10.1890/0012-9658(1997)078[1157:ihdrfb]2.0.co;2.

[33] G. E. Barnes. "The behaviour of Anodonta Cygnea L., and its neurophysiological basis". In: *Journal of Experimental Biology* 32.1 (Mar. 1955), pp. 158–174. ISSN: 1477-9145. DOI: 10.1242/jeb.32.1.158.

[34] A. Barthel et al. "Immune defence strategies of generalist and specialist insect herbivores". In: *Proceedings of the Royal Society B: Biological Sciences* 281.1788 (Aug. 2014), p. 20140897. ISSN: 1471-2954. DOI: 10.1098/rspb.2014.0897.

[35] Y. Onoda et al. "Global patterns of leaf mechanical properties". In: *Ecology Letters* 14.3 (Jan. 2011), pp. 301–312. DOI: 10.1111/j.1461-0248.2010.01582.x.

[36] A. J. J. Crumière et al. "The multidimensional nutritional niche of fungus-cultivar provisioning in free-ranging colonies of a neotropical leafcutter ant". In: *Ecology Letters* 24.11 (Aug. 2021). Ed. by N. Pinter-Wollman, pp. 2439–2451. ISSN: 1461-0248. DOI: 10.1111/ele.13865.

[37] G. A. Howe and G. Jander. "Plant Immunity to Insect Herbivores". In: *Annual Review of Plant Biology* 59.1 (June 2008), pp. 41–66. ISSN: 1545-2123. DOI: 10.1146/annurev.arplant.59.032607.092825.

[38] R. R. Kariyat et al. "Plant spines deter herbivory by restricting caterpillar movement". In: *Biology Letters* 13.5 (May 2017), p. 20170176. ISSN: 1744-957X. DOI: 10.1098/rsbl.2017.0176.

[39] G. Sun et al. "Plant chemical defenses against insect herbivores—ssing the wild tobacco as a model". In: *Phyton* 93.4 (2024), pp. 641–659. ISSN: 1851-5657. DOI: 10.32604/phyton.2024.049285.

[40] A. S. Indrakant K. Singh. *Plant-Pest Interactions: From Molecular Mechanisms to Chemical Ecology*. Ed. by C. Ecology. Chemical Ecology, 2021.

[41] J. D. Hare. "Ecological role of volatiles produced by plants in response to damage by herbivorous insects". In: *Annual Review of Entomology* 56.1 (Jan. 2011), pp. 161–180. ISSN: 1545-4487. DOI: 10.1146/annurev-ento-120709-144753.

[42] R. V. Barbehenn and C. Peter Constabel. "Tannins in plant–herbivore interactions". In: *Phytochemistry* 72.13 (Sept. 2011), pp. 1551–1565. ISSN: 0031-9422. DOI: 10.1016/j.phytochem.2011.01.040.

[43] H. Tiimonen et al. "Does lignin modification affect feeding preference or growth performance of insect herbivores in transgenic silver birch (Betula pendula Roth)?" In: *Planta* 222.4 (June 2005), pp. 699–708. ISSN: 1432-2048. DOI: 10.1007/s00425-005-0002-5.

[44] H. Yu et al. "Biogenic secondary organic aerosol participates in plant interactions and herbivory defense". In: *Science* 385.6714 (Sept. 2024), pp. 1225–1230. ISSN: 1095-9203. DOI: 10.1126/science.ado6779.

[45] M. Erb and C. A. Robert. "Sequestration of plant secondary metabolites by insect herbivores: molecular mechanisms and ecological consequences". In: *Current Opinion in Insect Science* 14 (Apr. 2016), pp. 8–11. ISSN: 2214-5745. DOI: 10.1016/j.cois.2015.11.005.

[46] C. W. Hoy, G. P. Head, and F. R. Hall. "Spatial hetrogenity and insect adaptaion to toxins". In: *Annual Review of Entomology* 43.1 (Jan. 1998), pp. 571–594. ISSN: 1545-4487. DOI: 10.1146/annurev.ento.43.1.571.

[47] G. E. Belovsky et al. "Effects of spines and thorns on Australian arid zone herbivores of different body masses". In: *Oecologia* 88.4 (Dec. 1991), pp. 521–528. ISSN: 1432-1939. DOI: 10.1007/bf00317715.

[48] S. D. Eigenbrode and K. E. Espelie. "Effects of plant epicuticular lipids on insect herbivores". In: *Annual review of entomology* 40.1 (1995), pp. 171–194. DOI: 10.1146/annurev.en.40.010195.001131.

[49] W. Federle et al. "Slippery ant-plants and skilful climbers: selection and protection of specific ant partners by epicuticular wax blooms in Macaranga (Euphorbiaceae)". In: *Oecologia* 112.2 (Oct. 1997), pp. 217–224. ISSN: 1432-1939. DOI: 10.1007/s004420050303.

[50] W. Federle, K. Rohrseitz, and B. Hölldobler. "Attachment forces of ants measured with a centrifuge: better 'wax-runners' have a poorer attachment to a smooth surface". In: *Journal of Experimental Biology* 203.3 (Feb. 2000), pp. 505–512. ISSN: 1477-9145. DOI: 10.1242/jeb.203.3.505.

[51] S. A. Tunstad et al. "The cuticular wax composition and crystal coverage of leaves and petals differ in a consistent manner between plant species". In: *Open Biology* 14.5 (May 2024). ISSN: 2046-2441. DOI: 10.1098/rsob.230430.

[52] P. Dalin et al. "Leaf trichome formation and plant resistance to herbivory". In: *Induced Plant Resistance to Herbivory*. Springer Netherlands, 2008, pp. 89–105. ISBN: 9781402081828. DOI: 10.1007/978-1-4020-8182-8_4.

[53] G. M. Stack et al. "Cannabinoids function in defense against chewing herbivores in Cannabis sativa L." In: *Horticulture Research* 10.11 (Oct. 2023). ISSN: 2052-7276. DOI: 10.1093/hr/uhad207.

[54] P. López Carretero et al. "Glandular trichomes affect mobility and predatory behavior of two aphid predators on medicinal cannabis". In: *Biological Control* 170 (July 2022), p. 104932. ISSN: 1049-9644. DOI: 10.1016/j.biocontrol.2022.104932.

[55] F. Püffel et al. "Biomechanics of cutting: sharpness, wear sensitivity, and the scaling of cutting forces in leaf-cutter ant mandibles". In: *Philosophical Transactions of the Royal Society B* 378.1891 (2023), p. 20220547. DOI: 10.1098/rstb.2022.0547.

[56] J. G. Williams and Y. Patel. "Fundamentals of cutting". In: *Interface Focus* 6.3 (June 2016), p. 20150108. ISSN: 2042-8901. DOI: 10.1098/rsfs.2015.0108.

[57] P. J. Peeters. "Leaf biomechanical properties and the densities of herbivorous insect guilds". In: *Functional Ecology* (2007), pp. 246–255.

[58] J. J. Howard. "Leafcutting and Diet Selection: Relative Influence of Leaf Chemistry and Physical Features". In: *Ecology* 69.1 (Feb. 1988), pp. 250–260. DOI: 10.2307/1943180.

[59] P. M. Barrer and J. M. Cherret. "Some factors affecting the site and pattern of leaf-cutting activity in the ant Atta cephalotes L." In: *Journal of Entomology Series A, General Entomology* 47.1 (Apr. 2009), pp. 15–27. DOI: 10.1111/j.1365-3032.1972.tb00002.x.

[60] J. M. Cherrett. "Some factors involved in the selection of vegetable substrate by Atta cephalotes (L.) (Hymenoptera: Formicidae) in tropical rain forest". In: *The Journal of Animal Ecology* 41.3 (Oct. 1972), p. 647. DOI: 10.2307/3200.

[61] M. Malishev and G. D. Sanson. "Leaf mechanics and herbivory defence: How tough tissue along the leaf body deters growing insect herbivores". In: *Austral Ecology* 40.3 (Jan. 2015), pp. 300–308. ISSN: 1442-9993. DOI: 10.1111/aec.12214.

[62] P. Lucas. "Mechanical defences to herbivory". In: *Annals of Botany* 86.5 (Nov. 2000), pp. 913–920. DOI: 10.1006/anbo.2000.1261.

[63] J. K. Wilson et al. "The nutritional landscape of host plants for a specialist insect herbivore". In: *Ecology and Evolution* 9.23 (Nov. 2019), pp. 13104–13113. ISSN: 2045-7758. DOI: 10.1002/ece3.5730.

[64] S. Biemelt, H. Tschiersch, and U. Sonnewald. "Impact of altered gibberellin metabolism on biomass accumulation, lignin biosynthesis, and photosynthesis in transgenic tobacco plants". In: *Plant Physiology* 135.1 (May 2004), pp. 254–265. ISSN: 0032-0889. DOI: 10.1104/pp.103.036988.

[65] P. He et al. "Leaf mechanical strength and photosynthetic capacity vary independently across 57 subtropical forest species with contrasting light requirements". In: *New Phytologist* 223.2 (Apr. 2019), pp. 607–618. ISSN: 1469-8137. DOI: 10.1111/nph.15803.

[66] E. T. F. Witkowski and B. B. Lamont. "Leaf specific mass confounds leaf density and thickness". In: *Oecologia* 88.4 (Dec. 1991), pp. 486–493. ISSN: 1432-1939. DOI: 10.1007/bf00317710.

[67] E. Caldwell, J. Read, and G. D. Sanson. "Which leaf mechanical traits correlate with insect herbivory among feeding guilds?" In: *Annals of Botany* (Dec. 2015), p. mcv178. ISSN: 1095-8290. DOI: 10.1093/aob/mcv178.

[68] E. O. W. Bert Hölldobler. *The Leafcutter Ants: Civilization by Instinct*. Ed. by W. W. N. Company. W. W. Norton Company, 2010.

[69] J. Montoya-Lerma et al. "Leaf-cutting ants revisited: Towards rational management and control". In: *International Journal of Pest Management* 58.3 (Sept. 2012), pp. 225–247. ISSN: 1366-5863. DOI: 10.1080/09670874.2012.663946.

[70] S. T. Meyer et al. "Leaf-cutting ants as ecosystem engineers: topsoil and litter perturbations around Atta cephalotes nests reduce nutrient availability". In: *Ecological Entomology* 38.5 (June 2013), pp. 497–504. ISSN: 1365-2311. DOI: 10.1111/een.12043.

[71] A. C. Z. Musuna. "Cereal Crop Losses Caused by Locusts in Eastern, Central and Southern Africa Region". In: *International Journal of Tropical Insect Science* 9.06 (Dec. 1988), pp. 701–707. ISSN: 1742-7592. DOI: 10.1017/s1742758400005579.

[72] K. Cressman. *Biological and Environmental hazards, risks, and disasters*. Ed. by E. Inc. Elsevier Inc, 2016.

[73] S. J. Simpson, G. A. Sword, and A. De Loof. "Advances, controversies and consensus in locust phase polyphenism research". In: *Journal of Orthoptera Research* 14.2 (Dec. 2005), pp. 213–222. ISSN: 1937-2426. DOI: 10.1665/1082-6467(2005)14[213:acacil]2.0.co;2.

[74] T. Haye et al. "Range expansion of the invasive brown marmorated stinkbug, Halyomorpha halys: an increasing threat to field, fruit and vegetable crops worldwide". In: *Journal of Pest Science* 88.4 (May 2015), pp. 665–673. ISSN: 1612-4766. DOI: 10.1007/s10340-015-0670-2.

[75] D.-H. Lee. "Current status of research progress on the biology and management of Halyomorpha halys (Hemiptera: Pentatomidae) as an invasive species". In: *Applied Entomology and Zoology* 50.3 (June 2015), pp. 277–290. ISSN: 1347-605X. DOI: 10.1007/s13355-015-0350-y.

[76] F. J. Clissold. *The biomechanics of chewing and plant fracture: mechanisms and implications*. Elsevier, 2007, pp. 317–372. DOI: 10.1016/s0065-2806(07)34006-x.

[77] H. Krenn. *Insect mouthparts: form, function, development and performance*. Springer, 2019.

[78] Chapman. *Regulatory mechanisms in insect feeding*. Ed. by S. Science. Springer Science, 1995.

[79] R. Chapman. *The insects structure and function*. Ed. by C. U. Press. Cambridge University Press, 1998.

[80] G. Sanson. "The biomechanics of browsing and grazing". In: *American Journal of Botany* 93.10 (Oct. 2006), pp. 1531–1545. DOI: 10.3732/ajb.93.10.1531.

[81] T. Atkins. *The science and engineering of cutting: The mechanics and processes of separating, scratching and puncturing biomaterials, metals and non-metals*. Ed. by Butterworth-Heineman. Butterworth-Heineman, 2009.

[82] J. F. Vincent and U. G. Wegst. "Design and mechanical properties of insect cuticle". In: *Arthropod Structure amp; Development* 33.3 (July 2004), pp. 187–199. ISSN: 1467-8039. DOI: 10.1016/j.asd.2004.05.006.

[83] X. Liu, J. Zhang, and K. Y. Zhu. "Chitin in arthropods: biosynthesis, modification, and metabolism". In: *Targeting Chitin-containing Organisms*. Springer Singapore, 2019, pp. 169–207. ISBN: 9789811373183. DOI: 10.1007/978-981-13-7318-3_9.

[84] R. A. A. Muzzarelli. "Chitin nanostructures in living organisms". In: *Chitin*. Springer Netherlands, Aug. 2010, pp. 1–34. ISBN: 9789048196845. DOI: 10.1007/978-90-481-9684-5_1.

[85] Y. Politi, B. Bar-On, and H.-O. Fabritius. "Mechanics of arthropod cuticle-versatility by structural and compositional variation". In: *Architectured Materials in Nature and Engineering*. Springer International Publishing, 2019, pp. 287–327. ISBN: 9783030119423. DOI: 10.1007/978-3-030-11942-3_10.

[86] Z. Liu et al. "Functional gradients and heterogeneities in biological materials: Design principles, functions, and bioinspired applications". In: *Progress in Materials Science* 88 (July 2017), pp. 467–498. ISSN: 0079-6425. DOI: 10.1016/j.pmatsci.2017.04.013.

[87] V. Birkenfeld, S. N. Gorb, and W. Krings. "Mandible elemental composition and mechanical properties from distinct castes of the leafcutter ant Atta laevigata (Attini; Formicidae)". In: *Interface Focus* 14.2 (Apr. 2024). ISSN: 2042-8901. DOI: 10.1098/rsfs.2023.0048.

[88] R. Schofield et al. "Zinc is incorporated into cuticular "tools" after ecdysis: The time course of the zinc distribution in "tools" and whole bodies of an ant and a scorpion". In: *Journal of Insect Physiology* 49.1 (Jan. 2003), pp. 31–44. DOI: 10.1016/s0022-1910(02)00224-x.

[89] F. Püffel et al. "Morphological determinants of bite force capacity in insects: a biomechanical analysis of polymorphic leaf-cutter ants". In: *Journal of The Royal Society Interface* 18.182 (Sept. 2021). DOI: 10.1098/rsif.2021.0424.

[90] F. Püffel, F. Roces, and D. Labonte. "Strong positive allometry of bite force in leaf-cutter ants increases the range of cuttable plant tissues". In: *Journal of Experimental Biology* 226.13 (July 2023). DOI: 10.1242/jeb.245140.

[91] F. Püffel, R. Johnston, and D. Labonte. "A biomechanical model for the relation between bite force and mandibular opening angle in arthropods". In: *Royal Society Open Science* 10.2 (Feb. 2023). DOI: 10.1098/rsos.221066.

[92] F. Puffel. "Biomechanics of the insect bite apparatus". PhD thesis. Imperial College London, 2022. DOI: 10.25560/104867.

[93] S. E. Santana, E. R. Dumont, and J. L. Davis. "Mechanics of bite force production and its relationship to diet in bats". In: *Functional Ecology* 24.4 (July 2010), pp. 776–784. ISSN: 1365-2435. DOI: 10.1111/j.1365-2435.2010.01703.x.

[94] T. A. McMahon. *Muscles, reflexes, and locomotion*. Ed. by P. U. Press. Princeton University Press, 1984.

[95] D. Labonte. "A theory of physiological similarity in muscle-driven motion". In: *Proceedings of the National Academy of Sciences* 120.24 (June 2023). ISSN: 1091-6490. DOI: 10.1073/pnas.2221217120.

[96] T. Cao and J.-P. Jin. "Evolution of flight muscle contractility and energetic efficiency". In: *Frontiers in Physiology* 11 (Oct. 2020). ISSN: 1664-042X. DOI: 10.3389/fphys.2020.01038.

[97] J. Lighton. *Measuring Metabolic Rates: A Manual for Scientists*. Ed. by O. U. Press. Oxford University Press, 2008.

[98] J. R. B. Lighton. "Limitations and requirements for measuring metabolic rates: a mini review". In: *European Journal of Clinical Nutrition* 71.3 (Jan. 2017), pp. 301–305. ISSN: 1476-5640. DOI: 10.1038/ejcn.2016.265.

[99] E. O. H.T. Odum. *Energy basis for man and nature*. 1976.

[100] R. L. Baldwin and A. C. Bywater. "Nutritional energetics of animals". In: *Annual Review of Nutrition* 4.1 (July 1984), pp. 101–114. ISSN: 1545-4312. DOI: 10.1146/annurev.nu.04.070184.000533.

[101] J. R. B. Lighton, G. A. Bartholomew, and D. H. Feener. "Energetics of locomotion and load carriage and a model of the energy cost of foraging in the leaf-cutting ant Atta colombica Guer". In: *Physiological Zoology* 60.5 (Sept. 1987), pp. 524–537. ISSN: 0031-935X. DOI: 10.1086/physzool.60.5.30156127.

[102] P. E. Schilman and F. Roces. "Foraging energetics of a nectar-feeding ant: metabolic expenditure as a function of food-source profitability". In: *Journal of Experimental Biology* 209.20 (Oct. 2006), pp. 4091–4101. ISSN: 0022-0949. DOI: 10.1242/jeb.02478.

[103] N. C. Holt and G. N. Askew. "Locomotion on a slope in leaf-cutter ants: metabolic energy use, behavioural adaptations and the implications for route selection on hilly terrain". In: *Journal of Experimental Biology* 215.15 (Aug. 2012), pp. 2545–2550. ISSN: 0022-0949. DOI: 10.1242/jeb.057695.

[104] U. Somjee et al. "The hidden cost of sexually selected traits: the metabolic expense of maintaining a sexually selected weapon". In: *Proceedings of the Royal Society B: Biological Sciences* 285.1891 (Nov. 2018), p. 20181685. ISSN: 1471-2954. DOI: 10.1098/rspb.2018.1685.

[105] D. Berrigan and L. Partridge. "Influence of temperature and activity on the metabolic rate of adult Drosophila melanogaster". In: *Comparative Biochemistry and Physiology Part A: Physiology* 118.4 (Dec. 1997), pp. 1301–1307. ISSN: 0300-9629. DOI: 10.1016/s0300-9629(97)00030-3.

[106] R. M. Sibly, J. H. Brown, and A. Kodric-Brown. *Metabolic ecology: a scaling approach*. Ed. by J. W. Sons. John Wiley Sons, 2012.

[107] J. Schmitt and P. Holmes. "Mechanical models for insect locomotion: active muscles and energy losses". In: *Biological Cybernetics* 89.1 (July 2003), pp. 43–55. ISSN: 1432-0770. DOI: 10.1007/s00422-003-0404-z.

[108] L. Reinhardt and R. Blickhan. "Level locomotion in wood ants: evidence for grounded running". In: *Journal of Experimental Biology* (Jan. 2014). ISSN: 0022-0949. DOI: 10.1242/jeb.098426.

[109] A. Lipp, H. Wolf, and F.-O. Lehmann. "Walking on inclines: energetics of locomotion in the antCamponotus". In: *Journal of Experimental Biology* 208.4 (Feb. 2005), pp. 707–719. ISSN: 0022-0949. DOI: 10.1242/jeb.01434.

[110] L. A. Peyré-Tartaruga et al. "Mechanical work as a (key) determinant of energy cost in human locomotion: recent findings and future directions". In: *Experimental Physiology* 106.9 (July 2021), pp. 1897–1908. ISSN: 1469-445X. DOI: 10.1113/ep089313.

[111] P. di Prampero. "The Energy Cost of Human Locomotion on Land and in Water*". In: *International Journal of Sports Medicine* 07.02 (Apr. 1986), pp. 55–72. ISSN: 1439-3964. DOI: 10.1055/s-2008-1025736.

[112] J. J. M. van Alphen and M. A. Jervis. "Foraging Behaviour". In: *Insect Natural Enemies*. Springer Netherlands, 1996, pp. 1–62. ISBN: 9789401100137. DOI: 10.1007/978-94-011-0013-7_1.

[113] M. Brian. *Social Insects: Ecology and Behavioural Biology*. Ed. by Chapman and Hall. Chapman and Hall, 1983.

[114] E. O. Wilson. "Social Insects". In: *Science* 172.3981 (Apr. 1971), pp. 406–406. ISSN: 1095-9203. DOI: 10.1126/science.172.3981.406.

[115] D. Sumpter and S. Pratt. "A modelling framework for understanding social insect foraging". In: *Behavioral Ecology and Sociobiology* 53.3 (Feb. 2003), pp. 131–144. ISSN: 1432-0762. DOI: 10.1007/s00265-002-0549-0.

[116] F.-X. Dechaume-Moncharmont et al. "The hidden cost of information in collective foraging". In: *Proceedings of the Royal Society B: Biological Sciences* 272.1573 (July 2005), pp. 1689–1695. ISSN: 1471-2954. DOI: 10.1098/rspb.2005.3137.

[117] K. Moll, W. Federle, and F. Roces. "The energetics of running stability: costs of transport in grass-cutting ants depend on fragment shape". In: *Journal of Experimental Biology* 215.1 (Jan. 2012), pp. 161–168. ISSN: 0022-0949. DOI: 10.1242/jeb.063594.

[118] F. Roces and J. R. B. Lighten. "Larger bites of leaf-cutting ants". In: *Nature* 373.6513 (Feb. 1995), pp. 392–392. ISSN: 1476-4687. DOI: 10.1038/373392a0.

[119] M. Burd. "Foraging behaviour of Atta cephalotes (leaf-cutting ants): an examination of two predictions for load selection". In: *Animal Behaviour* 60.6 (Dec. 2000), pp. 781–788. ISSN: 0003-3472. DOI: 10.1006/anbe.2000.1537.

[120] U. Rothe and W. Nachtigall. "Flight of the honey bee: IV. Respiratory quotients and metabolic rates during sitting, walking and flying". In: *Journal of Comparative Physiology B* 158.6 (1989), pp. 739–749. ISSN: 1432-136X. DOI: 10.1007/bf00693012.

[121] T. J. Wolf et al. "Physiological correlates of foraging efforts in honey-bees: oxygen consumption and nectar load". In: *Functional Ecology* 3.4 (1989), p. 417. ISSN: 0269-8463. DOI: 10.2307/2389615.

[122] C. T.M. *Oxygen consumption during flight. In CRC Handbook of Insect Flight*. Ed. by G. Goldsworthy. Boca Raton, 1988.

[123] L. G. Halsey et al. "Exploring key issues of aerobic scope interpretation in ectotherms: absolute versus factorial". In: *Reviews in Fish Biology and Fisheries* 28.2 (Mar. 2018), pp. 405–415. ISSN: 1573-5184. DOI: 10.1007/s11160-018-9516-3.

[124] J. R. B. Lighton. "Discontinuous gas exchange in insects". In: *Annual Review of Entomology* 41.1 (Jan. 1996), pp. 309–324. ISSN: 1545-4487. DOI: 10.1146/annurev.en.41.010196.001521.

[125] Harrison. *Encyclopedia of Insects*. Ed. by Resh and Carde. Elsevier, 2003.

[126] J. F. Harrison. "Tracheal System". In: *Encyclopedia of Insects*. Elsevier, 2009, pp. 1011–1015. ISBN: 9780123741448. DOI: 10.1016/b978-0-12-374144-8.00265-4.

[127] G. Snyder et al. "Gas exchange in the insect tracheal system". In: *Journal of Theoretical Biology* 172.3 (Feb. 1995), pp. 199–207. ISSN: 0022-5193. DOI: 10.1006/jtbi.1995.0016.

[128] L. Hanna and A. Popadić. "A hemipteran insect reveals new genetic mechanisms and evolutionary insights into tracheal system development". In: *Proceedings of the National Academy of Sciences* 117.8 (Feb. 2020), pp. 4252–4261. ISSN: 1091-6490. DOI: 10.1073/pnas.1908975117.

[129] T. D. Förster and H. A. Woods. "Mechanisms of tracheal filling in insects". In: *Biological Reviews* 88.1 (May 2012), pp. 1–14. ISSN: 1469-185X. DOI: 10.1111/j.1469-185x.2012.00233.x.

[130] M. Kleiber. *The fire of life. An introduction to animal energetics.* Ed. by J. W. Sons. John Wiley Sons, 1961.

[131] J. F. Gillooly et al. "Effects of size and temperature on metabolic rate". In: *Science* 293.5538 (Sept. 2001), pp. 2248–2251. ISSN: 1095-9203. DOI: 10.1126/science.1061967.

[132] T. M. Della Lucia, L. C. Gandra, and R. N. Guedes. "Managing leaf-cutting ants: peculiarities, trends and challenges: Managing leaf-cutting ants". In: *Pest Management Science* 70.1 (Oct. 2013), pp. 14–23. ISSN: 1526-498X. DOI: 10.1002/ps.3660.

[133] A. C. Swanson et al. "Welcome to the Atta world: A framework for understanding the effects of leaf-cutter ants on ecosystem functions". In: *Functional Ecology* 33.8 (Mar. 2019). Ed. by A. Bennett, pp. 1386–1399. ISSN: 1365-2435. DOI: 10.1111/1365-2435.13319.

[134] E. O. Wilson. "Caste and division of labor in leaf-cutter ants (Hymenoptera: Formicidae: Atta)". In: *Behavioral Ecology and Sociobiology* 7.2 (July 1980), pp. 157–165. DOI: 10.1007/bf00299521.

[135] L. L. Rockwood. "Plant selection and foraging patterns in two species of leaf-cutting ants (Atta)". In: *Ecology* 57.1 (Jan. 1976), pp. 48–61. ISSN: 1939-9170. DOI: 10.2307/1936397.

[136] E. O. Wilson. "Caste and division of labor in leaf-cutter ants (Hymenoptera: Formicidae: Atta): III. Ergonomic resiliency in foraging by A. cephalotes". In: *Behavioral Ecology and Sociobiology* 14.1 (Dec. 1983), pp. 47–54. ISSN: 1432-0762. DOI: 10.1007/bf00366655.

[137] J. K. Wetterer. "Forager polymorphism, size-matching, and load delivery in the leaf-cutting ant, Atta cephalotes". In: *Ecological Entomology* 19.1 (Feb. 1994), pp. 57–64. DOI: 10.1111/j.1365-2311.1994.tb00390.x.

[138] E. Clark. "Dynamic matching of forager size to resources in the continuously polymorphic leaf-cutter ant,Atta colombica (Hymenoptera, Formicidae)". In: *Ecological Entomology* 31.6 (Nov. 2006), pp. 629–635. ISSN: 1365-2311. DOI: 10.1111/j.1365-2311.2006.00826.x.

[139] R. M. S. Schofield et al. "Leaf-cutter ants with worn mandibles cut half as fast, spend twice the energy, and tend to carry instead of cut". In: *Behavioral Ecology and Sociobiology* 65.5 (Dec. 2010), pp. 969–982. DOI: 10.1007/s00265-010-1098-6.

[140] I. R. Leal, R. Wirth, and M. Tabarelli. "The multiple impacts of leaf-cutting ants and their novel ecological role in human-modified Neotropical forests". In: *Biotropica* 46.5 (June 2014), pp. 516–528. ISSN: 1744-7429. DOI: 10.1111/btp.12126.

[141] J. K. Wetterer. "Forager polymorphism and foraging ecology in the leaf-cutting ant Atta columbica". In: *Psyche: A Journal of Entomology* 102.3-4 (1995), pp. 131–145. DOI: 10.1155/1995/10717.

[142] N. Imirzian et al. "Large deformation diffeomorphic mapping ofshape variation reveals two distinct mandible and head capsule morphs in Atta vollenweideri leaf-cutter worker ants". In: *Ecology and Evolution* 14.4 (Apr. 2024). ISSN: 2045-7758. DOI: 10.1002/ece3.11236.

[143] J. Röschard and F. Roces. "Fragment-size determination and size-matching in the grass-cutting ant iAtta vollenweideri/i depend on the distance from the nest". In: *Journal of Tropical Ecology* 19.6 (Oct. 2003), pp. 647–653. DOI: 10.1017/s0266467403006047.

[144] F. Roces. "Leaf-cutting ants cut fragment sizes in relation to the distance from the nest". In: *Animal Behaviour* 40.6 (Dec. 1990), pp. 1181–1183. DOI: 10.1016/s0003-3472(05)80185-x.

[145] M. Burd. "Foraging performance by Atta colombica, a leaf-cutting ant". In: *The American Naturalist* 148.4 (Oct. 1996), pp. 597–612. DOI: 10.1086/285942.

[146] C. M. Nichols-Orians and J. C. Schultz. "Leaf toughness affects leaf harvesting by the aeaf cutter ant, Atta cephalotes (L.) (Hymenoptera: Formicidae)". In: *Biotropica* 21.1 (Mar. 1989), p. 80. DOI: 10.2307/2388446.

[147] C. M. Nichols-Orians and J. C. Schultz. "Interactions among leaf toughness, chemistry, and harvesting by attine ants". In: *Ecological Entomology* 15.3 (Aug. 1990), pp. 311–320. DOI: 10.1111/j.1365-2311.1990.tb00813.x.

[148] J. A. Gatehouse. "Plant resistance towards insect herbivores: a dynamic interaction". In: *New Phytologist* 156.2 (Oct. 2002), pp. 145–169. ISSN: 1469-8137. DOI: 10.1046/j.1469-8137.2002.00519.x.

[149] J. Ehrlén and O. Eriksson. "Large-scale spatial dynamics of plants: a response to Freckleton amp; Watkinson". In: *Journal of Ecology* 91.2 (Apr. 2003), pp. 316–320. ISSN: 1365-2745. DOI: 10.1046/j.1365-2745.2003.00753.x.

[150] C. J. E. Metcalf et al. "Evolution of flowering decisions in a stochastic, density-dependent environment". In: *Proceedings of the National Academy of Sciences* 105.30 (July 2008), pp. 10466–10470. ISSN: 1091-6490. DOI: 10.1073/pnas.0800777105.

[151] J. P. Sexton et al. "Evolution and ecology of species range limits". In: *Annual Review of Ecology, Evolution, and Systematics* 40.1 (Dec. 2009), pp. 415–436. ISSN: 1545-2069. DOI: 10.1146/annurev.ecolsys.110308.120317.

[152] K. C. Baer and J. L. Maron. "Declining demographic performance and dispersal limitation influence the geographic distribution of the perennial forb Astragalus utahensis (Fabaceae)". In: *Journal of Ecology* 107.3 (Nov. 2018). Ed. by N. Emery, pp. 1250–1262. ISSN: 1365-2745. DOI: 10.1111/1365-2745.13086.

[153] A. T. Kramer et al. "Sourcing native plants to support ecosystem function in different planting contexts". In: *Restoration Ecology* 27.3 (Mar. 2019), pp. 470–476. ISSN: 1526-100X. DOI: 10.1111/rec.12931.

[154] A. A. Agrawal and J. L. Maron. "Long-term impacts of insect herbivores on plant populations and communities". In: *Journal of Ecology* 110.12 (Oct. 2022), pp. 2800–2811. ISSN: 1365-2745. DOI: 10.1111/1365-2745.13996.

[155] T. Johnson. *An introduction to the studies of insects*. Cole Publishers, 2005.

[156] D. Pimental et al. "Environmental and economic costs of nonindigenous species in the United States". In: *BioScience* 50.1 (2000), p. 53. ISSN: 0006-3568. DOI: 10.1641/0006-3568(2000)050[0053:eaecon]2.3.co;2.

[157] C. Oliveira et al. "Crop losses and the economic impact of insect pests on Brazilian agriculture". In: *Crop Protection* 56 (Feb. 2014), pp. 50–54. ISSN: 0261-2194. DOI: 10.1016/j.cropro.2013.10.022.

[158] M. E. Hanley et al. "Plant structural traits and their role in anti-herbivore defence". In: *Perspectives in Plant Ecology, Evolution and Systematics* 8.4 (July 2007), pp. 157–178. ISSN: 1433-8319. DOI: 10.1016/j.ppees.2007.01.001.

[159] H. C. Sharma, G. Sujana, and D. Manohar Rao. "Morphological and chemical components of resistance to pod borer, Helicoverpa armigera in wild relatives of pigeonpea". In: *Arthropod-Plant Interactions* 3.3 (June 2009), pp. 151–161. ISSN: 1872-8847. DOI: 10.1007/s11829-009-9068-5.

[160] M. F. Choong. "What makes a leaf tough and how this affects the pattern of Castanopsis fissa leaf consumption by caterpillars". In: *Functional Ecology* 10.5 (Oct. 1996), p. 668. DOI: 10.2307/2390178.

[161] K. Y. Ang, P. W. Lucas, and H. T. W. Tan. "Novel way of measuring the fracture toughness of leaves and other thin films using a single inclined razor blade". In: *New Phytologist* 177.3 (Dec. 2007), pp. 830–837. DOI: 10.1111/j.1469-8137.2007.02302.x.

[162] R. Karban. "The ecology and evolution of induced resistance against herbivores". In: *Functional Ecology* 25.2 (Oct. 2010), pp. 339–347. ISSN: 1365-2435. DOI: 10.1111/j.1365-2435.2010.01789.x.

[163] A. R. Evans et al. "The scaling of tooth sharpness in mammals". In: *Annales Zoologici Fennici* 42.6 (2005), pp. 603–613.

[164] J. Goyens et al. "Biomechanical determinants of bite force dimorphism in Cyclommatus metalliferstag beetles". In: *Journal of Experimental Biology* 217.7 (Apr. 2014), pp. 1065–1071. ISSN: 0022-0949. DOI: 10.1242/jeb.091744.

[165] T. Weihmann et al. "Fast and powerful: biomechanics and bite forces of the mandibles in the american cockroach Periplaneta americana". In: *PLOS ONE* 10.11 (Nov. 2015). Ed. by W. Gronenberg, e0141226. ISSN: 1932-6203. DOI: 10.1371/journal.pone.0141226.

[166] B. Zhang and P. S. L. Anderson. "Modelling biological puncture: a mathematical framework for determining the energetics and scaling". In: *Journal of The Royal Society Interface* 19.195 (Oct. 2022). ISSN: 1742-5662. DOI: 10.1098/rsif.2022.0559.

[167] B. A. Goda and M. Bacca. *Cutting mechanics of soft compressible solids: force-radius scaling versus bulk modulus*. 2024. DOI: 10.48550/ARXIV.2409.02665.

[168] F. Püffel et al. "Developmental biomechanics and age polyethism in leaf-cutter ants". In: *Proceedings of the Royal Society B: Biological Sciences* 290.2000 (June 2023). DOI: 10.1098/rspb.2023.0355.

[169] S. Pielström and F. Roces. "Sequential soil transport and its influence on the spatial organisation of collective digging in leaf-cutting ants". In: *PLoS ONE* 8.2 (Feb. 2013). Ed. by S. Pratt, e57040. DOI: 10.1371/journal.pone.0057040.

[170] R. M. S. Schofield, M. H. Nesson, and K. A. Richardson. "Tooth hardness increases with zinc-content in mandibles of young adult leaf-cutter ants". In: *Naturwissenschaften* 89.12 (Dec. 2002), pp. 579–583. ISSN: 1432-1904. DOI: 10.1007/s00114-002-0381-4.

[171] R. F. Chapman. "The structure and wear of the mandibles in some african grasshoppers". In: *Proceedings of the Zoological Society of London* 142.1 (Jan. 1964), pp. 107–122. DOI: 10.1111/j.1469-7998.1964.tb05157.x.

[172] D. S. Brown. "The morphology and functioning of the mouthparts of Chileon Dipterum and Baetis Rhodani". In: *Proceedings of the Zoological Society of London* 136.2 (Mar. 1961), pp. 147–176. DOI: 10.1111/j.1469-7998.1961.tb06169.x.

[173] L. Kundanati et al. "Cutting mechanics of wood by beetle larval mandibles". In: *Journal of the Mechanical Behavior of Biomedical Materials* 112 (Dec. 2020), p. 104027. DOI: 10.1016/j.jmbbm.2020.104027.

[174] B. Hölldobler and E. O. Wilson. *The ants*. Harvard Univeristy Press, 1990.

[175] J. Tautz, F. Roces, and B. Hölldobler. "Use of a sound-based vibratome by leaf-cutting ants". In: *Science* 267.5194 (Jan. 1995), pp. 84–87. DOI: 10.1126/science.267.5194.84.

[176] J.-N. Jasmin and C. Devaux. "Laterality of leaf cutting in the attine ant Acromyrmex echinatior". In: *Insectes Sociaux* 62.1 (Dec. 2014), pp. 109–114. ISSN: 1420-9098. DOI: 10.1007/s00040-014-0379-x.

[177] R. Seghir and S. Arscott. "Extended PDMS stiffness range for flexible systems". In: *Sensors and Actuators A: Physical* 230 (July 2015), pp. 33–39. DOI: 10.1016/j.sna.2015.04.011.

[178] J. C. Lötters et al. "The mechanical properties of the rubber elastic polymer polydimethylsiloxane for sensor applications". In: *Journal of Micromechanics and Microengineering* 7.3 (Sept. 1997), pp. 145–147. DOI: 10.1088/0960-1317/7/3/017.

[179] A. Mata, A. J. Fleischman, and S. Roy. "Characterization of polydimethylsiloxane (PDMS) properties for biomedical micro/nanosystems". In: *Biomedical Microdevices* 7.4 (Dec. 2005), pp. 281–293. DOI: 10.1007/s10544-005-6070-2.

[180] K. Khanafer et al. "Effects of strain rate, mixing ratio, and stress–strain definition on the mechanical behavior of the polydimethylsiloxane (PDMS) material as related to its biological applications". In: *Biomedical Microdevices* 11.2 (Dec. 2008), pp. 503–508. DOI: 10.1007/s10544-008-9256-6.

[181] M. Liu et al. "Thickness-dependent mechanical properties of polydimethylsiloxane membranes". In: *Journal of Micromechanics and Microengineering* 19.3 (Feb. 2009), p. 035028. DOI: 10.1088/0960-1317/19/3/035028.

[182] D. Corning. *Sylgard184 technical datasheet*. URL: https://www.dow.com/content/dam/dcc/documents/en-us/productdatasheet/11/11-31/11-3184-sylgard-184-elastomer.pdf.

[183] R. Hopf et al. "Experimental and theoretical analyses of the age-dependent large-strain behavior of Sylgard 184 (10:1) silicone elastomer". In: *Journal of the Mechanical Behavior of Biomedical Materials* 60 (July 2016), pp. 425–437. DOI: 10.1016/j.jmbbm.2016.02.022.

[184] P. Lucas. "The fracture toughness of the leaf of the dicotyledon Calophyllum inophyllum L. (Guttiferae)". In: *Philosophical Transactions of the Royal Society of London. Series B: Biological Sciences* 334.1269 (Oct. 1991), pp. 95–106. DOI: 10.1098/rstb.1991.0099.

[185] H.-C. Spatz, L. Köhler, and K. J. Niklas. "Mechanical behaviour of plant tissues: composite materials or structures?" In: *Journal of Experimental Biology* 202.23 (Dec. 1999), pp. 3269–3272. DOI: 10.1242/jeb.202.23.3269.

[186] G. Cordoba-Barco, F. Casanova, and J. L. Ealo. "Determination of poro-viscoelastic properties of vegetal tissues as a function of moisture content by means of stress relaxation tests". In: *Rheologica Acta* 59.4 (Feb. 2020), pp. 201–208. DOI: 10.1007/s00397-020-01200-0.

[187] D. Taylor. "Seasonal variations in the toughness of leaves: a case study using Griselinia littoralis". In: *Integrative And Comparative Biology* (Mar. 2024). ISSN: 1557-7023. DOI: 10.1093/icb/icae004.

[188] L. W. Bielczynski et al. "Leaf and plant age affects photosynthetic performance and photoprotective capacity". In: *Plant Physiology* 175.4 (Oct. 2017), pp. 1634–1648. ISSN: 1532-2548. DOI: 10.1104/pp.17.00904.

[189] G. Li, D. Yang, and S. Sun. "Allometric relationships between lamina area, lamina mass and petiole mass of 93 temperate woody species vary with leaf habit, leaf form and altitude". In: *Functional Ecology* 22.4 (Aug. 2008), pp. 557–564. DOI: 10.1111/j.1365-2435.2008.01407.x.

[190] D. Römer, R. Exl, and F. Roces. "Two feedback mechanisms involved in the control of leaf fragment size in leaf-cutting ants". In: *Journal of Experimental Biology* 226.12 (June 2023). DOI: 10.1242/jeb.244246.

[191] Y. Su et al. "Leaf functional traits vary in urban environments: influences of leaf age, land-use type, and urban–rural gradient". In: *Frontiers in Ecology and Evolution* 9 (Dec. 2021). ISSN: 2296-701X. DOI: 10.3389/fevo.2021.681959.

[192] R. Oguchi et al. "Leaf anatomy and function". In: *Advances in Photosynthesis and Respiration*. Springer International Publishing, 2018, pp. 97–139. ISBN: 9783319935942. DOI: 10.1007/978-3-319-93594-2_5.

[193] D. Roylance. *Mechanics of Materials*. John Wiley Sons, 1996.

[194] C. Creton and M. Ciccotti. "Fracture and adhesion of soft materials: a review". In: *Reports on Progress in Physics* 79.4 (Mar. 2016), p. 046601. DOI: 10.1088/0034-4885/79/4/046601.

[195] I. D. Johnston et al. "Mechanical characterization of bulk Sylgard 184 for microfluidics and microengineering". In: *Journal of Micromechanics and Microengineering* 24.3 (Feb. 2014), p. 035017. DOI: 10.1088/0960-1317/24/3/035017.

[196] R. N. Palchesko et al. "Development of polydimethylsiloxane substrates with tunable elastic modulus to study cell mechanobiology in muscle and nerve". In: *PLoS ONE* 7.12 (Dec. 2012). Ed. by N. M. Neves, e51499. DOI: 10.1371/journal.pone.0051499.

[197] O. Akogwu et al. "Large strain deformation and cracking of nano-scale gold films on PDMS substrate". In: *Materials Science and Engineering: B* 170.1–3 (June 2010), pp. 32–40. ISSN: 0921-5107. DOI: 10.1016/j.mseb.2010.02.023.

[198] K. Song et al. "Investigating mechanical behaviours of PDMS films under cyclic loading". In: *Polymers* 14.12 (June 2022), p. 2373. ISSN: 2073-4360. DOI: 10.3390/polym14122373.

[199] B. Zhang et al. "Y-shaped cutting for the systematic characterization of cutting and tearing". In: *Experimental Mechanics* 59.4 (Feb. 2019), pp. 517–529. DOI: 10.1007/s11340-019-00479-2.

[200] J.-Y. Sun et al. "Highly stretchable and tough hydrogels". In: *Nature* 489.7414 (Sept. 2012), pp. 133–136. DOI: 10.1038/nature11409.

[201] D. Labonte and W. Federle. "Rate-dependence of 'wet' biological adhesives and the function of the pad secretion in insects". In: *Soft Matter* 11.44 (2015), pp. 8661–8673. DOI: 10.1039/c5sm01496d.

[202] G. J. Lake and O. H. Yeoh. "Measurement of rubber cutting resistance in the absence of friction". In: *International Journal of Fracture* 14.5 (Oct. 1978), pp. 509–526. DOI: 10.1007/bf01390472.

[203] A. N. Gent. "Adhesion and strength of viscoelastic solids. Is there a relationship between adhesion and bulk properties?" In: *Langmuir* 12.19 (Jan. 1996), pp. 4492–4496. ISSN: 1520-5827. DOI: 10.1021/la950887q.

[204] A. Atkins. "Toughness and cutting: a new way of simultaneously determining ductile fracture toughness and strength". In: *Engineering Fracture Mechanics* 72.6 (Apr. 2005), pp. 849–860. DOI: 10.1016/j.engfracmech.2004.07.014.

[205] S. Schuldt et al. "Analysis of the sharpness of blades for food cutting". In: *Journal of Food Engineering* 188 (Nov. 2016), pp. 13–20. DOI: 10.1016/j.jfoodeng.2016.04.022.

[206] A. G. Atkins and Y. W. Mai. "On the guillotining of materials". In: *Journal of Materials Science* 14.11 (Nov. 1979), pp. 2747–2754. DOI: 10.1007/bf00610649.

[207] S. B. Crofts et al. "How do morphological sharpness measures relate to puncture performance in viperid snake fangs?" In: *Biology Letters* 15.4 (Apr. 2019), p. 20180905. DOI: 10.1098/rsbl.2018.0905.

[208] S. B. Crofts and P. S. L. Anderson. "The influence of cactus spine surface structure on puncture performance and anchoring ability is tuned for ecology". In: *Proceedings of the Royal Society B: Biological Sciences* 285.1891 (Nov. 2018), p. 20182280. DOI: 10.1098/rspb.2018.2280.

[209] J. G. Pattrick, D. Labonte, and W. Federle. "Scaling of claw sharpness: mechanical constraints reduce attachment performance in larger insects". In: *Journal of Experimental Biology* (Jan. 2018). ISSN: 0022-0949. DOI: 10.1242/jeb.188391.

[210] Fields. *Discovering Statistics Using R*. John Wiley Sons, 2012.

[211] W. N. Sharpe. *Springer handbook of experimental solid mechanics*. Ed. by Springer. Springer, 2008.

[212] P. R. Ehrlich. "Some axioms of taxonomy". In: *Systematic Zoology* 13.3 (Sept. 1964), p. 109. ISSN: 0039-7989. DOI: 10.2307/2411485.

[213] D. Treutter. "Significance of flavonoids in plant resistance: a review". In: *Environmental Chemistry Letters* 4.3 (July 2006), pp. 147–157. ISSN: 1610-3661. DOI: 10.1007/s10311-006-0068-8.

[214] P. Usha Rani and Y. Jyothsna. "Biochemical and enzymatic changes in rice plants as a mechanism of defense". In: *Acta Physiologiae Plantarum* 32.4 (Jan. 2010), pp. 695–701. ISSN: 1861-1664. DOI: 10.1007/s11738-009-0449-2.

[215] A. R. War et al. "Herbivore and elicitor induced resistance in groundnut to asian armyworm, Spodoptera litura". In: *Plant Signaling & Behavior* 6.11 (Nov. 2011), pp. 1769–1777. ISSN: 1559-2324. DOI: 10.4161/psb.6.11.17323.

[216] G. Arimura, K. Matsui, and J. Takabayashi. "Chemical and molecular ecology of herbivore-induced plant volatiles: proximate factors and their ultimate functions". In: *Plant and Cell Physiology* 50.5 (Feb. 2009), pp. 911–923. ISSN: 1471-9053. DOI: 10.1093/pcp/pcp030.

[217] J. Vincent. "Fracture properties of plants". In: *Advances in Botanical Research Volume 17*. Elsevier, 1990, pp. 235–287. ISBN: 9780120059171. DOI: 10.1016/s0065-2296(08)60135-4.

[218] S. J. Wright. "Phenological responses to seasonality in tropical forest plants". In: *Tropical Forest Plant Ecophysiology*. Springer US, 1996, pp. 440–460. ISBN: 9781461311638. DOI: 10.1007/978-1-4613-1163-8_15.

[219] G. Sanson et al. "Measurement of leaf biomechanical properties in studies of herbivory: Opportunities, problems and procedures". In: *Austral Ecology* 26.5 (Oct. 2001), pp. 535–546. DOI: 10.1046/j.1442-9993.2001.01154.x.

[220] J. Read and A. Stokes. "Plant biomechanics in an ecological context". In: *American Journal of Botany* 93.10 (Oct. 2006), pp. 1546–1565. ISSN: 1537-2197. DOI: 10.3732/ajb.93.10.1546.

[221] E. A. Bernays. "Diet-Induced Head Allometry Among Foliage-Chewing Insects and Its Importance for Graminivores". In: *Science* 231.4737 (Jan. 1986), pp. 495–497. ISSN: 1095-9203. DOI: 10.1126/science.231.4737.495.

[222] E. Bernays and R. Chapman. "The evolution of deterrent responses in plant-feeding insects". In: *Perspectives in Chemoreception and Behavior*. Springer New York, 1987, pp. 159–173. ISBN: 9781461246442. DOI: 10.1007/978-1-4612-4644-2_10.

[223] Bernays. "Evolution of insect morphology in relation to plants". In: *Philosophical Transactions of the Royal Society of London. Series B: Biological Sciences* 333.1267 (Aug. 1991), pp. 257–264. ISSN: 1471-2970. DOI: 10.1098/rstb.1991.0075.

[224] E. A. Bernays. "Evolution of feeding behavior in insect herbivores". In: *BioScience* 48.1 (Jan. 1998), pp. 35–44. ISSN: 1525-3244. DOI: 10.2307/1313226.

[225] R. M. S. Schofield et al. "Is fracture a bigger problem for smaller animals? Force and fracture scaling for a simple model of cutting, puncture and crushing". In: *Interface Focus* 6.3 (June 2016), p. 20160002. DOI: 10.1098/rsfs.2016.0002.

[226] A. Blanke. "The early evolution of biting–chewing performance in hexapoda". In: *Insect Mouthparts*. Springer International Publishing, 2019, pp. 175–202. ISBN: 9783030296544. DOI: 10.1007/978-3-030-29654-4_6.

[227] I. Kamyab, S. Chakrabarti, and J. G. Williams. In: *Journal of Materials Science* 33.11 (1998), pp. 2763–2770. DOI: 10.1023/a:1017517332112.

[228] T. Millar et al. "An investigation of cutting resistance in stretched polymer films". In: *Procedia Structural Integrity* 2 (2016), pp. 190–196. ISSN: 2452-3216. DOI: 10.1016/j.prostr.2016.06.025.

[229] S. Goh, M. Charalambides, and J. Williams. "On the mechanics of wire cutting of cheese". In: *Engineering Fracture Mechanics* 72.6 (Apr. 2005), pp. 931–946. ISSN: 0013-7944. DOI: 10.1016/j.engfracmech.2004.07.015.

[230] B. Blackman et al. "Tool sharpness as a factor in machining tests to determine toughness". In: *Engineering Fracture Mechanics* 101 (Mar. 2013), pp. 47–58. ISSN: 0013-7944. DOI: 10.1016/j.engfracmech.2012.09.020.

[231] C. McCarthy, M. Hussey, and M. Gilchrist. "On the sharpness of straight edge blades in cutting soft solids: Part I – indentation experiments". In: *Engineering Fracture Mechanics* 74.14 (Sept. 2007), pp. 2205–2224. ISSN: 0013-7944. DOI: 10.1016/j.engfracmech.2006.10.015.

[232] P. W. Lucas and B. Pereira. "Estimation of the Fracture Toughness of Leaves". In: *Functional Ecology* 4.6 (1990), p. 819. DOI: 10.2307/2389448.

[233] J. F. V. Vincent. "The influence of water content on the stiffness and fracture properties of grass leaves". In: *Grass and Forage Science* 38.2 (June 1983), pp. 107–114. ISSN: 1365-2494. DOI: 10.1111/j.1365-2494.1983.tb01628.x.

[234] G. S. a. R. N. Aranwela. *Methods of assessing leaf-fracture properties*. Ed. by C. U. Press. Cambridge University Press, 1999.

[235] Lucas. "The toughness of plant cell walls". In: *Philosophical Transactions of the Royal Society of London. Series B: Biological Sciences* 348.1325 (May 1995), pp. 363–372. ISSN: 1471-2970. DOI: 10.1098/rstb.1995.0074.

[236] H. Xiao, X. Wang, and C. Long. "Theoretical model for determining elastic modulus of ceramic materials by nanoindentation". In: *Materialia* 17 (June 2021), p. 101121. ISSN: 2589-1529. DOI: 10.1016/j.mtla.2021.101121.

[237] M. F. Choong et al. "Leaf fracture toughness and sclerophylly: their correlations and ecological implications". In: *New Phytologist* 121.4 (Aug. 1992), pp. 597–610. DOI: 10.1111/j.1469-8137.1992.tb01131.x.

[238] J. Read and G. D. Sanson. "Characterizing sclerophylly: the mechanical properties of a diverse range of leaf types". In: *New Phytologist* 160.1 (Aug. 2003), pp. 81–99. DOI: 10.1046/j.1469-8137.2003.00855.x.

[239] P. Lucas. *Dental functional morphology: how teeth work*. Cambridge University Press, 2004.

[240] M. J. Raupp. "Effects of leaf toughness on mandibular wear of the leaf beetle, Plagiodera versicolora". In: *Ecological Entomology* 10.1 (Feb. 1985), pp. 73–79. DOI: 10.1111/j.1365-2311.1985.tb00536.x.

[241] R. H. Köhler and M. R. Hanson. "Plastid tubules of higher plants are tissue-specific and developmentally regulated". In: *Journal of Cell Science* 113.1 (Jan. 2000), pp. 81–89. ISSN: 1477-9137. DOI: 10.1242/jcs.113.1.81.

[242] B. D. Roitberg et al. "The cost of being an omnivore: mandible wear from plant feeding in a true bug". In: *Naturwissenschaften* 92.9 (Aug. 2005), pp. 431–434. DOI: 10.1007/s00114-005-0013-x.

[243] R. A. Depieri, C. G. Andrade, and A. R. Panizzi. "A new methodology for processing mouthparts of hemipterans (Hemiptera) for microscopic studies". In: *Micron* 41.2 (Feb. 2010), pp. 169–171. ISSN: 0968-4328. DOI: 10.1016/j.micron.2009.09.006.

[244] K. Kuřavová, L. Hajduková, and P. Kočárek. "Age-related mandible abrasion in the groundhopper Tetrix tenuicornis (Tetrigidae, Orthoptera)". In: *Arthropod structure &; development* 43.3 (May 2014), pp. 187–192. ISSN: 1467-8039. DOI: 10.1016/j.asd.2014.02.002.

[245] W. W. K. Houston. "The life cycles and age of Carabus glabratus Paykull and C.problematicus Herbst (Col.: Carabidae) on moorland in northern England". In: *Ecological Entomology* 6.3 (Aug. 1981), pp. 263–271. ISSN: 1365-2311. DOI: 10.1111/j.1365-2311.1981.tb00613.x.

[246] W. Arens. "Wear and tear of mouthparts: a critical problem in stream animals feeding on epilithic algae". In: *Canadian Journal of Zoology* 68.9 (Sept. 1990), pp. 1896–1914. ISSN: 1480-3283. DOI: 10.1139/z90-269.

[247] R. Schofield. "The homogenous alternative to biomineralization: Zn- and Mn-rich materials enable sharp organismal "tools" that reduce force requirements". In: *scientific reports* (2021).

[248] O. L. Kvedaras et al. "Influence of plant silicon and sugarcane cultivar on mandibular wear in the stalk boreriEldana saccharina/i". In: *Agricultural and Forest Entomology* 11.3 (Aug. 2009), pp. 301–306. DOI: 10.1111/j.1461-9563.2009.00430.x.

[249] O. Reynolds, M. Keeping, and J. Meyer. "Silicon-augmented resistance of plants to herbivorous insects: a review". In: *Annals of Applied Biology* 155.2 (Oct. 2009), pp. 171–186. DOI: 10.1111/j.1744-7348.2009.00348.x.

[250] K. Moll, F. Roces, and W. Federle. "Foraging grass-cutting ants (Atta vollenweideri) maintain stability by balancing their loads with controlled head movements". In: *Journal of Comparative Physiology A* 196.7 (May 2010), pp. 471–480. ISSN: 1432-1351. DOI: 10.1007/s00359-010-0535-3.

[251] K. Moll, F. Roces, and W. Federle. "How load-carrying ants avoid falling over: mechanical stability during foraging in Atta vollenweideri grass-cutting ants". In: *PLoS ONE* 8.1 (Jan. 2013). Ed. by C. M. Aegerter, e52816. ISSN: 1932-6203. DOI: 10.1371/journal.pone.0052816.

[252] J. R. B. Lighton, J. A. Weier, and D. H. Feener. "The energetics of locomotion and load carriage in the desert harvester ant Pogonomyrmex rugosus". In: *Journal of Experimental Biology* 181.1 (Aug. 1993), pp. 49–62. ISSN: 1477-9145. DOI: 10.1242/jeb.181.1.49.

[253] F. D. Duncan and J. R. B. Lighton. "The burden within: The energy cost of load carriage in the honeypot ant, Myrmecocystus". In: *Physiological Zoology* 67.1 (Jan. 1994), pp. 190–203. ISSN: 0031-935X. DOI: 10.1086/physzool.67.1.30163842.

[254] R. B. Armstrong et al. "Metabolism of rats running up and down an incline". In: *Journal of Applied Physiology* 55.2 (Aug. 1983), pp. 518–521. ISSN: 1522-1601. DOI: 10.1152/jappl.1983.55.2.518.

[255] B. A. Wunder and P. R. Morrison. "Red squirrel metabolism during incline running". In: *Comparative Biochemistry and Physiology Part A: Physiology* 48.1 (May 1974), pp. 153–161. ISSN: 0300-9629. DOI: 10.1016/0300-9629(74)90863-9.

[256] R. J. Full and A. Tullis. "Energetics of ascent: insects on inclines". In: *Journal of Experimental Biology* 149.1 (Mar. 1990), pp. 307–317. ISSN: 1477-9145. DOI: 10.1242/jeb.149.1.307.

[257] R. Margaria. "Positive and negative work performances and their efficiencies in human locomotion". In: *Internationale Zeitschrift for Angewandte Physiologie Einschlienlich Arbeitsphysiologie* 25.4 (1968), pp. 339–351. ISSN: 1439-6327. DOI: 10.1007/bf00699624.

[258] S. Hunt. "Measurements of photosynthesis and respiration in plants". In: *Physiologia Plantarum* 117.3 (Feb. 2003), pp. 314–325. ISSN: 1399-3054. DOI: 10.1034/j.1399-3054.2003.00055.x.

[259] F. Roces and B. Hölldobler. "Leaf density and a trade-off between load-size selection and recruitment behavior in the ant Atta cephalotes". In: *Oecologia* 97.1 (Feb. 1994), pp. 1–8. DOI: 10.1007/bf00317902.

[260] F. Roces. "Both evaluation of resource quality and speed of recruited leaf-cutting ants (Acromyrmex lundi) depend on their motivational state". In: *Behavioral Ecology and Sociobiology* 33.3 (Sept. 1993), pp. 183–189. ISSN: 1432-0762. DOI: 10.1007/bf00216599.

[261] S. L. Chown et al. "Scaling of insect metabolic rate is inconsistent with the nutrient supply network model". In: *Functional Ecology* (2007).

[262] E. Hemmingsen and P. F. Scholander. "Specific transport of oxygen through hemoglobin solutions: why is this transport abolished when opposed by a slight back pressure of oxygen?" In: *Science* 132.3437 (Nov. 1960), pp. 1379–1381. ISSN: 1095-9203. DOI: 10.1126/science.132.3437.1379.

[263] M. J. Carter, P. A. Cortes, and E. L. Rezende. "Temperature variability and metabolic adaptation in terrestrial and aquatic ectotherms". In: *Journal of Thermal Biology* 115 (July 2023), p. 103565. ISSN: 0306-4565. DOI: 10.1016/j.jtherbio.2023.103565.

[264] J. B. Lighton, M. C. Quinlan, and D. Feener. "Is bigger better? Water balance in the polymorphic desert harvester ant Messor pergandei". In: *Physiological Entomology* 19.4 (Dec. 1994), pp. 325–334. ISSN: 1365-3032. DOI: 10.1111/j.1365-3032.1994.tb01059.x.

[265] R. Singh et al. "Wolbachia-infected pharaoh ant colonies have higher egg production, metabolic rate and worker survival". In: *Journal of Experimental Biology* 227.16 (Aug. 2024). ISSN: 1477-9145. DOI: 10.1242/jeb.247168.

[266] J. Lois-Milevicich, P. E. Schilman, and R. Josens. "Viscosity as a key factor in decision making of nectar feeding ants". In: *Journal of Insect Physiology* 128 (Jan. 2021), p. 104164. ISSN: 0022-1910. DOI: 10.1016/j.jinsphys.2020.104164.

[267] J. R. B. Lighton. "Discontinuous CO2 emission in a small insect, the Formicine ant Camponotus vicixus". In: *Journal of Experimental Biology* 134.1 (Jan. 1988), pp. 363–376. ISSN: 1477-9145. DOI: 10.1242/jeb.134.1.363.

[268] J. R. B. Lighton and G. A. Bartholomew. "Standard energy metabolism of a desert harvester ant, Pogonomyrmex rugosus: Effects of temperature, body mass, group size, and humidity". In: *Proceedings of the National Academy of Sciences* 85.13 (July 1988), pp. 4765–4769. ISSN: 1091-6490. DOI: 10.1073/pnas.85.13.4765.

[269] J. R. B. Lighton. "Cost of tokking: the energetics of substrate communication in the tok-tok beetle,Psammodes striatus". In: *Journal of Comparative Physiology B* 157.1 (1987), pp. 11–20. ISSN: 1432-136X. DOI: 10.1007/bf00702723.

[270] G. A. Bartholomew, J. R. B. Lighton, and G. N. Louw. "Energetics of locomotion and patterns of respiration in tenebrionid beetles from the Namib Desert". In: *Journal of Comparative Physiology B* 155.2 (1985), pp. 155–162. ISSN: 1432-136X. DOI: 10.1007/bf00685208.

[271] V. Kang, F. Püffel, and D. Labonte. "Three-dimensional kinematics of leaf-cutter ant mandibles: not all dicondylic joints are simple hinges". In: *Philosophical Transactions of the Royal Society B: Biological Sciences* 378.1891 (Oct. 2023). ISSN: 1471-2970. DOI: 10.1098/rstb.2022.0546.

[272] J. Schindelin et al. "Fiji: an open-source platform for biological-image analysis". In: *Nature Methods* 9.7 (June 2012), pp. 676–682. ISSN: 1548-7105. DOI: 10.1038/nmeth.2019.

[273] R Core Team. *R: A Language and Environment for Statistical Computing*. R Foundation for Statistical Computing. Vienna, Austria, 2022. URL: https://www.R-project.org/.

[274] J. R. Lighton. "Slow discontinuous ventilation in the Namib dune-sea ant Camponotus detritus(Hymenoptera, Formicidae)". In: *Journal of Experimental Biology* 151.1 (July 1990), pp. 71–82. ISSN: 1477-9145. DOI: 10.1242/jeb.151.1.71.

[275] J. S. Terblanche et al. "Scaling of gas exchange cycle frequency in insects". In: *Biology Letters* 4.1 (Dec. 2007), pp. 127–129. ISSN: 1744-957X. DOI: 10.1098/rsbl.2007.0522.

[276] T. R. Schultz and S. G. Brady. "Major evolutionary transitions in ant agriculture". In: *Proceedings of the National Academy of Sciences* 105.14 (Apr. 2008), pp. 5435–5440. ISSN: 1091-6490. DOI: 10.1073/pnas.0711024105.

[277] E. O. Wilson. "Causes of ecological success: the case of the ants". In: *The Journal of Animal Ecology* 56.1 (Feb. 1987), p. 1. ISSN: 0021-8790. DOI: 10.2307/4795.

[278] H. Herz, W. Beyschlag, and B. Hölldobler. "Herbivory rate of leaf-cutting ants in a tropical moist forest in panama at the population and ecosystem scales". In: *Biotropica* 39.4 (May 2007), pp. 482–488. ISSN: 1744-7429. DOI: 10.1111/j.1744-7429.2007.00284.x.

[279] D. J. de Souza et al. "Ectosymbionts and immunity in the leaf-cutting ant Acromyrmex subterraneus subterraneus". In: *Brain, Behavior, and Immunity* 28 (Feb. 2013), pp. 182–187. ISSN: 0889-1591. DOI: 10.1016/j.bbi.2012.11.014.

[280] K. Schmidt-Nielsen, L. Bolis, and C. R. Taylor. *Comparative Physiology: Primitive Mammals*. Vol. 4. Cambridge University Press, 1980.

[281] V. Ducret et al. "Do female frogs have higher resting metabolic rates than males? A case study with Xenopus allofraseri". In: *Journal of Zoology* 312.4 (Aug. 2020), pp. 221–226. ISSN: 1469-7998. DOI: 10.1111/jzo.12820.

[282] J. R. Lighton. "Respiratory biology: why insects evolved discontinuous gas exchange". In: *Current Biology* 17.16 (Aug. 2007), R645–R647. ISSN: 0960-9822. DOI: 10.1016/j.cub.2007.06.007.

[283] P. Kestler. "Respiration and respiratory water loss". In: *Environmental Physiology and Biochemistry of Insects*. Springer Berlin Heidelberg, 1984, pp. 137–183. ISBN: 9783642700200. DOI: 10.1007/978-3-642-70020-0_6.

[284] N. Hadley. *The water relations of terrestrial arthropods*. Ed. by Arthropoda. Arthropoda, 1994.

[285] J. R. B. Lighton. "Ventilation in namib Ddsert Tenebrionid beetles: mass scaling and evidence of a novel quantized flutter-phase". In: *Journal of Experimental Biology* 159.1 (Sept. 1991), pp. 249–268. ISSN: 0022-0949. DOI: 10.1242/jeb.159.1.249.

[286] K. J. Greenlee, C. Nebeker, and J. F. Harrison. "Body size-independent safety margins for gas exchange across grasshopper species". In: *Journal of Experimental Biology* 210.7 (Apr. 2007), pp. 1288–1296. ISSN: 0022-0949. DOI: 10.1242/jeb.001982.

[287] E. P. Snelling, P. G. D. Matthews, and R. S. Seymour. "Allometric scaling of discontinuous gas exchange patterns in the locust Locusta migratoria throughout ontogeny". In: *Journal of Experimental Biology* (Jan. 2012). ISSN: 0022-0949. DOI: 10.1242/jeb.072769.

[288] A. L. V. Davis, S. L. Chown, and C. H. Scholtz. "Discontinuous gas-exchange cycles in Scarabaeus dung beetles (Coleoptera: scarabaeidae): mass-scaling and temperature dependence". In: *Physiological and Biochemical Zoology* 72.5 (Sept. 1999), pp. 555–565. ISSN: 1537-5293. DOI: 10.1086/316698.

[289] W. R. Stahl. "Scaling of respiratory variables in mammals". In: *Journal of Applied Physiology* 22.3 (Mar. 1967), pp. 453–460. ISSN: 1522-1601. DOI: 10.1152/jappl.1967.22.3.453.

[290] I. J. Aitkenhead et al. "Tracheal branching in ants is area-decreasing, violating a central assumption of network transport models". In: *PLOS Computational Biology* 16.4 (Apr. 2020). Ed. by V. M. Savage, e1007853. ISSN: 1553-7358. DOI: 10.1371/journal.pcbi.1007853.

[291] J. Nunome. "Studies on the respiration of the silkworm: on the air current of respiration". In: *The Journal of Sericultural Science of Japan* (1951).

[292] J. R. Vogt and M. E. Dillon. "Allometric scaling of tracheal morphology among bumblebee sisters (Apidae:Bombus): compensation for oxygen limitation at large body sizes?" In: *Physiological and Biochemical Zoology* 86.5 (Sept. 2013), pp. 576–587. ISSN: 1537-5293. DOI: 10.1086/672211.

[293] K. J. Greenlee et al. "Hypoxia-induced compression in the tracheal system of the tobacco hornworm caterpillar,Manduca sextaL." In: *Journal of Experimental Biology* (Jan. 2013). ISSN: 0022-0949. DOI: 10.1242/jeb.082479.

[294] J. F. Harrison et al. "How to be a giant: hypermetric scaling of the leg in cockroaches and scarab beetles suggests oxygen transport to the legs limits maximal insect size". In: *The FASEB Journal* 34.S1 (Apr. 2020), pp. 1–1. ISSN: 1530-6860. DOI: 10.1096/fasebj.2020.34.s1.06388.

[295] S. K. Hetz and T. J. Bradley. "Insects breathe discontinuously to avoid oxygen toxicity". In: *Nature* 433.7025 (Feb. 2005), pp. 516–519. ISSN: 1476-4687. DOI: 10.1038/nature03106.

[296] T. J. Roberts, M. S. Chen, and C. R. Taylor. "Energetics Of bipedal running II. limb design and running mechanics". In: *Journal of Experimental Biology* 201.19 (Oct. 1998), pp. 2753–2762. ISSN: 1477-9145. DOI: 10.1242/jeb.201.19.2753.

[297] D. Labonte and N. C. Holt. "Beyond power limits: the kinetic energy capacity of skeletal muscle". In: *Journal of Experimental Biology* (Sept. 2024). ISSN: 1477-9145. DOI: 10.1242/jeb.247150.

[298] C. R. Taylor. "Force development during sustained locomotion: a determinant of gait, speed and metabolic power". In: *Journal of Experimental Biology* 115.1 (Mar. 1985), pp. 253–262. ISSN: 1477-9145. DOI: 10.1242/jeb.115.1.253.

[299] S. Kipp, A. M. Grabowski, and R. Kram. "What determines the metabolic cost of human running across a wide range of velocities?" In: *Journal of Experimental Biology* (Jan. 2018). ISSN: 0022-0949. DOI: 10.1242/jeb.184218.

[300] R. T. R. Kram. "Energetics of running: a new perspective". In: *Letters to Nature* (1990).

[301] T. J. van der Zee and A. D. Kuo. "The high energetic cost of rapid force development in muscle". In: *Journal of Experimental Biology* 224.9 (May 2021). ISSN: 1477-9145. DOI: 10.1242/jeb.233965.

[302] O. T. Lewis, M. Martin, and T. J. Czaczkes. "Effects of trail gradient on leaf tissue transport and load size selection in leaf-cutter ants". In: *Behavioral Ecology* 19.4 (2008), pp. 805–809. ISSN: 1045-2249. DOI: 10.1093/beheco/arn032.

[303] A. Arenas and F. Roces. "Avoidance of plants unsuitable for the symbiotic fungus in leaf-cutting ants: Learning can take place entirely at the colony dump". In: *PLOS ONE* 12.3 (Mar. 2017). Ed. by N. Chaline, e0171388. ISSN: 1932-6203. DOI: 10.1371/journal.pone.0171388.

[304] R. J. Stuart and R. E. Page. "Genetic component to division of labor among workers of a leptothoracine ant". In: *Naturwissenschaften* 78.8 (Aug. 1991), pp. 375–377. ISSN: 1432-1904. DOI: 10.1007/bf01131615.

[305] S. J. and L. D. "Colony disassociation following diet partitioning in a unicolonial ant". In: *Naturwissenschaften* 88.2 (Mar. 2001), pp. 73–77. ISSN: 1432-1904. DOI: 10.1007/s001140000198.

[306] N. Kikuta and K. Tsuji. "Queen and worker policing in the monogynous and monandrous ant, Diacamma sp." In: *Behavioral Ecology and Sociobiology* 46.3 (Aug. 1999), pp. 180–189. ISSN: 1432-0762. DOI: 10.1007/s002650050608.

[307] A. Falibene, F. Roces, and W. Wassler. "Long-term avoidance memory formation is associated with a transient increase in mushroom body synaptic complexes in leaf-cutting ants". In: *Frontiers in Behavioral Neuroscience* 9 (Apr. 2015). ISSN: 1662-5153. DOI: 10.3389/fnbeh.2015.00084.

[308] F. Roces and B. Hölldobler. "Use of stridulation in foraging leaf-cutting ants: mechanical support during cutting or short-range recruitment signal?" In: *Behavioral Ecology and Sociobiology* 39.5 (Nov. 1996), pp. 293–299. ISSN: 1432-0762. DOI: 10.1007/s002650050292.

[309] M. M. Martin, R. M. Carman, and J. G. MacConnell. "Nutrients derived from the fungus cultured by the fungus-growing ant Atta colombica". In: *Annals of the Entomological Society of America* 62.1 (Jan. 1969), pp. 11–13. ISSN: 0013-8746. DOI: 10.1093/aesa/62.1.11.

[310] E. Kolb. "Particle Physics and Cosmology". In: *arXiv* (1994).

[311] W. Gronenberg et al. "Mandible muscle fibers in ants: fast or powerful?" In: *Cell and Tissue Research* 289.2 (July 1997), pp. 347–361. ISSN: 1432-0878. DOI: 10.1007/s004410050882.

[312] J. K. Wetterer. "Allometry and the geometry of leaf-cutting in Atta cephalotes". In: *Behavioral Ecology and Sociobiology* 29.5 (Dec. 1991), pp. 347–351. DOI: 10.1007/bf00165959.

[313] F. P. Massey and S. E. Hartley. "Physical defences wear you down: progressive and irreversible impacts of silica on insect herbivores". In: *Journal of Animal Ecology* 78.1 (Dec. 2008), pp. 281–291. ISSN: 1365-2656. DOI: 10.1111/j.1365-2656.2008.01472.x.

[314] G. Hofstra and J. D. Hesketh. "Effects of temperature on the gas exchange of leaves in the light and dark". In: *Planta* 85.3 (1969), pp. 228–237. ISSN: 1432-2048. DOI: 10.1007/bf00389400.

[315] F. Plum. "Computational Methods to Study the Behaviour of Social Insects". PhD thesis. Imperial College London, 2023.

[316] S. O. Oladipupo et al. "Why do insects close their spiracles? a meta-analytic evaluation of the adaptive hypothesis of discontinuous gas exchange in insects". In: *Insects* 13.2 (Jan. 2022), p. 117. ISSN: 2075-4450. DOI: 10.3390/insects13020117.